MICROWAVE PROMOTED ADDITION OF ORGANOSILOXANES TO

HYDROXYL CONTAINING SUBSTRATES FOR FACILE

SYNTHESIS OF CHEMICAL AND BIOLOGICAL

WARFARE AGENT REACTIVE POLYMERS

Except where reference is made to the work of others, the work described in this thesis is my own or was done in collaboration with my advisory committee. This thesis does not include proprietary or classified information

Jeffery Ray Owens

Certificate of Approval:

Edward J. Parish
Professor
Chemistry & Biochemistry

Shelby D. Worley, Chair
Professor
Chemistry & Biochemistry

Peter D. Livant
Associate Professor
Chemistry & Biochemistry

Royall M. Broughton Jr.
Professor
Polymer & Fiber Engineering

George T. Flowers
Interim Dean
Graduate School

MICROWAVE PROMOTED ADDITION OF ORGANOSILOXANES TO HYDROXYL CONTAINING SUBSTRATES FOR FACILE SYNTHESIS OF CHEMICAL AND BIOLOGICAL WARFARE AGENT REACTIVE POLYMERS

Jeffery Ray Owens

A Dissertation

Submitted to

the Graduate Faculty of

Auburn University

in Partial Fulfillment of the

Requirements for the

Degree of

Doctor of Philosphy

Auburn, Alabama

May 10, 2007

MICROWAVE PROMOTED ADDITION OF ORGANOSILOXANES TO HYDROXYL CONTAINING SUBSTRATES FOR FACILE SYNTHESIS OF CHEMICAL AND BIOLOGICAL WARFARE AGENT REACTIVE POLYMERS

Jeffery Ray Owens

_____
Signature of Author

_____
Date of Graduation

This work was funded and carried out using USAF equipment, personnel, and facilities, under contract number F08636-02-C-7020. As such, the United States Air Force may possess certain rights to any intellectual property contained herein, in accordance with Executive Order 10096.

DISSERTATION ABSTRACT

MICROWAVE PROMOTED ADDITION OF ORGANOSILOXANES TO HYDROXYL CONTAINING SUBSTRATES FOR FACILE SYNTHESIS OF CHEMICAL AND BIOLOGICAL WARFARE AGENT REACTIVE POLYMERS

Jeffery Ray Owens

Doctor of Philosophy, May 10, 2007
(B.S. Fort Hays State University, 1997)
(B.S. Fort Hays State University, 1996)

149 Typed Pages

Directed by Professor Shelby D. Worley

The primary focus of this work was the synthesis and characterization of materials efficacious in detoxifying/killing chemical and/or biological threat agent surrogates, including *Bacillus anthracis* spores, in militarily relevant environments. To this end, it was shown: that polymers containing ≥5 ppt active chlorine in the form of polymer linked hydantoin chloramides demonstrated significant activity against biological and chemical threat agent surrogates; that ≥5 ppt active chlorine is easily attained on polymeric

substrates containing hydroxyl groups using a minimum amount of solvent and reduced amounts of reagents by the microwave grafting of 3-(3-triethoxysilylpropyl)-5,5-dimethylhydantoin (BA-1) onto the substrate, followed by exposure to an appropriate chlorinating agent; through environmental stability experiments that attenuation of active chlorine from the chlorinated hydantoin−bound polymers over time, with the degree of loss dependent on the conditions; and finally, that, in all cases in this work, rechlorination of the spent polymer bound−hydantoin moieties was achieved.

Recognizing the advantages of using microwave irradiation as an alternate means to conventional heating for the attachment of siloxanes to hydroxyl containing substrates and the recognition of the differences between the heat-treated analogs remains the most significant discoveries reported in this work. Compared to the most effective heat treatment for addition of BA-1 to boehmite, controlled application of microwave energy enhanced the capacity for incorporation of active chlorine more than fourfold—from a lower relative concentration of BA-1. To demonstrate the generality of this method of enhancing silicone coupling, microwave irradiation was used to synthesize discrete hypervalent silicon compounds faster, using less solvent, and in higher purity and yield compared to traditional synthetic processes. Finally, the tactical purpose of this program was realized: the microwave-enhanced BA-1-treated substrates caused 5-log reductions in viable counts of *B. anthracis* Sterne spores.

ACKNOWLWDGEMENTS

I would like to thank Professor Worley for his patience, Dr. Wander for his impatience (in a constructive way), and all my friends at Air Force Research Laboratory that supported me. Additionally, I would like to thank my brother for making me laugh when I needed it the most, my dad for possessing the will to pull through, my mother, for serving as my role model for strength and perseverance, and Dr. Wander; the guidance he provided truly does deserve double recognition. I would like to give special thanks to my loving wife, who has stood by me and helped to ease my stress during difficult times, who has laughed and cried with me, and who is always there when I need her the most. Finally, I would like to thank my son, Sebastian, who was conceived, born, and grew to >1 year old during the course of this work. He loves to help me type, and manages to push the power button to the laptop at the most inopportune times.

THANK YOU!

Style manual or journal used: Hybrid of The Journal of Organic Chemistry and Air Force Technical Report

Computer software used: Microsoft Word, Microsoft Excel, Chemdraw 7.0, Omnic, Endnote X

TABLE OF CONTENTS

LIST OF FIGURES

LIST OF TABLES

I. INTRODUCTION

I.1—Statement of the Problem:

The global purpose of this investigation was:

To expand the scope of a class of effective disinfectants containing *N*-halogenated heterocyclic rings (halamines) to encompass materials for protection of humans, their implements, and their habitat from attack by a chemical (CW) or biological weapon (BW).

Toward this end the following series of steps was proposed:

1. To validate the expectation that a readily available halamine will oxidize a –C–S–R unit—using two CW agent (CWA) surrogates—to the corresponding sulfoxide, and to test the halamine's ability to promote the hydrolysis of a P–F bond of a third CWA surrogate.

2. To exploit the reactivity of halamines toward surrogate BW agents and at least two CWA surrogates. It was proposed to systematically functionalize a series of macroscopic and nanoscopic substrates using a silyl coupling reaction to incorporate chloramine functionality. The resulting materials were further proposed to be potentially protective against CW and BW agents because of their reactivity, which was to be evaluated by measuring the efficacy with which each reacts with the three CWA surrogates and kills three surrogate BW agents.

3. To characterize the durability of polymer−siloxane linked heterocyclic chloramines in common military operational environments through controlled measurement of heat stability, UV stability, and susceptibility to hydrolysis.

4. Finally, to better characterize the mode of attachment through the siloxyl bonds to these various polymeric substrates, it was proposed to prepare and characterize a cyclic, monomeric siloxane product by reaction of a 3-(trialkoxy-silyl)propyl compound with a multifunctional small organic molecule.

I.2—Historical Background:

Nobel Laureate Fritz Haber formally introduced the world to chemical warfare at the Battle of Ypres, April 22, 1915.[1] The world has not been idle since that time. The dynamic and rapidly evolving Science and Technology world has driven the threat from newly developed chemical and biological warfare (CBW) agents to new heights.[2] Moreover, the availability of the Internet and global networking has made it easy and economically feasible for anyone with the inclination and a relatively modest budget to acquire the technology, instrumentation, and starting materials to develop both traditional and next-generation threat agents. The challenge then lies in developing the capability to deal with the multitude of identified and unidentified threats that will inevitably become available to terrorist organizations.

The daunting task of protecting personnel and materiel assets from these unforeseen threats requires a sound approach that encompasses broad vision and economic feasibility. Defense technologies developed to meet this challenge must remain as versatile as the multitude of potential threats while maintaining a robustness and ease of use that allows for practical field application. Current systems do not adequately protect personnel and assets against threat agents developed 75 years ago, much less more recently developed agents. Consequently, action is required in the science community for the development of the technologies that will define the

protective systems that can protect against current and future terrorist actions.

While the terrorist method of choice has traditionally been the use of explosives, events such as the Tokyo subway sarin nerve gas attack, and the weaponized anthrax mail attack clearly point to a trend towards chemical and biological warfare.[2, 3] Unfortunately, while the world of chemistry has advanced exponentially since the 1930s, the systems employed to protect against chemical agents remain essentially the same as they were in the 1930s: passive exclusion barrier materials, such as butyl rubber and poly(vinyl alcohol)s, solid-state adsorbents, such as activated carbon and diatomaceous earth, and hypochlorite solutions for chemical agent decontamination/neutralization.[2-5] Biological agent protection has come a bit farther in the realm of medicine, with the development of new vaccines and antibiotics, but still remains grossly inadequate compared to the wide variety of highly adaptive pathogens available in Mother Nature's arsenal, and their availability to practically anyone who has the motivation to use them.[6]

After 9/11, and the weaponized anthrax terrorist attacks, the US adopted a more vigilant posture with respect to potential threats and threat agents. This increased emphasis placed a high priority on protection from biological warfare agents, in addition to traditional chemical threat agents.[2, 3] US treaty agreements strictly regulate the use of chemical and biological

warfare agents.[2, 3] The common chemical threat agents and reasonable surrogates are shown in Figure 1.

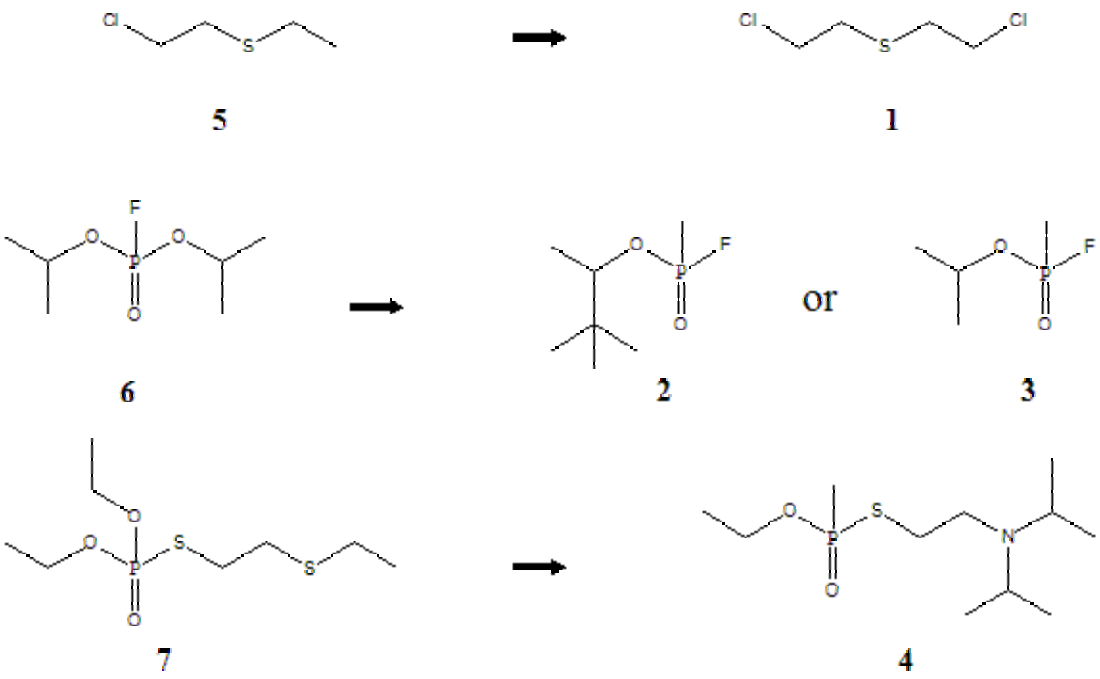

Figure 1. CWA Surrogate Comparison to Actual CWA

Respectively they are: HD, sulfur mustard, mustard gas, or bis(2-chloroethyl)sulfide (1) and its surrogate ½ mustard, 2-CEES, or 2-chloroethyl ethyl sulfide (5); soman, GD, or *O*-pinacolyl methylphosphonofluoridate (2) and sarin, GB, or isopropyl methylphosphonofluoridate (3) and their surrogate, DFP, or diisopropyl phosphorofluoridate (6); VX, or methylphosphonothioic acid *S*-[2-[bis(1-methylethyl)amino]ethyl] *O*-ethyl ester (4) and its surrogate, D-S, demeton-S or S-[2-(ethylthio)ethyl] O,O-diethyl phosphorothioate (7).

The biological threat is much more dynamic than the chemical threat, so representative, non-pathogenic organisms for each "class" of potential pathogens are:

Escherichia coli—Gram negative bacterium

Staphylococcus aureus—Gram positive bacterium

Bacillus atrophaeus or B. anthracis (Sterne strain)—Gram positive spore

Aspergillus niger—Fungal spore

MS-2 coli phage—Virus

To solve a problem, one must first understand the dynamics of the problem. The protection of aggregates of people is called collective protection (CP), and encompasses shelter systems, buildings, and air handling. The protection of a single individual is called individual protection (IP) and consists of protective clothing and a supply of clean breathable air. State-of-the-art, fielded CP systems include a poly(vinyl alcohol) CBW protective liner, to keep chemical and biological (CB) threats from entering an area; an activated charcoal filter, to remove any chemical threats in the air; and a high efficiency particle-arresting (HEPA) filter, to remove any biological pathogens from air. Unfortunately, current systems remain inadequate.[7]

"Barrier materials" rely on passive exclusion, with protection based on low-surface-energy materials that possess low permeation coefficients to the target threats. The problem is simple physics—no material is "impermeable"

to anything. Permeability is simply a function of time and environmental conditions.[5, 8] To deal with this challenge, one applies limits corresponding to the limitations of state-of-the-art barrier materials, and adjust the military concept of operations accordingly. Unfortunately for us, chemicals are chosen as chemical warfare agents (CWAs) because they have a variety of characteristics in addition to simple lethality that make them effective, *i.e.*, most will readily permeate polymers that are normally employed in CP and IP systems.[4, 5, 8-10]

Solid-state adsorbent materials rely on high surface areas and high affinities for target compounds to remove target chemicals from air streams. These types of systems are commonly used to purify air for CP and IP, and are employed for making "breathable" fabrics in IP systems.[11] Unfortunately, this type of capture is reversible and is dependent on the mass transfer rate into and out of the adsorbent. The mass transfer equilibrium of such a system is highly variable depending on the concentration of the target compound in the air vs. concentration of the target compound in the adsorbent (adsorbate), on temperature, and on competitive kinetics of interferants (*e.g.*, commonly encountered solvents, pesticides, diesel exhaust, fuel vapors, etc.).[12, 13] Additionally, such systems can reach their saturation point, at which they have exhausted their adsorbent capacity for the target compound. The high variability within these materials, coupled with the huge numbers of unknown variables in a practical environment, make it extremely difficult to predict the amount of time these systems will function properly

before needing to be replaced; consequently, extremely conservative parameters have been established that govern the system's working life based on worst-case environmental conditions. Also, when using these adsorbent systems as breathable protective garments, the level of protection from submicron-sized biological particles provided by such adsorbent breathable protective garments remains in question.[14]

HEPA filtration is a generic name for a particle filtration technology that removes 99.97% of 0.3-µm particles.[15] HEPA filters are the primary means of protection from biological warfare agents, but they carry several associated liabilities. One major problem in HEPA systems is pressure drop—the difference in pressure on the front side of the filter, where dirty air enters the system, compare to the back side, where filtered air leaves the system—a direct consequence of forcing large volumes of air through small-diameter pores or orifices to achieve the specified removal efficiency. Additionally, particles 0.1–0.3-µm in diameter, such as some viruses, are not captured completely, so many of them penetrate and create a potential infectious hazard. Finally, the HEPA filter is not discriminatory; it is a simple particle exclusion filter and catch-all.[16] Unfortunately, the more particles it catches, the higher the pressure drop rises. This is problematic, considering that many of the areas that the United States military conducts operations in today, such as deserts, have extremely high concentrations of aerosolized particles.

I.3. Reactive Materials

One way of dealing with the problems of currently fielded systems is to incorporate active barrier materials (ABMs)—materials that employ more than physical processes to achieve the required protection. ABMs would employ a combination of physical properties and chemically reactive properties to achieve the required protection. In an ABM system the physical barrier properties of a substrate, be it air filtration media, garments or tentage, need only slow down the permeation of the target compounds enough for the embedded chemical reactivity to react with, or "neutralize" the target compounds.

The concept of using reactive chemistries to neutralize threat agents for protective systems is not new. In fact, research on chemical warfare agent decontaminants coincides with the end of World War I and the stockpiling of HD, the deadly vesicant agent bis(2-chlorethyl)sulfide (1), commonly known as sulfur mustard or mustard gas.[9, 10, 13] Scientists immediately identified chloramines as efficient decontaminants for sulfur mustard (Figure 2).

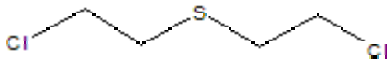

1

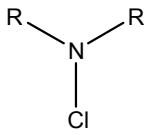

Figure 2. Chloramine Structure

These compounds were appealing as decontaminants because they were commercially available for water disinfection. Chloramines liberate chlorine in the form of hypochlorite in the presence of moisture, which also makes them very effective biocides (Figure 3).[17-25]

Figure 3. Secondary Amine—Chloramine Equilibrium

Additionally, hypochlorite is capable of oxidizing mustard to the sulfoxide and, under certain conditions, the sulfone (Figure 4).[9]

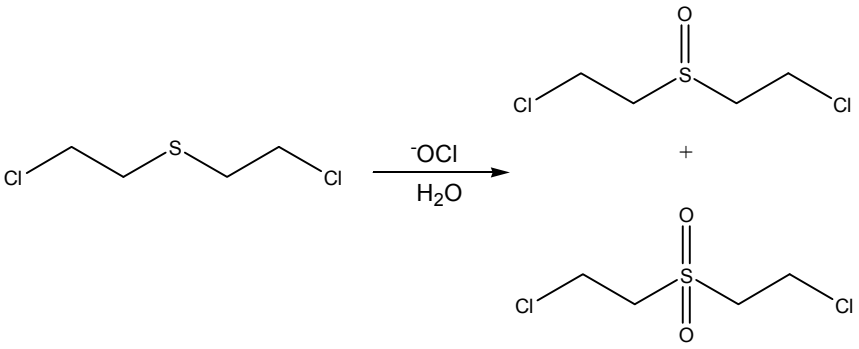

Figure 4. Reaction of HD with Hypochlorite Ion

The ability to stabilize the N–Cl bond through inductive and steric effects induced by the R and R' groups attached to the nitrogen steered research toward reactive protection.[26, 27] In general, electron-donating groups and bulky R and R' groups will stabilize the N–Cl bond, while electron withdrawing groups and small R and R' groups destabilize the N–Cl bond.[13, 17, 25] The stability of this N–Cl bond determines the oxidative potential of the chlorine, as well as the rate at which the chlorine will dissociate from the amine into water. Consequently, not all chloramines are suitable for protection, decontamination or disinfection purposes. Cyclic chloramines that are generated from heterocycles were found to be the most effective at chlorine stabilization, while maintaining enough oxidative potential to decontaminate. Figure 5 illustrates select examples of commercially available chloramines used for water disinfection that were also used as chemical warfare agent decontaminants. They are chloroisocyanurates (8), 1,3,5-trichloro-2,4-dioxohexahydrotriazene (9), 1,3-dichloro-5,5-dimethyl hydantoin (10), *N*-chlorosuccinimide (11), 1,4-dichloro-2,2,5,5-tetramethyl-3,6-piperazinedione (12), and chloroglycolurils (13), each of which has no hydrogens alpha to the chloramine group.[13, 17] The presence of an alpha hydrogen destabilizes the chloramine by allowing intramolecular elimination of HCl to form a double bond between the nitrogen and the protonated alpha carbon.[17]

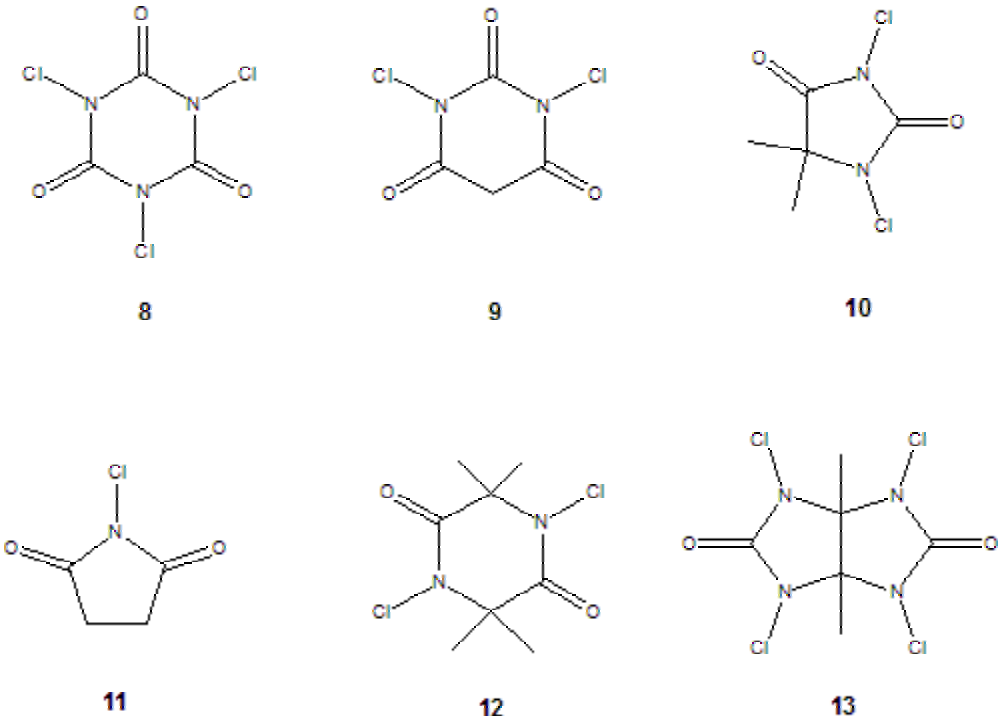

Figure 5. Commercially Available Chloramines

1,3-dichloro-5,5-dimethylhydantoin (10) was used extensively as a sulfur mustard decontaminant and was the active ingredient in the composition of Decontamination Agent, Non-Corrosive (DANC), which was used as a decontaminant until 1972. DS2 (Decontaminating Solution #2) replaced DANC because of its inability to decontaminate G-agents, the toxicity of the solvent system (1,1,2,2-tetrachloroethane), and because DANC is corrosive to select metal alloys.[4]

In addition to decontaminant solutions, chloramines were also pursued extensively as impregnants to chemical and biological protective suits.

However, these experimental textile garments displayed poor durability, strongly irritated skin, leached upon washing, and tended to lose their reactivity in less than a month.[8] Polymers inherently containing the chloramine or amines capable of forming the chloramine were also synthesized. Unfortunately, these materials were difficult to make, demonstrated poor durability, and did not possess the chlorine capacity needed to adequately decontaminate.[26, 27]

The synthesis and integration of heterocyclic chloramines into/onto polymeric coatings/surfaces for biocidal utility has been the focus of Professor Worley's research group at Auburn University for over a decade. Recently several of these heterocyclic amine precursors have shown superior versatility for incorporation into a variety of polymeric substrates, while still retaining biocidal activity, presumably through an oxidation mechanism.[23, 24, 28] Once formed, the chloramine-grafted materials retain considerable amounts of available Cl^+.

Although of limited interest for broad protection applications, the synthesis of polystyrene hydantoin (PSH), and its chlorinated analog, by Worley's group was a significant first step in the evolution of stable polymer-bound chloramines for purposes of protection (Figure 6).[19]

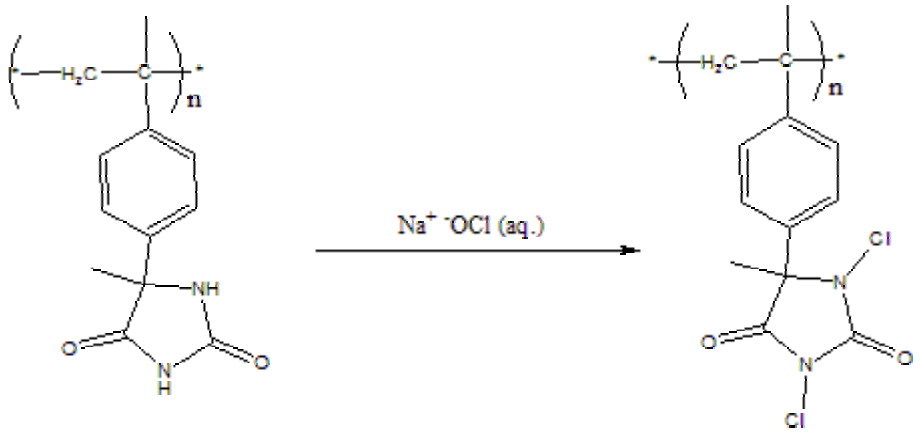

Figure 6. Chlorination of PSH

Another significant stepping stone was the ability to covalently link chloramine-forming heterocyclic amines (specifically hydantoin derivatives) to cotton. This linkage involved the coupling of either *N*-methylol-5,5-dimethylhydantoin (MDMH), or *N*,*N*'-dimethylol-5,5-dimethylhydantoin (DMDMH) to O-6 of cellulose within the cotton polymer.[21] While this graft does work, in the case of DMDMH, it requires hydrolysis or elimination of one of the methylol groups before a chloramine can form. Unfortunately, the resulting coupling of both compounds is linked through a hemiaminal, which can hydrolyze or eliminate to form formaldehyde (Figure 7).

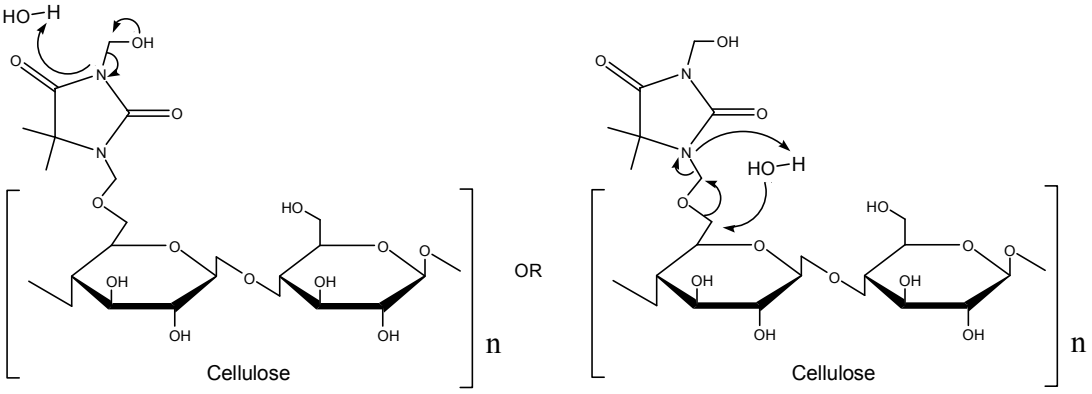

Figure 7. Elimination of formaldehyde from DMDMH

A more stable coupling to O-6 of cellulose, by radical addition of *N*-allyldimethylhydantoin (ADMH), was later developed by Professor Gang Sun at UC Davis.[28-a] Concurrently Professor Worley, *et al*., synthesized 3-(3-triethoxysilylpropyl)-5,5-dimethylhydantoin (BA-1), and demonstrated that it was also capable of grafting to O-6 of cellulose in addition to a variety of other polymers containing hydroxyl groups (Figure 8).[24, 29]

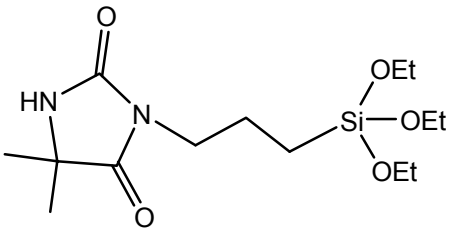

Figure 8. Strucure of BA-1

An easy, scaleable synthetic route to chloramine-forming polymers has distinct advantages over past efforts at chloramine-treated materials, particularly if enough chlorine is present to effectively decontaminate. Given that many of the polymers commonly found in protection systems contain

hydroxyl groups, BA-1 emerges as a good candidate for the synthesis and demonstration of inherently biocidal and CWA-reactive polymers.

I.4. Microwave Chemistry

Microwave chemistry is a rapidly growing area in organic synthesis.[30, 31] This is not surprising considering that microwave-assisted reactions often dramatically increase yields, decrease reaction times, and many times allow for solvent-free reactions. Microwave irradiation is defined as electromagnetic irradiation in the frequency range of 0.3 to 300 GHz. All domestic microwave ovens operate at a frequency of 2.45 GHz (wavelength of 12.24 cm), to avoid interference with telecommunication and cellular phone frequencies.[30] Since the energy of the microwave photon in this frequency region is only 0.0016 eV, which is too low to break chemical bonds, it is generally assumed that microwaves cannot induce chemical reactions based solely on this energy absorption—although this is hotly disputed.[32-37] Consequently, It is generally accepted that microwave-enhanced chemistry is based on the efficient and selective excitation of the materials by microwave dielectric heating effects.[30] This phenomenon is dependent on the ability of a specific material to absorb microwave energy and convert it into heat. The electric component of an electromagnetic field causes heating by two mechanisms, dipolar polarization and ionic conduction. Irradiation of the sample at microwave frequencies results in the dipoles or ions aligning in the applied electric field. As the applied field oscillates, the dipole or ion field attempts to realign itself with the alternating electric field and, in the process, energy is dissipated in the form of heat, through molecular collision and dielectric loss (Figure 9).[38]

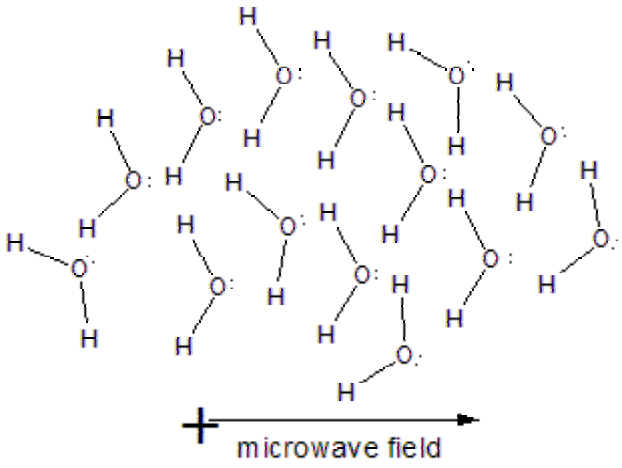

Figure 9. Polarization of Water during Microwave Heating

Microwave heating differs from conventional heating in that in conventional heating, heating occurs through dissipation of energy via molecular collision without organized alignment of dipoles within the substrate (Figure 10).

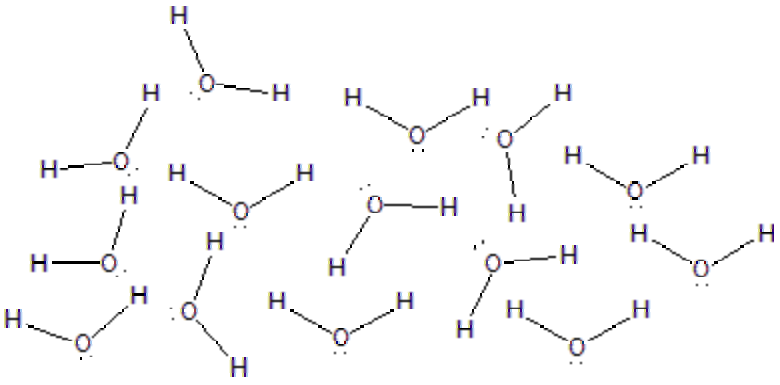

Figure 10. Conventional Heating of Water

The amount of heat generated by microwave heating is directly related to the ability of the matrix to realign itself with the frequency of the applied field; if the dipoles and/or ion pairs do not have enough time to realign, or reorient too quickly with the applied field as it oscillates, no heating occurs.[38] In most

cases, the allocated frequency of 2.45 GHz used in all conventional microwave systems lies between these two extremes and allows the molecular dipole enough time to align in the field, but not enough time to follow the alternating field precisely, thus leading to efficient internal heating of ionic or polar/polarizable materials.

The heating characteristics of a particular material under microwave irradiation conditions are dependent on its dielectric properties. The ability of a specific substance to convert electromagnetic energy into heat at a given frequency and temperature is determined by the loss factor $\tan \delta = \epsilon''/\epsilon'$, where ϵ'' is the dielectric loss, which is indicative of the efficiency with which electromagnetic radiation is converted into heat, and ϵ', which represents the dielectric constant and describes the ability of molecules to be polarized by the electric field.[30] A reaction medium with a high $\tan \delta$ value is required for efficient absorption, which results in rapid heating. In general, solvents can be classified as high ($\tan \delta > 0.5$), medium ($0.1 > \tan \delta > 0.5$), and low ($\tan \delta < 0.1$) microwave absorbing.[30] The loss factors for three solvents used in the microwave graft of silanols, silyl esters, and silyl ethers to various hydroxyl-containing substrates that will be described and discussed in this paper are: ethanol ($\tan \delta = 0.941$), water ($\tan \delta = 0.123$), and acetone ($\tan \delta = 0.054$). Either ethanol or water was used when ambient heating of the solvent was desired and acetone was used when the reaction solvent was used more as a heat sink for the reactants.

Non-thermal effects (NTEs) are other, more controversial mechanisms that may account for some of the results presented in this work. NTEs are defined as phenomena that result from direct interaction of the electric field with specific molecules in the reaction medium.[36] NTEs are considered to be independent of thermal processes, and thus are appropriately named nonthermal effects. The theoretical explanation for NTEs involves consideration of additional charge separation and molecular orientation induced by the electromagnetic field leading to stabilization of reaction intermediates.[33] Unlike conventional heating, the presence of an electric field leads to orientation effects of dipolar molecules without significantly affecting nonpolar molecules, and hence, has the potential to change the frequency at which molecular collisions associated with dipolar molecular species in chemical reactions occur. This phenomenon can create potentially favorable reaction conditions for the facilitation of reactions that would otherwise be kinetically less favored. This is a highly controversial theory that has met with considerable resistance, and it is not the primary focus of this work.

I.5. Hypervalent Silicon

Experiments in this work demonstrate microwave-assisted synthesis of hypervalent silicon compounds. Consequently a brief background of the differing schools of thought surrounding hypervalent silicon compounds is merited. Hypervalent molecules were first defined by Musher as a class of molecules or ions that are formed from elements bound to a greater number of ligands than accommodated by their lowest energy stable valence.[39] He addressed the problem by defining these compounds as having expanded octets. The classic definition of the Valence Shell Electron Pair Repulsion (VSEPR) model states that an atom such as silicon, with valence electrons $3s^2 3p^2$, will form four sp^3 hybridized atomic orbitals to make four σ bonds to four ligands, each with unpaired electrons.[39] To bond to an additional ligand, it is theorized that Si promotes a lower-lying electron into an unoccupied, higher-energy *d*-orbital to form five hybridized orbitals, sp^3d.[39-45]

Many have recognized that this classical definition works well for compounds with normal valencies, but not for hypervalent compounds. This is because promotion of a low-lying *ns* or *np* electron into an *nd*-orbital requires a large amount of excitation energy, making this hybridization energetically unfavorable. Also, in non-metals, *d*-orbitals are highly diffuse and heavily shielded by low lying *s*- and *p*-orbitals, resulting in poor overlap with neighboring atomic orbitals.[46, 47] These difficulties with the theory are often explained by the fact that these hypervalent states are found only when silicon is bound to relatively electronegative ligands compared to silicon. In

this explanation, electronegative ligands, such as oxygen, increase the net positive charge on the silicon and cause compression of the *d*-orbital. These *d*-orbitals that are compressed by the inductive effects from electronegative ligands can then hybridize to form $3sp^3d$- and $3sp^3d^2$-orbitals and participate in σ-bond formation.

With the development of computers able to calculate the possible positions of electrons in small molecules, physicists are now able to judge whether *d*-orbital participation is probable. For hypervalent silane species, calculations do indicate that *d*-orbital populations are existent, but to a small extent.[45, 48] In fact, the populations are so small that the results do not indicate that *d*-orbitals are involved in bond hybridization.[49] While the role of these *d*-orbitals is still under speculation, several theories have so far been presented. The most common argument is that the *d*-orbitals allow for greater polarizability. This explanation is consistent with the ease at which second-row elements polarize in comparison to the first-row elements, the obvious conclusion being that *d*-orbitals behave as polarization functions.[50] A second theory states that the *d*-orbital occupation is the result of *π*-backbonding with ligand lone pairs.[51] Pimentel and Rundle presented yet a third theory, based on reexamining the VSPER model to explain the behavior of hypervalent molecules formed with nonmetallic centers. Their idea presented a new type of bonding behavior, the three–center–four electron bond (3c-4e).[49] A 3c-4e bond is defined as an elongated, linear, electronically delocalized arrangement of two electronegative ligands on a

central atom. 3c-4e bonds are commonly explained as a delocalized σ bond. This type of bonding is usually formed by the overlap of an unhybridized *p*-orbital on the central atom and two terminal ligand orbitals.[46-48, 52-53]

II. EXPERIMENTAL

Methods:

1. M1—*Chlorination procedure*—The material to be charged with chlorine is completely immersed in 0.5 % aqueous sodium hypochlorite solution for 10 minutes if the material is a fabric or powder, 30 minutes if the material is a modified polymer coating. The material is then removed and washed with distilled water until the wash solution tests negative for active chlorine. A negative active chlorine response is determined by the absence of a color change when ~50 mg of potassium iodide and 1.0 mL of starch indicator are added to the wash solution AFTER the material has been removed from the wash solution. Once a negative active chlorine response has been determined, the material is dried at 35 ºC overnight.

2. M2—*Qualitative test method for determining oxidative reactivity for nonporous surfaces*—Solid potassium iodide (50 mg) is placed directly on the test surface. 5 drops of distilled water is added to the potassium iodide and allowed to react for 10 minutes. If no color change is apparent, then one drop of starch indicator is added. A positive test is indicated by the oxidation of iodide to elemental iodine and is detected by a color

change from colorless to yellow–brown in the absence of starch indicator, and blue–black when starch indicator is added.

3. M3—*Qualitative test method for determining oxidative reactivity for porous materials*—Solid potassium iodide (50 mg) is placed in a 20-mL scintillation vial. A 5-mL portion of distilled water is added along with ~100 mg of material to be tested. The solution is allowed to react for 5 minutes. If no color change is apparent, then one drop of starch indicator is added. The test is evaluated as in M2.

4. M4—*Quantitative test method for determining abundance of active chlorine*—All standard method protocols and procedures of *National Environmental Methods Index* method # 4500-Cl B, *Iodometric Method I: Chlorine by Iodometry*, were followed with the following modification: the sample to be tested is added to deionized, chlorine-free water along with glacial acetic acid, as indicated in method 4500-Cl B, and stirred gently at room temperature for 5 minutes.[54] The solution is then titrated with standardized $Na_2S_2O_3$ solution until only a hint of yellow color remains. A 1-mL portion of starch indicator is added and the solution is then titrated to a clear and colorless state. The solution is then allowed to stand for 1 hour and re-titrated to a clear and colorless state. The titration is performed in triplicate on samples from the same batch.

5. M5—*Quantitative test method for reactivity to chemical agent surrogates in solution*—A 100-mg sample of material to be tested is placed in a

3.0-mL sample vial, and 1.0 mL of acetonitrile is added. The vial is capped and sealed with a septum cap and 1.0 μL of surrogate is injected. The vial is then placed on a GC autoinjector shaker table, and agitated throughout the experiment. 1.0 μL samples are taken from the vial and injected into the GC via autoinjector at the specified time intervals. The steady state, time dependent nature of this reaction limits the sample number for each time interval to one.

6. M6—*Semi-quantitative test method for measuring reactivity and permeation of vaporous chemical agent surrogates through a gas-permeable polymeric system*—A 63.5-mm diameter, (31.65 cm^2) material sample disc is placed in a permeation cell. The diameter of the sample test aperture is 3/4 in (3.81 cm), which means the surface area exposed to the challenge is 2.85×10^{-4} m^2. The chemical agent vapor surrogate challenge for a gas-permeable test samples is 1.0 μL. The chemical agent surrogate is deposited into the bottom of the reservoir through the injection port. The system is maintained at 75 ºC throughout the experiment. Zero-air carrier gas is maintained at a constant flow across the opposite side of the test material at a rate of 1.5 L/min, and bubbled into a cold trap containing 100 mL of acetonitrile maintained at a constant temperature of 3 ºC. 1.0 μL of acetonitrile from the cold trap is injected into a GCMS at regular time intervals. The steady state, time dependent

nature of this reaction, limits the sample number for each time interval to one.

7. M7—*Qualitative test method to screen for biocidal efficacy*—American Association of Textile Chemists and Colorists (AATCC) test method 147, *Antibacterial Assessment of Textile Materials: Parallel Streak Method* involves the aseptic transfer of the test material directly onto the surface of inoculated nutrient agar slurries for a specified incubation contact time, after which the test material is removed and any growth, or lack thereof, beneath the test material surface is recorded.[55] Examples of positive (left) and negative (right) tests are shown in Figure 11.

Figure 11. Examples of Positive (left) and Negative (right) AATCC 147 Results

8. M8—*Qualitative test method for determining the biocidal efficacy of hydrophobic surfaces and substrates*—ASTM method E2180-1, *Standard Test for Determining the Activity of Incorporated Antimicrobial Agent(s) in Polymeric or Hydrophobic Materials* involves aseptic transfer of the test material directly onto the surface of inoculated nutrient agar slurries for a

specified incubation contact time series, after which the test material is removed and any growth, or lack thereof, beneath the test material surface is recorded.[56] The test material is then washed to re-suspend nutrient agar plates. The plates are incubated for a specified period of time and the resulting colonies counted. This method reveals contact efficacy times as well as growth trends associated with the test material. Three general trends are meaningful: uninhibited growth, bacteriostasis, and inhibited growth.

9. M9—*Quantitative test method for measuring the biocidal efficacy of textiles*—AATCC method 100, *Antibacterial Finishes on Textile Materials, Assessment of*, involves aseptic transfer of a known concentration of inoculum directly onto the surface of the test material for a specified incubation contact time series.[57] For the test to be valid, the material must absorb all of the inoculum. After each incubation period the test material is removed and washed to resuspend any remaining viable organisms, and the wash solution is serially diluted and plated onto nutrient agar plates. The plates are incubated for a specified period of time and the resulting colonies counted.

10. M10—*Quantitative test method for measuring the biocidal efficacy of immobilized biocides*—As specified in ASTM E2149-01, *Standard Test Method for Determining the Antimicrobial Activity of Immobilized Antimicrobial Agents Under Dynamic Contact Conditions*, a 100-mg

sample of test material is placed in a 250-mL capped Erlenmeyer flask along with a known concentration of test organism.[58] The flask is shaken on a shaker table for an hour, and the solution is then serially diluted onto nutrient agar plates. The plates are incubated overnight and the colonies counted.

11. M11—*Microwave reaction program series*—This program controls the power level and duration of each microwave interval. This program consists of five 30-second intervals, two of which (intervals 2 and 4) are cooling intervals and three periods (intervals 1, 3, 5) wherein the magnetron is engaged. Intervals 1 and 3 operate at 50% power, and interval 5 is conducted at 100% power. Microwave information: CEM MDS-2100, model 924070; 208/230V; 60 Hz; 2400 W max power; 1000 W max output; 2450 MHz magnetron frequency.

II.1—Experiment 1 (E1): *Proof of Concept*

Polystyrene hydantoin (PSH) was chlorinated according to M1, and tested according to M3 and M4. The M3 test yielded a dark black color without the addition of starch indicator. M4 titration yielded titrant values equating to 1.68×10^{-4} mols Cl^+/g, or 5.57 ppt Cl^+. A 100-mg sample of the chlorinated polystyrene hydantoin (PSH-Cl) was tested according to M5 with demeton-S or *O,O*-diethyl *S*-2-ethylthioethyl phosphorothioate (D-S), diisopropyl fluorophosphate (DFP) and 2-chloroethyl ethyl sulfide (CEES). Samples were taken at approximately 15-minute intervals, and the data were plotted.

II.2—Experiment Series 2 (E2): *Synthesis of Biocidal AlO(OH)*

1. (E2.1)— A 1.050-g (10.30 mmol) portion of nanoscale (300 nm mean diameter) boehmite [AlO(OH)] was placed in a 250-mL, three-neck, round-bottom flask to which 35.0 mL of acetone and 5.0 mL of distilled water were added. A water-cooled fractionating column was attached to the middle neck. A 300 ºC mercury thermometer was inserted through a Teflon™ stopper in a second neck for monitoring headspace vapor temperature. The third neck was fitted with a one-holed rubber stopper fitted with a 50.0-mL volumetric pipette. A 1.642-g (4.946 mmol) portion of 3-(3-triethoxysilylpropyl)-5,5-dimethylhydantoin (BA-1), provided by the Worley group, was dissolved in 10.0 mL of acetone and added to the volumetric pipette. The solution in the round-bottom was brought to a boil, whereupon the solution of BA-1 was added dropwise at a rate of ~5 drops/minute over a 60-minute time period. After addition of the solution was complete, the mixture was allowed to reflux for two hours. The solution was then refrigerated at 5 ºC in a standard-taper-stopper-sealed container overnight. The clear, colorless liquid top layer was decanted, and the fine white powder sediment was washed via vacuum filtration twice with 5.0-mL portions of chilled acetone and twice with 5-mL portions of distilled water. The sediment was then dried at 35 ºC for 48 hours. A finely divided white powder (E2P1, 782 mg) was collected upon drying. *note: significant loss of product during the sediment washing.*

The product was chlorinated according to M1 and then tested according to M3, which yielded no color change with no indicator, but a faint purple tint after the indicator was added.

2. (E2.2) —Following the procedure of E2.1, 1.002 g (9.829 mmol) of boehmite was placed in a 250-mL three-neck round-bottom flask, and absolute ethanol (35.0 mL) and distilled water (5.0 mL) were added. The *p*H of the solution was then adjusted to 4.5 with 0.10 *M* HCl, and 1.667 g (5.021 mmol) of BA-1 was dissolved in 10.0 mL absolute ethanol, and added to the volumetric pipette and delivered under reflux. After the addition of BA-1 was complete, the mixture was allowed to reflux for 2 h and worked up to yield a clear and slightly yellow top layer that was decanted, and a slightly gray “gel” sediment that was washed twice with acetone, and twice with distilled water before drying at 35 ºC for 48 hours.
   *Note: significant loss of product during the sediment washing. *
   The resulting, finely divided, white, powdery product (990 mg, E2P2) was chlorinated according to M1 and then tested according to M3, which yielded an immediate dark yellow–brown color in the absence of indicator. Elemental analysis: 2.31% C; 0.61% N. FTIR (diamond single point ATR): strong broad band 556–909 cm^{-1}; sharp, strong bands at 1072 and 1098 cm^{-1}; sharp, strong band at 1708 cm^{-1}; sharp, weak band at 1774 cm^{-1}; weak bands at 2976 and 2874 cm^{-1}.

3. (E2.3)—Procedure E2.1 was repeated with 1.022 g (10.03 mmol) boehmite and 1.729 g (5.208 mmol) BA-1, with the exception that the *p*H of the solution was adjusted to 9.0 using 0.50 *M* KOH solution. The reaction and workup yielded a finely divided white powder (790 mg, E2P3) collected upon drying. E2P3 was chlorinated according to M1 and tested according to M3, which yielded a medium yellow color with no indicator and a dark purple–black with the indicator. Elemental analysis: 1.64% C; 0.40% N. FTIR (diamond single point ATR) strong broad band between 561–900 cm^{-1}; sharp, strong bands at 1071 and 1081 cm^{-1}; sharp, strong band at 1713 cm^{-1}; sharp, weak band at 1768 cm^{-1}; weak bands at 2976 and 2877 cm^{-1}.

4. (E2.4)—The steps of E2.3 were repeated using 1.054 g (10.34 mmol) boehmite and 1.670 g (5.030 mmol) of BA-1, with the exception that the *p*H of the solution was adjusted to 9.0 5% (wt/wt) aqueous solution of sodium hypochlorite. The experiment yielded a clear and slightly yellow liquid top layer that was decanted and a finely divided white powder (1.075 g, E2P4) after washing and drying. E2P4 was chlorinated according to M1 and tested according to M3, which yielded an immediate dark yellow–brown color with no indicator. Elemental analysis: 2.48% C; 0.65% N. FTIR (diamond single point ATR) strong broad band ~500–910 ~cm^{-1}; sharp, strong bands at ~1070 and ~1100 cm^{-1}; sharp, strong band at ~1710 cm^{-1}; sharp, weak band at ~1770 cm^{-1}; weak bands at ~2980 and ~2870 cm^{-1}.

5. (E2.5)—1.010 g boehmite (9.908 mmol) was placed in a 20.0-mL scintillation vial, to which 5.0 mL acetone and 0.5 mL 0.5% aqueous sodium hypochlorite were added, before 1.028 g (3.096 mmol) of BA-1 was added all at once. The unsealed reaction mixture was mixed thoroughly, then irradiated in a conventional microwave oven at full power for three one-minute intervals, and allowed to cool to room temperature between successive intervals. Additional acetone was added between intervals if the reaction mixture was "dry." The reaction mixture was then irradiated in the microwave at full power for three minutes to drive off any remaining solvent. The finely divided, dark-brown "powder" sediment was washed as in E2.1–2.4, with significant loss of product, to yield a dark brown powder product (1.023 mg, E2P5) after drying. The product was chlorinated according to M1 and then tested according to M3, which yielded an immediate dark yellow–brown color with no indicator. FTIR (diamond single point ATR): strong broad band ~500–910 ~cm^{-1}; sharp, strong absorbance bands at ~1070 and ~1100 cm^{-1}; sharp, strong band at ~1710 cm^{-1}; sharp, weak band at ~1770 cm^{-1}; weak bands at ~2980 and ~2870 cm^{-1}.

6. (E2.6)—A 20.0-mL scintillation vial was charged with 1.021 g (10.02 mmol) of boehmite, and a mixture of 5.0 mL of ethanol, 10 drops of 0.5% aqueous sodium hypochlorite, and 1.003 g BA-1 (3.021 mmol) was added all at once. The unsealed reaction mixture was mixed thoroughly, and then irradiated in a conventional microwave oven at

full power for three one-minute intervals. The mixture was allowed to cool to room temperature between heating intervals, and additional ethanol was added if the reaction mixture was “dry”. The reaction mixture was then irradiated in the microwave at full power for three minutes to remove remaining solvent. The finely divided white “powder” sediment was washed on a vacuum filter twice with 5.0-mL portions of chilled acetone and twice with 5.0-mL portions of distilled water before being dried at 35 ºC for 48 hours to yield a finely divided white powder (1.014 g, E2P6).

Note: significant loss of product during the sediment washing.

The product was chlorinated according to M1 and tested according to M3, which yielded an immediate dark yellow–brown color with no indicator. Elemental analysis: 3.06% C; 0.97% N. FTIR (diamond single point ATR) strong, broad band ~500–910 ~cm^{-1}; sharp, strong bands ~1070 and ~1100 cm^{-1}; sharp, strong band at ~1710 cm^{-1}; sharp, weak band at ~1770 cm^{-1}; weak bands at ~2980 and ~2870 cm^{-1}.

7. (E2.7)—The procedure of E2.6 was repeated with 1.064 g (10.44 mmol) boehmite and 990 mg BA-1 (2.982 mmol) with the exception that 10 drops 0.1 molar hydrochloric acid were added instead of hypochorite. The experiment yielded a finely divided white powder (992 mg E2P7). The product was chlorinated according to M1 and

then tested according to M3, which yielded a faint yellow color with no indicator and a medium purple color with starch indicator.

8. (E2.8)—The procedure of E2.6 was repeated with 1.083 g (10.62 mmol) boehmite and 1.001 g of BA-1 (3.015 mmol), with the exception that the 10 drop 0.50 *M* KOH solution were added. The reaction yielded a finely divided white powder (1.091 g, E2P8). The product was chlorinated according to M1 and then tested according to M3, which yielded an immediate dark yellow–brown color with no indicator. Elemental analysis: 3.0% C; 0.91% N. E2P8 was evaluated for biocidal efficacy in solution according to M10 against *Staphylococcus aureus*, *Klebsiella pneumoniae*, and *Aspergillus niger*. E2P8 was evaluated for efficacy against chemical warfare agent surrogates according to M5. FTIR (diamond single point ATR) strong broad band ~500–910 ~cm^{-1}; sharp, strong bands at ~1070 and ~1100 cm^{-1}; sharp, strong band at ~1710 cm^{-1}; sharp, weak band at ~1770 cm^{-1}; weak bands at ~2980 and ~2870 cm^{-1}.

9. (E2.9)—The procedure of E2.6 was repeated, except that acetone was used as the solvent, and no hypochlorite was added. To the acetone, 1.057 g (10.37 mmol) boehmite and 1.003 g BA-1 (3.021 mmol) were added. A fine white powder (1.080 g) was collected upon drying (E2P9), chlorinated according to M1 and then tested according to M3, which yielded a dark yellow color with no indicator. Elemental

analysis: 2.41% C; 0.66% N. FTIR (diamond single point ATR) strong broad band ~500–910 ~cm^{-1}; sharp, strong absorbance bands at ~1070 and ~1100 cm^{-1}; sharp, strong band at ~1710 cm^{-1}; sharp, weak band at ~1770 cm^{-1}; weak bands at ~2980 and ~2870 cm^{-1}.

10. (E2.10)—A solution of 25.00 g BA-1 (75.30 mmol) and 100 mL absolute ethanol was added to 52.18 g (511.9 mmol) boehmite in a 500-mL beaker. After the mixture was mixed thoroughly with a metal spatula, 10.0 mL of 0.5 M aqueous sodium hydroxide solution was added with continued stirring. The reaction mixture was then divided equally into four 100-mL microwave acid digestion vessels and irradiated with microwaves in a microwave reactor in the open vessels according to M11 for two cycles. The resulting product was washed and separated by centrifugation twice with chilled acetone and twice with distilled water, then dried at 35 ºC for 48 hours to yield a finely divided white powder (54.77 g, E2P10). E2P10 was chlorinated according to M1 and tested according to M3, which yielded a black color with no indicator. Elemental analysis: 9.36% C; 2.95% N. E2P10 was evaluated for biocidal efficacy in solution according to M10 against *S. aureus*, *B. atrophaeus* spores, and *A. niger*. FTIR (diamond single point ATR) strong broad band ~500–910 ~cm^{-1}; sharp, strong absorbance bands at ~1070 and ~1100 cm^{-1}; sharp, strong band at ~1710 cm^{-1}; sharp, weak band at ~1770 cm^{-1}; weak bands at ~2980 and ~2870 cm^{-1}.

11. (E2.11)—The procedure of E2.10 was repeated with 52.01 g (510.2 mmol) of boehmite and 25.00 g of [3-(trimethoxysilyl)propyl]octadecyldimethylammonium chloride (QAC-1, Aldrich), (50 mmol) delivered in a mixture of 72% QAC-1, 13% methanol and 15% 3-chloropropyltrimethoxysilane to yield a finely divided white powder (57.81 g E2P11). Elemental analysis: 15.94% C; 1.10% N. E2P11 was evaluated for biocidal efficacy in solution according to M10 against *S. aureus*, *B. atrophaeus* spores, and *A. niger*. FTIR (diamond single point ATR) strong broad band at ~500–940 ~cm^{-1}; broad strong bands ~990–1130 cm^{-1}; sharp, strong bands at ~1480, ~2930 and ~2870 cm^{-1}.

II.3—Experiment Series 3 (E3): *Fabric Treatments*—

Four wash solutions were prepared:

Wash I—336 mg of BA-1 (Auburn) were dissolved in 10.0 mL absolute ethanol in a 20.0-mL scintillation vial. The vial was capped when not in use, to prevent evaporation of the solvent.

Wash II—In a 20.0-mL scintillation vial, 332 mg of BA-1 (Auburn) were dissolved in 10.0 mL of absolute ethanol, 2.0 mL of distilled water and 0.5 mL of 10% HCl, and mixed thoroughly by capping and shaking the mixture. The vial was capped when not in use to prevent evaporation of the solvent.

Wash III—In a 20.0-mL scintillation vial 334 mg of BA-1 (Auburn) were dissolved in 10.0 mL of acetone. The vial was capped when not in use, to prevent evaporation of the solvent.

Wash IV—In a 20.0-mL scintillation vial 332 mg of BA-1 (Auburn) were dissolved in 10.0 mL of absolute ethanol and 2.0 mL 0.50 % sodium hypochlorite solution were added and mixed thoroughly by capping and shaking the mixture. The vial was capped when not in use, to prevent evaporation of the solvent.

1. (E3.1)—Individual 300-mg (± 5 mg) squares of 50:50 nylon–cotton Battle Dress Uniform (BDU) fabric samples, provided by Natick Soldier Center, were dipped to saturation in one of the wash solutions I–IV and irradiated in a conventional microwave oven at the highest power

setting (760 W) in a Teflon™ vessel for three one-minute intervals. Each sample was allowed to cool and was turned between intervals. Each BDU sample was then washed consecutively with two 5.0-mL portions of chilled acetone and with two 5.0-mL portions of distilled water before drying at 35 ºC overnight to produce fabric samples (E3P1.1)– (E3P1.4) from Wash I–IV, respectively. The dried samples were chlorinated according to method M1, cut into three approximately equal sample sizes, and titrated according to M4 using 2.527×10^{-4} *N* $Na_2S_2O_3$ solution.

2. (E3.2)—The procedure of E3.1 was repeated with 300-mg (± 5 mg) squares of BDU fabric, except that the dipping-and-microwaving sequence was repeated four times before workup and chlorination, to produce fabric samples (E3P2.1)–(E3P2.2) from Wash I–IV, respectively.

3. (E3.3)—The procedure of E3.1 was repeated with 300-mg (± 5 mg) squares of BDU fabric, except that microwave irradiation was applied for two three-minute intervals, to produce fabric samples (E3P3.1)–(E3P3.4) from Wash I–IV, respectively.

4. (E3.4)—The procedure of E3.1 was repeated with 300 mg (± 5 mg) squares of BDU, except that no microwave irradiation was applied, to produce fabric samples (E3P4.1)–(E3P4.4) from Wash I–IV, respectively.

5. (E3.5)—The procedure of E3.4 was repeated with 300 mg (± 5 mg) squares of BDU, except that the dipped fabric samples were placed in a 75 ºC oven overnight, to produce fabric samples (E3P5.1)–(E3P5.4) from Wash I–IV, respectively.

II.4—Experimental Series 4 (E4): *Fabric Treatment Down-select and Enhancement*—

1. (E4.1)—A solution containing 20% wt/wt of QAC-1 or BA-1, or 10% wt/wt of 2,4-dioxo-7,7,9,9-tetramethyl-3-(3-triethoxysilylpropyl)-3,8-diazaspirobicyclo[5.4]decane (TTDD, Auburn) was prepared in 5:1 acetone–water containing 1.0 mL/L of Triton 100 surfactant. Twelve-inch squares of 50:50 nylon–cotton BDU material were saturated with this solution, wrung dry, and irradiated with microwaves in a conventional microwave oven on the highest setting for two minutes on a half-inch Teflon™ plate. This saturate-and-microwave cycle was performed a total of three times, after which the material cooled and was irradiated with microwaves for three additional two-minute intervals, with cooling between heating intervals. The material was then washed thoroughly with tap water and an available surfactant (Ajax™ dish soap), and the chloramine-forming products in fabric samples E4P1.1–E4P3.1 (from BA-1 and TTDD, respectively) were chlorinated according to M1 and titrated for active chlorine content according to M4.

2. (E4.2)—Identical to E4.1, except that before each saturation step the dry fabric sample was shaken in a 1-gal bag containing nanoscale (300 nm mean diameter) boehmite (Sasol, Puralox) to produce fabric samples (E4P1.2)–(E4P3.2) from the respective silanes.

3. (E4.3)—Identical to E4.1, except that in lieu of microwave heating the materials were dried in a 75 ºC oven for one hour between saturations and then cured at 75 ºC for 18 hours to produce fabric samples (E4P1.3)– (E4P3.3) from the respective silanes.

   Each of the products from series E4P1 and series E4P3 were chlorinated according to M1 and evaluated for efficacy against chemical agent surrogates according to M6 using CEES (5), D-S (7) and DFP (6).

   The products from E4 were evaluated for biocidal efficacy according to M9 against *S. aureus*, *B. anthracis* spores (Sterne strain), MS-2 coli phage, and *A. niger* spores.

II.5—Experimental Series 5 (E5): *Durability*

1. (E5.1)—Products E2P1,3,4, and 7–9 were evaluated for heat stability during a six-month period. Samples were chlorinated according to M1, weighed, and divided three ways equally. One set was kept at room temperature; the others were kept at 50 °C and 75 °C, respectively, inside dark enclosures. Triplicate samples from each temperature set were titrated at time zero, 1 day, 30 days, 90 days, 120 days and 180 days according to M4.

2. (E5.2)—A sample of each chloramine-forming product from E4 was cut into 4-inch squares, which were placed in separate netted laundry bags. The samples were washed in a Kenmore washer on a setting of permanent press 6 (regular), medium water load, cold water wash and rinse, with 1/3 cup of All® hypoallergenic, chlorine-free detergent. A sample from each product group was removed, air dried, and titrated according to M4. The washing process was repeated with the remaining samples except that during the rinse cycle 1/2 cup household chlorine bleach (5.25% NaOCl) was added. These samples were then put through an additional rinse cycle and dried in a Kenmore dryer on permanent press, high heat for 20 minutes. Representative samples from each product group were then titrated according to M4.

3. (E5.3)—A sample of each chloramine-forming product from E4 was cut into nine one-inch squares. The nine samples from each product

group were added to a separate beaker of boiling distilled water all at once. Triplicate samples from each product group were removed from the boiling water at time intervals of 15 min, 30 min, and 60 min, and titrated according to M4. The samples were *not* rechlorinated prior to titrating. Samples E4P1.2 and E4P3.2 contained a powdery white residue after boiling. The white residue was tested according to M2, E4P1.2 yielding dark yellow and E4P3.2 faint yellow color.

4. (E5.4) A sample of each chloramine-forming product from E4 was cut into three one-inch squares, placed in separate 250-mL beakers, and autoclaved for 15 minutes at 121 °C and 19 psi. Triplicate samples from each product group were removed and titrated according to M4.

5. (E5.5) A sample of each chloramine-forming product from E4 was cut into 24 one-inch squares and irradiated with UV light at 312 nm on a FBDLT-88 Transilluminator (Fisher Scientific) under ambient conditions. Triplicate samples from each product group were removed and titrated according to M4 at each time interval: time zero, 15 min, 30 min, 60 min, 120 min, 4 hrs, 8 hrs, and 24 hrs. The 24-hour samples were then rechlorinated according to M1 and titrated.

6. (E5.6)—A sample of each chloramine-forming product from E4 was cut into 21 one-inch squares. The squares were attached to a 3-ft x 3-ft plywood board using straight pins. The board was placed on the rooftop of a building at Tyndall Air Force Base, Florida, May 3,

2005. Triplicate samples from each product group were removed and titrated according to M4 at each time interval: time zero, 1 day, 3 days, 7 days, 14 days, 22 days, and 30 days. Local weather, including UV index, high temperature, humidity, and cloud conditions were monitored on a daily basis at http://www.accuweather.com/forecast-current-conditions and recorded. The samples were then rechlorinated according to M1 and titrated.

II.6—Experimental Series 6 (E6): *Utility of Microwave Graft*

(E6.1)—*Siloxane Reactivity*—

1. (E6.1.1)—1.0 mmol of octadecyltrimethoxysilane was delivered (Sigma–Aldrich, 90 % pure), (417 mg)] to 3.0 mL acetone. The acetone solution was added all at once to 9.7 mmol (9.9 g) nanoscale (300 nm mean diameter) boehmite (Sasol) in a 100-mL microwave acid digestion vessel. Distilled water (1.0 mL) was added, and the contents mixed thoroughly with a glass rod and irradiated with microwaves in a sealed vessel according to M11 for one cycle, then in an open vessel, according to M11, for three cycles. The resulting product was washed and separated via centrifugation twice with 5.0-mL portions of chilled acetone and twice with 5.0-mL portions of distilled water, and dried at 35 ºC for 48 hours to yield 1.076 g fine white powder (E6P1.1). Elemental Analysis: 1.988% C; 0.002% N (*n*=4). FTIR (diamond single point ATR): strong broad band ~550–910 cm^{-1}; sharp, strong bands at ~1090, ~1190, ~2860 and ~2950 cm^{-1}. E6P1.1 was compared to positive and negative controls. The positive control consisted of elemental analysis and FTIR diamond ATR of boehmite treated with the siloxane and then washed in a similar manner as the reaction products. The negative control consisted of the elemental analysis and FTIR diamond ATR of the neat boehmite washed in the same manner as the reaction products.

Negative control Elemental Analysis: 0.106% C; 0.082% N (*n*=3). Results from negative control elemental analysis were subtracted from elemental analysis values of reaction products. All positive controls were consistent within 5% of negative control values (*n*=3).

2. (E6.1.2)—E6.1.1 was repeated with 1.008 g (9.888 mmol) boehmite plus 210 mg (1.1 mmol) of methoxydimethyloctylsilane, (Aldrich, 98 % pure, b.p. 221 ºC) to yield 1.010 g fine white powder upon drying (E6P1.2). Elemental Analysis: 1.274% C; 0.000% N (*n*=3). FTIR (diamond single point ATR): strong broad m band m ~550–910 cm^{-1}; faint absorbance bands at ~1090, 1260, and 2930 cm^{-1}.*Note: spectrum enhancement algorithm required for FTIR detection.*

3. (E6.1.3)—E6.1.1 was repeated with 1.000 g (9.810 mmol) boehmite plus 180 mg (1.0 mmol) of triisopropylsilanol (Sigma–Aldrich, 98 % pure, b.p.196 ºC) to yield 1.010 g fine white powder upon drying (E6P1.3). Elemental Analysis: 1.124% C; 0.000% N (*n*=6). FTIR (diamond single point ATR): strong broad band ~550-910 cm^{-1}; faint bands at ~1470, 2860, and 2940 cm^{-1}; *Note: spectrum enhancement algorithm required for FTIR detection.

4. (E6.1.4)—E6.1.1 was repeated with 1.003 g (9.839 mmol) boehmite plus 150 mg (1.1 mmol) of potassium trimethylsilanolate (Sigma–Aldrich, 90 % pure, b.p. >100 ºC); 0.987 g fine white powder was collected upon drying (E6P1.4). Elemental Analysis: 0.157% C;

0.001% N (*n*=6). FTIR (diamond single point ATR): strong broad between ~550–910 cm^{-1}.

5. (E6.1.5)—E6.1.1 was repeated with 1.001 g (9.820 mmol) boehmite plus 250 mg (1.1 mmol) of (3-chloropropyl)triethoxysilane (Aldrich, 95 % pure, b.p. <100 ºC), except that only one cycle of irradiation was performed in the open reactor, to yield 1.011 g fine white powder collected upon drying (E6P1.5). Elemental Analysis: 0.473% C; 0.000% N (*n*=4). FTIR (diamond single point ATR): strong absorbance between ~550–910 cm^{-1}; strong, sharp bands at 1040 and 1100 cm^{-1}; weak, sharp bands at 1240, 1270, 1310, 1440, and 2930 cm^{-1}.

6. (E6.1.6)—E6.1.5 was repeated with 1.002 g (9.829 mmol) boehmite plus 190 mg (1.0 mmol) of (3-chloropropyl)dimethoxymethylsilane (Sigma–Aldrich, 99 % pure, b.p.70 ºC) to yield 0.987 g fine white powder collected upon drying (E6P1.6). Elemental Analysis: 0.581% C; 0.000% N (*n*=3). FTIR (diamond single point ATR): strong absorbance between ~550–910 cm^{-1}

7. (E6.1.7)—E6.1.1 was repeated with 1.001 g (9.820mmol) boehmite plus 230 mg (1.0 mmol) of 3-aminopropyltriethoxysilane (Sigma–Aldrich, 99 % pure, b.p. 213 ºC) to yield 1.096 g fine white powder collected upon drying (E6P1.7). Elemental Analysis: 0.565% C; 1.827% N (*n*=8). FTIR (diamond single point ATR): strong

absorbance bands at ~950, 1000, 1020, 1080, 1110, 1130, 3740, and 3750 cm^{-1}.

8. (E6.1.8)—E6.1.1 was repeated with 1.005 g (9.859 mmol) boehmite plus 290 mg (1.1 mmol) of *N*-[3-(trimethoxysilyl)propyl]ethylenediamine (Sigma–Aldrich, 80 % pure, b.p. 146 ºC) to yield 0.998 g fine white powder collected upon drying (E6P1.8). Elemental Analysis: 0.723% C; 1.175% N (*n*=8). FTIR (diamond single point ATR): strong absorbance band at ~550–950 cm^{-1}; strong sharp bands at ~1000 and ~1100 cm^{-1}; broad, weak bands from 1450–1650, 2850–2950 and 3200–3350 cm^{-1}; sharp weak absorbance at 3750 cm^{-1}.

9. (E6.1.9)—E6.1.1 was repeated with 1.001 g (9.820 mmol) boehmite plus 270 mg (1.1 mmol) of 3-(trimethoxysilyl)-propylmethacrylate (Sigma–Aldrich, 98 % pure, b.p. 190 ºC) to yield 1.007 g fine white powder collected upon drying (E6P1.9). Elemental Analysis: 1.112% C; 0.000% N (*n*=6). FTIR (diamond single point ATR): strong broad band at ~550–950 cm^{-1}; weak absorbance bands at 1010, 1170, 1310, 1340, 1650, and 1720 cm^{-1}.

10. (E6.1.10)—E6.1.1 was repeated with 1.010 g (9.908 mmol) boehmite plus 280 mg (1.2 mmol) of 3-glycidoxypropyltrimethoxysilane (Sigma–Aldrich, 98 % pure, b.p. 260 ºC) to yield 1.021 g fine white powder collected upon drying (E6P1.10). Elemental Analysis: 1.07% C; 0.000% N (*n*=6). FTIR (diamond single point ATR): strong broad band

at ~550–950 cm^{-1}; sharp bands at 1040, 1060, 1100, 2870 and 2940 cm^{-1}.

11. (E6.1.11)—E6.1.5 was repeated with 1.003 g (9.839 mmol) boehmite and 566 mg (1.0 mmol) of 3,3,4,4,5,5,6,6,7,7,8,8,9,9,10,10,10-heptadecafluorodecyltrimethoxysilane (SynQuest, 93%, 83 ºC b.p.) to yield 1.088 g fine white powder collected upon drying (E6P1.11). FTIR (diamond single point ATR): strong broad band at ~550–970 cm^{-1}; strong, sharp bands at 1070, 1110, 1150, 1200, and 1240 cm^{-1}.

(E6.2)—*Substrate Reactivity*—

1. (E6.2.1)—A solution of 333 mg (1.00mmol) BA-1 (GFS) in 3.0 mL absolute ethanol and 1.0 mL of 0.5 *M* aqueous KOH was added to 1.00 g of substrate (activated alumina) in a 100-mL microwave acid digestion vessel . After thorough mixing with a glass rod, the reaction mixture was irradiated with microwaves in an open vessel according to M11 for two cycles. The resulting product was washed and separated via centrifugation twice with 5.0-mL portions of chilled acetone and twice with 5.0-mL portions of distilled water. The product (E6P2.1) was dried at 35 ºC for 48 hours, chlorinated according to M1, and qualitatively tested for reactivity according to M3 to give a light yellow color that turned dark blue upon addition of starch indicator.

2. (E6.2.2)—E6.2.1 was repeated with 1.00 g SiO_2 (silica gel, grade 12, 28–200 mesh, Aldrich), and 332 mg BA-1. The white, powdery product (E6P2.2) tested light yellow, dark blue with indicator.

3. (E6.2.3)—E6.2.1 was repeated with 1.18 g 4-mm borosilicate glass beads (Fisher) and 335 mg BA-1. The treated beads (E6P2.3) tested yellow; black with indicator.

4. (E6.2.4)—E6.2.1 was repeated with 1.00 g TiO_2 , 60 mesh (Aldrich), and 332 mg BA-1. The white, powdery product (E6P2.4) tested dark yellow.

5. (E6.2.5)—E6.2.1 was repeated with 1.08 g $Mg_3SiO_{10}(OH)_2$ (talc, Aldrich) and 331 mg BA-1. The white, powdery product (E6P2.5) tested light yellow, dark blue with indicator.

6. (E6.2.6)—E6.2.1 was repeated with 1.00 g $CaAl_2O_{10}(OH)_2$ (montmorillonite) and 332 mg BA-1. The resulting powder(E6P2.6) tested dark brown.

7. (E6.2.7)—E6.2.1 was repeated with 1.03 g $Al_2\,Si_2O_5(OH)_4$ (kaolinite) and 334 mg BA-1. The white, powdery product (E6P2.7) tested dark brown.

8. (E6.2.8)—E6.2.1 was repeated with 1.08 g $(Mg_2,Fe_2^{++},Al_4)_3Si_4O_{10}(OH)_2 \cdot 4(H_2O)$, (vermiculite, Aldrich) and 335 mg BA-1. The product (E6P2.8) tested dark brown.

9. (E6.2.9)—E6.2.1 was repeated with 1.01 g $(Na_{16})(Al_{16}Si_{24}O_{80}) \cdot 16H_2O$ (zeolite molecular sieves, 13X, 3060 mesh, F&M Scientific) and 331 mg BA-1. The white, powdery product (E6P2.9) tested dark brown.

10. (E6.2.10)—E6.2.1 was repeated with 1.09 g 100% cotton fabric and 332 mg BA-1. The treated fabric (E6P2.10) tested dark brown.

11. (E6.2.11)—E6.2.1 was repeated with 1.08 g raw wool and 332 mg BA-1. The treated fabric (E6P2.11) tested light yellow.

12. - (E6.2.12)—E6.2.1 was repeated with 1.13 g cured cowhide leather and 333 mg BA-1. The treated leather (E6P2.12) tested dark yellow.

13. (E6.2.13)—E6.2.1 was repeated with 1.03 g commercial nylon hosiery (Leggs™) and 332 mg BA-1. The treated fabric (E6P2.13) displayed no color change even with starch indicator.

14. (E6.2.14)—E6.2.1 was repeated with 1.11 g hydroentangled hydroxyl-terminated nylon and 332 mg BA-1. The treated fabric (E6P2.14) tested dark yellow.

II.7—Experimental Series 7 (E7): *Model Monomer Synthesis*—

1. (E7.1)—BA-1 (338 mg, 1.02 mmol) was dissolved in 2.0 mL acetone. Methyl α-D-glucopyranoside (αMG, 199 mg, 1.03 mmol) was added to the solution, and 0.6 mL distilled water was added dropwise, with stirring, to dissolve the sugar. The reaction mixture was transferred to a 100-mL Teflon™ microwave reaction vessel and irradiated with microwaves for three cycles of M11 in an open-cup reactor. The reaction vessel was cooled to -5 °C before opening, to yield 362 mg of clear, pale yellow, glass-like solid (E7P1), insoluble in acetone, ethanol and water. Melting point: 147–169 °C; FTIR (diamond single point ATR): sharp bands at 1050–1100 cm^{-1}, 1640–1690, 1680–1755 and 1745–1795 cm^{-1}; broad weak band at 3140–3400 cm^{-1}. A portion (10 mg) was finely ground, chlorinated according to M1, and tested according to M3, showing a yellow color without indicator, dark blue to black with indicator.

2. (E7.2)—The procedure of E7.1 was repeated with 198 mg (1.02 mmol) αMG, 198 mg BA-1, 5.0 mL acetone and 0.4 mL water, applying only one cycle of M11 in the open-cup reactor, to yield 301 mg of the same clear, pale–yellow glass E7P2. Melting point: 149–170 °C; FTIR (diamond single point ATR) sharp bands at 1050–1100, 1645–1690, 1680–1755 and 1745–1790 cm^{-1}; broad weak band at 3140–3400 cm^{-1}; insoluble in acetone, ethanol, water. Grinding and chlorination of

~10 mg of product according to M1 and testing according to M3 yielded the same yellow and dark blue to black colors.

3. (E7.3)—The procedure of E7.2 was repeated with a solution of 198 mg (1.02 mmol) αMG in 5.0 mL acetone and 0.4 mL water in a 100-mL Teflon™ microwave reaction vessel, except that 225 mg of 3-aminopropyltriethoxysilane (APS) was added in two-drop portions to produce, after irradiation, a clear, pale yellow, glass-like solid (E7P3). Melting point: 152–173 °C; FTIR (diamond single point ATR): sharp band at 1045–1085 cm^{-1}; two distinct broad bands at 3000–3140 and 3225–3370 cm^{-1}; broad weak band at 3140–3400 cm^{-1}; insoluble in acetone, ethanol and water.

4. (E7.4)—In a 100-mL Teflon™ microwave reaction vessel, 214 mg of glycerol (2.32 mmol) was dissolved in 10 mL of 95% ethanol, and 1.0 mL 0.1 *M* NaOH (aq) solution was added. BA-1 (661 mg) was added in two-drop portions between 30-sec microwave irradiations in a closed-cup reaction until all the BA-1 was added (4 X 30s). The mixture was irradiated with microwaves for one cycle of M11 in an open-cup reaction and the vessel was cooled to -5 °C before opening to yield a clear, pale yellow–orange, soft solid (E7P4). FTIR (diamond single point ATR): sharp bands at 1040–1100, 1630–1690, 1660–1750 and 1745–1800 cm^{-1}; broad band at 3180–3300 cm^{-1}. Chlorination of ~10 mg of product according to M1 and testing according to M3

showed a yellow color without indicator, dark blue to black with indicator.

5. (E7.5)—APS (2.257 g, 10.21 mmol) was added to 1.063 g glycerol (11.55 mmol) all at once and irradiated with microwaves in a sealed 100-mL Teflon™ microwave reaction vessel under argon for three cycles of M11. The sealed reaction vessel was then cooled to -5 °C before opening to yield a hard, slightly yellow, clear, glass (E7P5). FTIR (diamond single point ATR): three strong sharp overlapping bands, 990–1150 cm^{-1}; multiple sharp, strong bands, 1320–1480 cm^{-1}; broad strong band, 1580–1620 cm^{-1}; three sharp, strong bands at 2860, 2930, and 2970 cm^{-1}; two strong overlapping absorbencies, 3170–3580 cm^{-1}.

6. (E7.6)—The procedure of E7.5 was repeated with 2.232 g. (10.10 mmol) APS and 1.040 g glycerol (11.29 mmol), except that 1.0 mL 10% HCl (aq) was added to the reaction mixture. The resulting light brown, clear, highly porous solid (E7P6) ws identical to E7P5.

7. (E7.7)—The procedure of E7.5 was repeated with 2.229 g (10.09 mmol) APS and 1.079 g glycerol (11.72 mmol), except that 1.0 mL 10% NaOH (aq) was added to the reaction mixture. The resulting light brown, clear, highly porous solid (E7P7) possessed identical properties to E7P5.

8. (E7.8)—The procedure of E7.5 was repeated with 2.208 g (9.991 mmol) APS and 1.056 g glycerol (11.47 mmol), except that 1.0 mL 0.5 % NaOCl (aq) was added to the reaction mixture. The resulting light brown, clear, highly porous solid (E7P8) possessed identical properties to E7P5.

9. (E7.9)— Ethylene glycol (930 mg, 15.0 mmol) was dissolved in 50 mL 95% ethanol. APS (2.217 g, 10.03 mmol) was added all at once and the reaction mixture was irradiated with microwaves in a sealed, 100-mL Teflon™ microwave reaction vessel for four intervals of M11. The sealed reaction vessel was cooled to -5 °C before opening. Sparse, white, opaque, needle-like crystals were observed in a clear colorless liquid, but the crystals turned into a clear, colorless, oil upon contact with air. The liquid was concentrated overnight in a rotary evaporator under vacuum at 75 °C, yielding a clear, viscous, slightly yellow oil (E7P9). FTIR (diamond single point ATR): three strong, overlapping bands, 990–1150 cm^{-1}; multiple sharp, strong bands, 1320–1480 cm^{-1}; broad strong band, 1580– 1620 cm^{-1}; sharp strong bands at 2870 and 2930 cm^{-1}; two strong overlapping bands, 3170–3580 cm^{-1}.

10. (E7.10)—Ethylene glycol (965 mg, 15.6 mmol) was dissolved in 10 mL 95% ethanol and 2.214 g APS (10.02 mmol) was added all at once. The *p*H was adjusted to 6.21 with 10% HCl (aq.) before the reaction

mixture was irradiated with microwaves in an open 100-mL Teflon™ microwave reaction vessel until no liquid remained. The product was a light brown, clear, highly porous solid that liquefied upon exposure to air to a light brown, clear oil (E7P10), that was spectroscopically identical in nature to E7P9.

11. (E7.11)—The procedure of E7.9 was repeated with 2.225 g (10.08 mmol) APS and 975 mg ethylene glycol (15.7 mmol), but without a solvent, producing a solid mass of white opaque needle-like crystals that turned upon contact with air into a clear, colorless, oil (E7P11), identical in nature to E7P9. ^{1}H NMR (300 MHz, $CDCl_3$): δ 0.60–0.68 (broad multiplet, 2.0 H), 1.15–1.20 (triplet, 14.0 H), 1.50–1.60 (broad multiplet, 2.0 H), 2.10–2.30 (broad multiplet, 13.0 H), 2.60–6.75 (broad multiplet, 1.5 H), 3.65–3.80 (sharp multiplet, 22.5 H), 3.75–3.80 (broad multiplet, 2.0 H).

12. (E7.12)— Catechol (2.259 g, 20.52 mmol) was dissolved in 10 mL absolute ethanol and added with stirring to 2.227 g (10.08 mmol) of APS. The reaction mixture was sealed under argon in a 100-mL Teflon™ microwave reaction vessel and irradiated with microwaves for three intervals of M11. A white, opaque precipitate formed with a small amount of opaque, colorless liquid. The solid was vacuum filtered and washed with cold 95% ethanol; yield 2.781 g (91.36%) of bis(1,2-phenylenedioxy)-(3-aminopropyl)silane (E7P12). ^{1}H NMR

(300-MHz, DMSO/d-6) δ 0.48–0.52 (triplet, 2H, $SiCH_2$–), 1.46–1.50 (multiplet, 2H, –CCH_2C–), 2.50–2.59 (multiplet, 2H, NCH_2–), 3.31–3.70 (broad multiplet, 3H, –NH), 6.43–6.47 (multiplet, 4H, H-4,5 of Ar), 6.51–6.55 (multiplet, 4H, H-3,6 of Ar). FTIR (diamond single point ATR) sharp band at 1000–1050 cm^{-1}, broad, overlapping bands at 2800–2970 and 2900–3150 cm^{-1}. MS *m/z* 302.8 (calc. for $_{15}H_{16}NO_4Si$: 303).

13. (E7.13)—BA-1 (3.391 g. 10.21 mmol) was mixed with 1.582 g triethanolamine (10.60 mmol) and irradiated with microwaves in a sealed 100-mL Teflon™ microwave reaction vessel under argon for two cycles of M11. The sealed reaction vessel was then cooled to -5 °C before opening. The white-to-slightly yellow, opaque precipitate was vacuum filtered and washed with cold 95% ethanol to give 3.311 g of a crude product that was recrystallized by dissolving in a minimum volume of boiling acetone, cooling the solution to room temperature, blanketing the solution with a layer of pentane, and allowing it to stand for a week. 1-[3-(5,5-Dimethylhydantoin-3-yl)propyl]-5-aza-2,8,9-trioxa-1-silabicyclo[3.3.3]undecane (E7P14) settled. ^1H NMR (300 MHz, $CDCl_3$) δ 0.39–0.43 (triplet, 2H, $SiCH_2$), 1.46–1.49 (singlet, 6H, -CH_3), 1.65–1.80 (multiplet, 2H, –CCH_2C–), 2.70–2.85 (triplet, 6H,–NCH_2 [CH_2O–]), 3.40–3.50 (triplet, 2H, –CH_2–hydantoin), 3.70–3.85 (triplet, 6H, CH_2O), 5.50 (broad singlet, 1H, N–H).

14. (E7.14)—A stirred mixture of APS (2.213 g. 10.0 mmol) and triethanolamine (1.593 g, 10.68 mmol) was irradiated with microwaves in a sealed 100-mL Teflon™ microwave reaction vessel under argon for two cycles of M11. The sealed reaction vessel was cooled to -5 °C before opening. The resulting white, opaque precipitate was vacuum filtered and washed with cold 95% ethanol to yield 2.097 g of crude product. Recrystallization by dissolving in acetone, evaporating solvent to the saturation point, and allowing the solution to stand under a loosened cap for a week gave 1.712 g of clear, colorless, needles of 1-(3-aminopropyl)-5-aza-2,8,9-trioxa-1-silabicyclo[3.3.3]undecane (E7P14).

Table 1. X-Ray Crystallography Results for E7P14.

Sample	E7P14
Empirical formula	$C_9H_{18}N_2O_3Si$
Formula weight	230.34
Temperature	173(2) K
Wavelength	0.71073 Å
Crystal system	Monoclinic
Space group	P 2_1
a	6.6339(10) Å
b	12.9876(19) Å
c	7.1373(11) Å
α	90°
β	107.026(2)°
γ	90°
Volume	587.99(15) $Å^3$
Z	2
Density (calculated)	1.301 Mg/m^3
Absorption coefficient	0.191 mm^{-1}
Reflections collected	3890
Independent reflections	2465
$R_1[I \geq 2\sigma(I)\text{data}]$[a]	0.0341
$wR_2[I \geq 2\sigma(I)\text{data}]$[b]	0.0886

[a] $R_1 = \sum(||Fo| - |Fc||) / \sum|Fo|$

[b] $\omega R_2 = [\sum[\omega(Fo^2 - Fc^2)^2] / \sum[\omega Fo^2]^2]^{1/2}$

X-ray Crystallography: Unit cell dimensions were obtained (Table 1) and intensity data were collected at The University of Florida, Gainesville, by Dr. Khalil A. Abboud on a Siemens SMART PLATFORM equipped with a CCD area detector and a graphite monochromator utilizing MoKα radiation (λ = 0.71073 Å) at 173 K. Cell parameters were refined using up to 8192 reflections. A full sphere of data (1850 frames) was collected using the ω-scan method (0.3° frame width). The first 50 frames were re-measured at the end of data collection to monitor instrument and crystal stability (maximum correction on I was < 1 %). The crystal-to-detector distance was 4.994 cm. Absorption corrections by integration were applied based on measured indexed crystal faces.

The structure was solved by the Direct Method in *SHELXTL6,* and refined using full-matrix least-squares. The space group was determined from examination of the systematic absences in the data, and the successful solution and refinement of the structure confirmed these assignments. The non-H atoms were treated anisotropically, whereas the hydrogen atoms were calculated in ideal positions and were riding on their respective carbon and nitrogen atoms. A total of 144 parameters were refined in the final cycle of refinement using 2465 reflections with $\lambda > 2\sigma$ (I) to yield R_1 and wR_2 of 3.41% and 8.86%, respectively. Refinement was done using F^2 *SHELXTL6* (2000). Bruker-AXS, Madison, Wisconsin.

III. RESULTS AND DISCUSSION

III.1—Proof-of-Concept: *Validation of Chloramines as Possible Countermeasures to Chemical Weapons*—

Previous work has established that chlorinated polystyrene halamines, such as PSH-Cl, are relatively indiscriminate biocides, that afford convenient storage of chlorine equivalents in the +1 oxidation state by exchange of amide and imide protons in reactions with Cl_2 or hypochlorites.[19] Because Cl^{+1} compounds are commonly used as oxidizing agents, this proof-of-concept experiment was designed to test the oxidative reactivity of PSH-Cl as a representative polymer-bound chloramine toward two commonly-used surrogates for chemical warfare agents (CWAs): 2-CEES (5) and D-S (7).

It is clear from Figure 12 that PSH-Cl was considerably more effective at reacting with 2-CEES and D-S in acetonitrile at room temperature than was the unchlorinated polystyrene hydantoin control. The chart also shows that CEES reacted faster under these reaction conditions than D-S. From the Cl^{+1} titration data for PSH-Cl, the results in figure 12, and knowing that, in the presence of water, oxidation to the sulfoxide is a proven method of neutralization of both HD and VX, we can conclude that hydantoin-modified polymers containing at least 5 ppt of active chlorine (measured under M4

conditions) possess sufficient activity to HD analogs to merit a systematic investigation of polymer-bound chloramines and related compounds. [9, 10, 13]

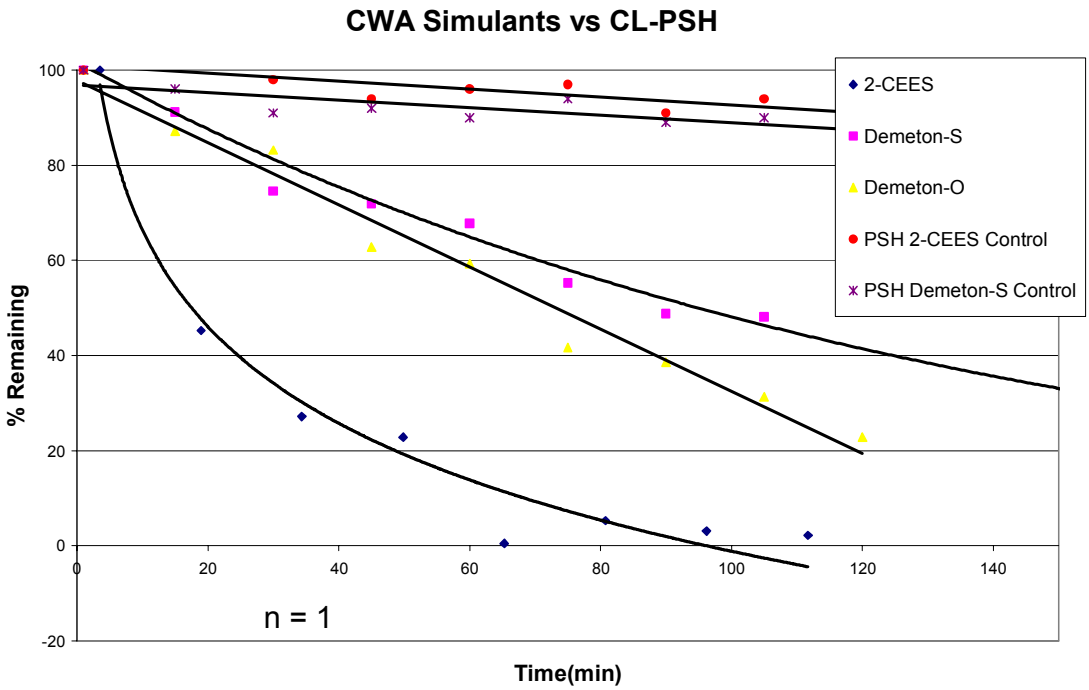

Figure 12. Degradation of Surrogates by Chlorinated Polystyrene—Hydantoin

In the absence of a control no statement is justified about the isomer D-O, but the likelihood of beneficial decreases in VX concentrations, although less certain, reinforces the conclusion that a complete study can be expected to produce reactive materials of interest to the military, Homeland Security and public health organizations.

III.2—Experiment 2 Discussion:

E2.1–E2.4—*Sol–Gel Attachment to Boehmite*

The experiments designated E2.*n* were performed to develop a practical synthesis of aluminum-oxide-bound siloxanes reactive against chemical and/or biological warfare agents. The primary focus of this experiment was the immobilization of hydantoin siloxanes onto nanoscale (300 nm diameter) boehmite Hydantoins were chosen because chlorinated hydantoins are known to be active against chemical and biological warfare agents, and nanoscale boehmite was chosen because it provides a high surface area (>300 m^2/g) and possesses an abundance of surface local hydroxyl groups to carry out the sol–gel addition of alkoxysilanes (Figure 13).[59-62, 63, 63-*a,b*]

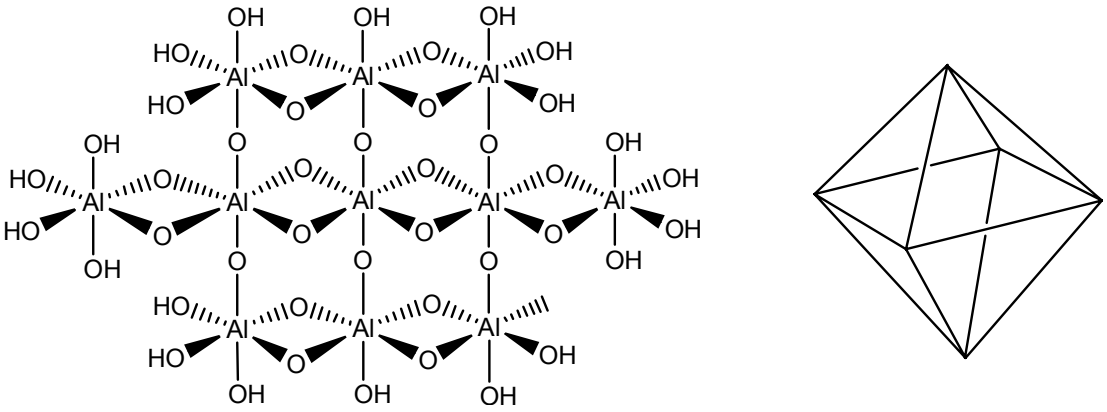

Figure 13. Structure of Boehmite

It was hypothesized that the aluminum oxide–hydantoin siloxane adduct would: 1. increase the stability of the chloramide with regard to UV, heat, and moisture; 2. increase the amount of available chloramide by providing a greater surface area to which hydantoin silane moieties can be bound; 3. provide a common substrate that is easily incorporated into a variety of polymers; 4. increase the residence time and contact time with the reactant; and 5. provide additional hydrolytic activity against select threat agents through its increased surface area, the amphoteric nature of the resulting aluminosilicate, and the innate reactivity of nanoscale metal oxides (Frenkel defects and Slotsky pairs).[63, 63-a]

Figure 14 depicts the accepted acid and base catalyzed sol–gel activation mechanisms of alkoxysilanes.[63-a]

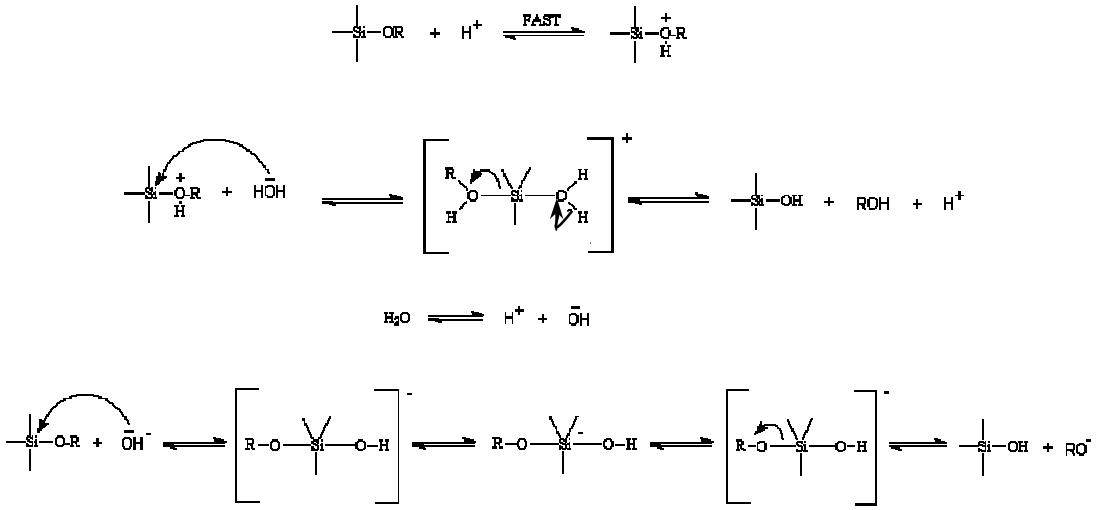

Figure 14. Sol–gel Reaction Activation Mechanism

Once activated, the alkoxysilanes rapidly undergo polycondensation followed by crosslinking. The Worley group has demonstrated that sol–gel addition of

BA-1 to silica gel.[29] Since It is well known that sol–gel chemistry also readily occurs between alkoxysilanes and aluminum oxides to form mixed aluminosilicate oxides, this reaction scheme was adopted for the initial attempt at synthesizing the hydantoin siloxane boehmite adduct (Figure 15).[29, 59-62, 63-*b*]

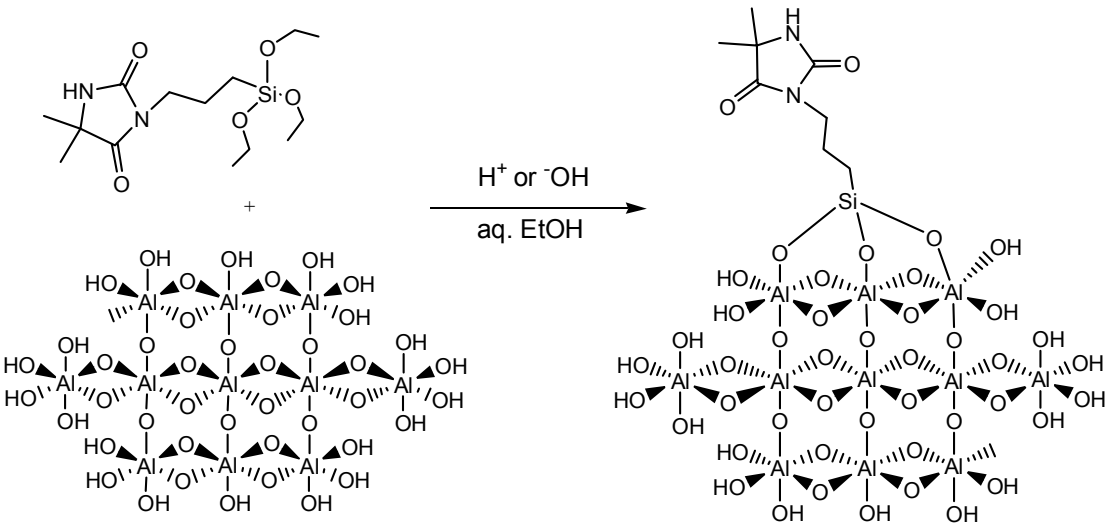

Figure 15. Proposed Sol–gel Reaction Scheme between BA-1 and Boehmite

Elemental analysis, redox titration data and color reaction results for the various reaction conditions employed in the synthesis of the E2 products are listed in Table 2. Durability will be addressed in the discussion of experiment series E5.

Table 2. Carbon, Chlorine[+1] and Nitrogen Content, and Infrared Spectral Characteristics of Chlorinated BA-1 Nanoparticles Prepared from Boehmite and Antimicrobial Trialkoxysilanes under Different Reaction Conditions.

R-[a]	E2-[b]	E2M3 color[c]		E2M4[d]	FTIR/	Elemental Analysis		
		Neat	+ starch	mmol Cl/g	ATR[e]	%C (+/- .13)	%N (+/- .06)	%C/%N
Control (boehmite)		No	no	0.00	N/A	N/M	N/M	N/M
BA-1	P1	No	wk purple	N/M[f]	-	N/M	N/M	N/M
BA-1	P2	dk yel/brn	N/M	0.120	+	2.31	0.61	3.79[g]
BA-1	P3	med yel	N/M	0.061	+	1.64	0.40	4.10
BA-1	P4	dk yel/brn	N/M	0.160	+	2.48	0.65	3.82
BA-1	P5	dk yel/brn	N/M	N/M	+	N/M	N/M	N/A
BA-1	P6	dk yel/brn	N/M	0.128	+	3.06	0.97	3.15
BA-1	P7	faint yel	N/M	N/M	-	N/M	N/M	N/A
BA-1	P8	dk yel/brn	N/M	0.207	+	3.00	0.91	3.30
BA-1	P9	dk yel/brn	N/M	0.142	+	2.41	0.66	3.65
BA-1	P10	Black	N/M	0.685	+	9.36	2.95	3.17
Q18[h]	P11	N/A	N/A	N/A	+	15.94	1.10	14.49

[a]—R- of $(EtO)_3Si(CH_2)_3$-R. [b]—Product index number keyed to Experimental Section. [c]—Iodine formed by reaction with KI. [d]—Determined by titration. [e]—+ indicates no starting material in FTIR spectrum of product. [f]—N/M = not measured. [g]—Ratio of %C to %N. [h]—Q18 = Octadecyldimethylammonium.

For each preparation the degree of substitution of BA-1 to boehmite was calculated independently (Table 3) from the respective carbon and nitrogen weight percentages measured by elemental analysis. Values of the observed carbon:nitrogen ratio were then compared with the theoretical carbon:nitrogen weight ratio for $C_8H_{13}N_2O_2Si$—8*12.011/2*14.007 = 3.43:1.00—which corresponds to substitution of all three of the ethoxy groups in BA-1 by boehmite hydroxyls (Figure 16). The M3 data recorded in Table 2

were measured for products E2P*n* after chlorination according to M1. The negative controls, which were simply prepared without addition of BA-1, retained no reactive chlorine.

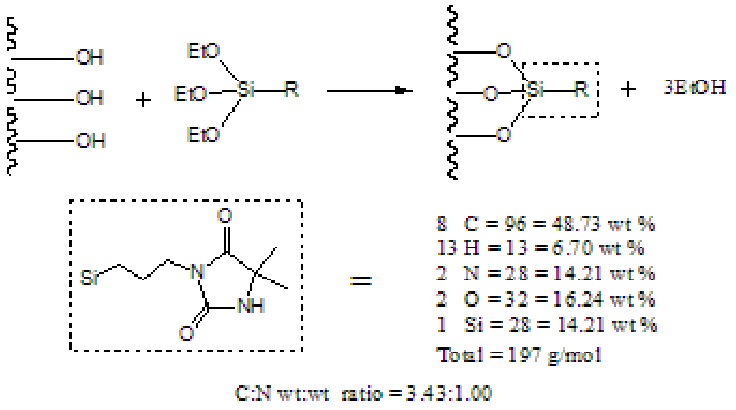

Figure 16. 3-point Attachment of BA-1 to a Substrate

This initial preparation, E2.1, was predicated on the expectation that the intrinsic acidity of boehmite (*pKa* 7.5) would be sufficient to drive the reaction to completion; however, M3 results indicated that product E2P1 retained only negligible amounts of BA-1. Experiments E2.2 and E2.3 incorporated sol–gel and non-neutral *p*H chemistry to promote attachment of BA-1 to the boehmite, as measured by the reactive chlorine content.[60-62] The M3, M4, and elemental analysis data in Table 3 confirm that significantly more BA-1 attached to the substrate nanoparticle than was bound at a neutral *p*H (reaction, E2.1).

Table 3. Cl^+ Content of Chlorinated Biocidal Nanoparticles Prepared from Boehmite and Antimicrobial Trialkoxysilanes under Various Reaction Conditions.

E2	ppt active Cl		wt % hydantoin added, calculated		
	Meas by M4[a] (+/- 0.52)	Calc from EA-N[b]	from M4[a] data	from EA-C[c]	from EA-N[b]
P2	4.20	7.63	2.35	4.74	4.27
P7	N/A	N/A	N/A	N/A	N/A
P3	2.14	5.00	1.20	3.37	2.81
P8	7.25	11.36	4.06	6.16	6.40
P10	23.98	36.84	13.43	19.21	20.76
P4	5.61	8.13	3.14	5.09	4.57
P6	4.48	12.11	2.51	6.28	6.83
P1	N/A	N/A	N/A	N/A	N/A
P9	4.96	8.25	2.78	4.95	4.64
P11	N/A	N/A	N/A	[21.20]	[28.95]

[a]—Redox titration with thiosulfate; [b,c]—Wt% N and C, respectively, measured by elemental analysis. *Note fully attached hydantoin silane MW addition is ~194 g/mol

Redox titration (M4) data show that E2P2, the product of acid catalysis, contains twice the active chlorine compared to the analogous base catalyzed product, (E2P3). Likewise, elemental analysis data show that the C:N ratio measured for product E2P2, 3.78:1.00, is much closer to the ideal theoretical C:N ratio, 3.43:1.00, than the C:N ratio of product E2P3, 4.10:1.00, from the base-catalyzed reaction. A carbon content higher than the ideal theoretical ratio may be interpreted as indicating retention of one (C:N calculated = 120.099/28.014 = 4.29) or more of the BA-1 ethoxy groups by some incorporated moieties, and possibly weaker attachment to the boehmite. That the weight percent values of BA-1 added, as calculated from wt-% C

elemental analysis, are slightly higher than the corresponding values calculated from wt-% N leads to the same conclusion.

While the agreement among both sets of calculated values lends confidence in the accuracy of the data, the M4 titration data suggests that, assuming that the measurements, calculations and interpretation are correct, not all of the free amide nitrogen atoms added are available to bind chlorine. Using wt-% N of the chlorinated, acid-catalyzed product E2P2 as the basis for comparison to the titration result, 45% of the chloramine-forming nitrogen centers added are either unable to form chloramines or are forming chloramines that are inert under M4 conditions. The former suggests bonding or occlusion of the amide nitrogen, whereas the latter suggests a highly stabilized chloramine, possibly because of electronic interactions between bound chorine and the boehmite matrix. It's known that both chlorine gas and phosgene will react with aluminum oxide, via nucleophilic addition, to form chlorinated aluminum oxide analogs.[63-*c*] However, since this work is dealing with chlorine in the Cl^+ state, it is unlikely that it will react in the same manner, if at all. If stabilization of the Cl^+ were to occur, it would likely be by association with the aluminum bound oxygen, since these oxygen atoms possess a high partial negative charge as a consequence of being bound to the aluminum. The corresponding calculation for the base-catalyzed product, E2P3, after chlorination, reveals an even higher percentage, 57%, of unreactive nitrogen centers.

In experiment E2.4 sodium hypochlorite was used in an attempt both to raise the *p*H and to form the chloramide of the BA-1–boehmite adduct in a single step. The rationale for immediate *N*-chlorination was to prevent binding or occlusion of the amide site during the sol–gel process. Comparing wt% N values for E2P4 and E2P2 shows similar attachment efficiency, 0.65 and 0.61%, respectively, as does comparing the elemental analysis C:N ratios, 3.82 and 3.79, respectively. The M4 titration data show a 2.6 fold increase in available chlorine compared to the base-catalyzed preparation of E2P3, and a 33% increase over the acid-catalyzed product E2P2. Finally, comparison of the M4 result with the value predicted from wt-% N analysis of E2P4 after chlorination reveals that 69% of the theoretically available chloramine-forming nitrogens are available, a 14% improvement over E2P2.

E2.5–E2.11—*Microwave-Induced Polymer Grafting*

Microwaves cause compounds to generate heat by oscillating the alignment of dipole moments within a compound.[30] Microwave absorption strength is dependent on the dielectric properties of a molecule. Molecules with larger dipole moments exhibit longer relaxation times and higher susceptibility to microwave excitation. A quick and easy method to determine relative dipole moment charge separation is to compare the electronegativities (ENs) of the atoms within the compound. Large differences create large bond dipole moments, implying efficient microwave excitation and consequent heating within that molecular region.

It is not surprising that the siloxanes are microwave active. First consider the hydroxyl group, whose O–H dipole moment is highly susceptible to microwave excitation. Hydrogen has EN 2.20 pauling units (PU) and oxygen has EN 3.44 PU, a difference (ΔEN_{O-H}) of 1.24 PU. From this one might expect compounds with a definite dipole moment of 1.24 PU or greater to possess a microwave excitation susceptibility equal to or greater than that of a hydroxyl group. The EN of Si is 1.90 PU, and ΔEN_{O-Si} (as in a silyl ether or silanol bond) is 1.54 PU, larger than ΔEN_{O-H} and much larger than ΔEN_{C-O} (0.89 PU). Consequently, one might expect compounds containing Si–O linkages to be extremely susceptible to microwave excitation. While this appears obvious in retrospect, relatively few microwave-mediated siloxane reactions are reported in the literature and, curiously, the few reactions reported center around cleavage of siloxane bonds, rather than their formation. [64-67] Reactions E2.5–E2.11 explore the utility of this phenomenon in the synthesis of the hydantoin silane.

E2.5 In this experiment, BA-1 was dispersed in acetone, to ensure homogeneous distribution of the siloxane onto the boehmite. From previous results it is apparent that BA-1 is present in gross excess, due to its high density as compared to the finely divided boehmite powder. Consequently, the reaction mixture remains inhomogeneous, resulting in uneven distribution of the siloxane onto the boehmite when the two neat materials are mixed prior to microwave irradiation. In this experiment the ethanol solvent employed in

reactions E2.1–E2.4 was replaced with acetone for three reasons:

1. acetone is more transparent to microwaves than ethanol, so less power is lost to heating the medium, 2. the rate-limiting step—hydrolytic cleavage of the ethoxy groups in BA-1 to form ethanol—is reversible, so drastically decreasing the concentration of the byproduct should favorably shift the equilibrium of this reaction; and 3. to increase the likelihood of forming the three-point attachment. However, darkening of the reaction mixture and formation of a pungent odor indicated that acetone is not inert under the reaction, presumably forming chlorintated aldol adducts through the reactions depicted in Figures 17-18, in addition to the classical halaform reaction, to form chloroform. This result is consistent with data reported in the literature.[72] Consequently, acetone was used in the remainder of this work only for reactions carried out at a relatively neutral *p*H and in the absence of strong nucleophiles.

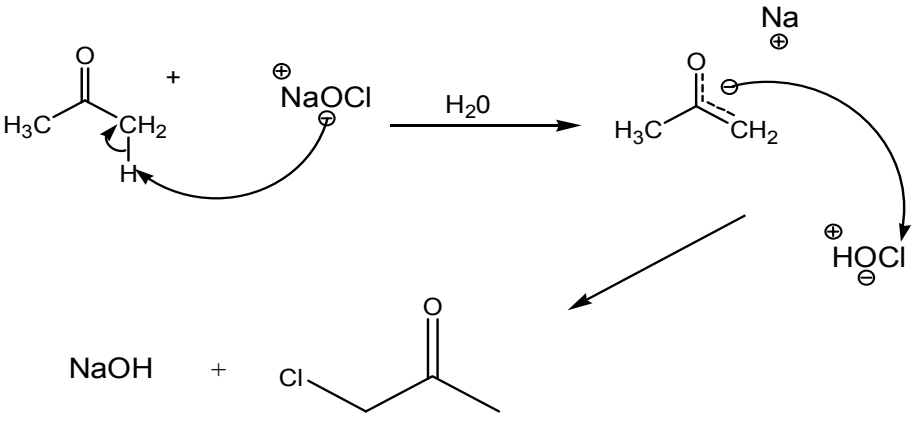

Figure 17. Reaction of Sodium Hypochlorite with Acetone

The reaction in Figure 17 will occur in conjunction with the competing reaction shown in Figure 18.

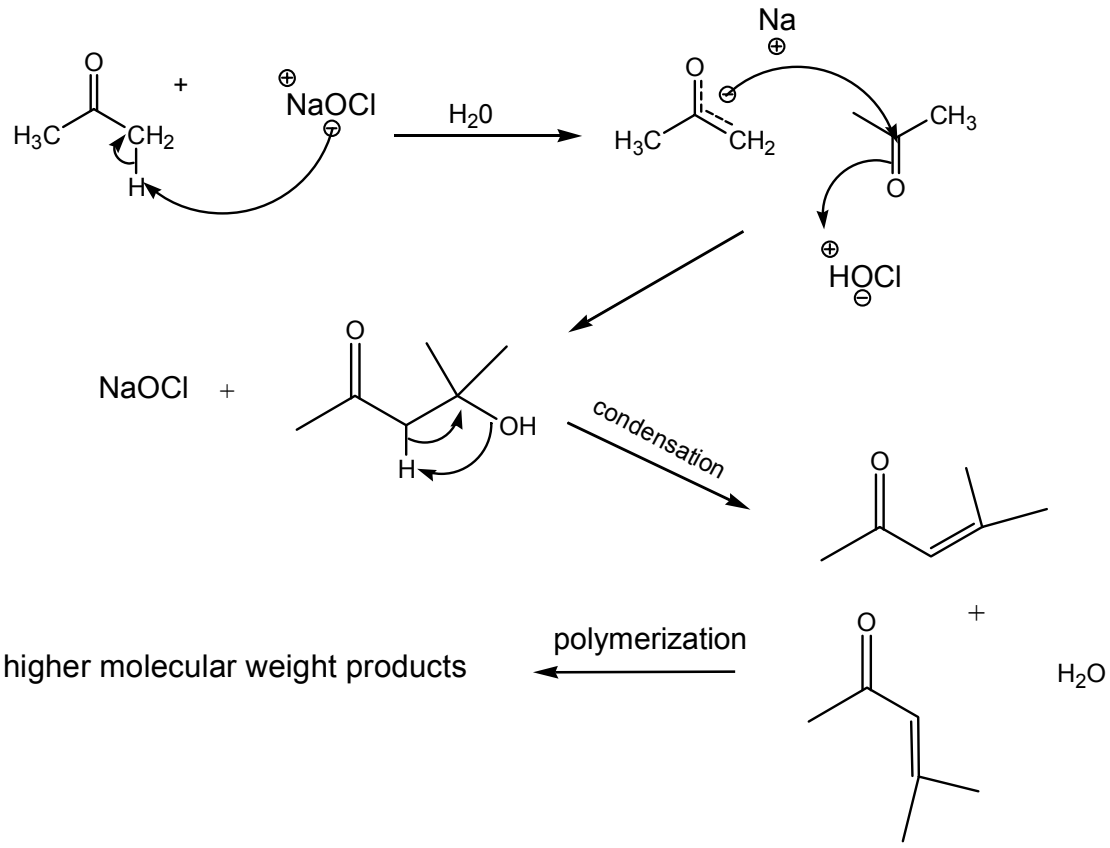

Figure 18. Aldol Formation and Condensation with Acetone and Hypochlorite Sodium Hypochlorite

E2.6 The base-catalyzed, microwave-activated reaction E2.5 was repeated in ethanol. Whereas the M4 titration measured only 4.48 ppt active chlorine, 20.14 % less than from E2P4, only ~3 mmol of BA-1 was used in this experiment, compared to ~5 mmol used in reaction E2.4, so the yield of active Cl per equivalent of BA-1 was increased by nearly 20%. Calculations of wt-% addition of BA-1 based on wt-%N and C by elemental analysis are in general agreement, but the value calculated from wt-% N was *higher* by 0.53% than

the equivalent value calculated from wt-% C—and the M4 titration result is barely 1/3 of these calculated values. The efficiency of attachment increased fourfold, but 2/3 of the BA-1 moieties attached are unable to bind chlorine in a usable form.

That the C:N ratio of this product—3.15:1.00—is lower than the ideal ratio, 3.43:1.00, requires that E2P4 possess less carbon than the simple BA-1–boehmite adduct. Assuming data accuracy and that BA-1 is the sole source of carbon and nitrogen in the product, the system must shed carbon species while retaining nitrogen atoms, certainly by some mode of decomposition of the hydantoin ring. The theoretical C:N ratio for the corresponding amine, $–Si(CH_2)_3NH_2$, is 3*12.011/14.007 = 2.57; the corresponding calculation for a 2:1 mixture of amine and hydantoin yields C:N 2.86; and a similar calculation for a 1:1:1 mixture of both structures plus a carbamate, $–Si(CH_2)_3NHC(O)OAl–$, yields C:N 3.15. Thus, “cracking” of the hydantoin ring and bonding of the subsequent “cracked” molecular nitrogen species to a silicon or aluminum center provides a plausible interpretation of these data and impetus to refine the coupling procedure. Further literature research indicates that this result is similar to the result of pyrolyzing amines in the presence of aluminum oxide.[72-*a*]

E2.7 Experiment E2.6 demonstrated that microwave heating in the presence of hypochlorite causes much more than just local heating. To isolate the influence of hypochlorite, experiment E2.7 reproduced the conditions of

reaction E2.2 using microwave heating in place of conventional heating so that the products of the two reactions could be compared. The reaction conditions in E2.7 were identical to E2.6, except that HCl solution was added to the reaction in place of sodium hypochlorite. From an academic perspective, the M3 data from the E2.7 product did indicate successful incorporation of chloramide forming moieties. However, from a practical chemical and biological agent detoxification perspective, the feeble yellow tint afforded by the amount of available Cl^+ is likely inadequate for stoichiometric detoxification purposes. Consequently, this set of reaction conditions was abandoned as a practical synthetic route.

E2.8 The failure to incorporate the hydantoins of BA-1 into E2P7 showed that the microwave coupling reaction benefits from the presence of sodium hypochlorite. Experiments E2.1–E2.4, employed conventional heating, wherein, NaOCl served as a superior catalyst to HCl and HCl catalyzed better than NaOH, with respect to the addition of active chloramine forming moieties to the substrate. Experiment E2.8 was included to complete the parallel set of microwave reactions for comparison to the equivalent heat-treated products, which will separate the effects of *p*H and converting the amide N—H bond. The reaction conditions were identical to E2.7 except the HCl was replaced with an equimolar amount of NaOH.

M4 data showed a 72.6% increase in active chlorine uptake over E2P2. As above, experiment E2.7 used 40% less BA-1 than E2.2 and was

complete in a fraction of the reaction time compared to the reaction time required for synthesis of product E2.2. The C:N ratio, 3.30:1.00, was comfortably close to the ideal 3.43:1.00, and that it was lower, suggests full incorporation of BA-1 Si–O valences into Al–O–Si structures. The M4 titration result was 64% of theoretical based on wt-% N from the elemental analysis. C:N calculated for 0.64 BA-1 + 0.36 $–Si(CH_2)_3NH_2$ is 3.70, so ring degradation to form this primary amine may contribute to product formation, but it is not the principal mode of carbon shedding in this reaction. Including a significant amount of carbamate formation builds a possible rationalization for the observations, but the extent of contribution by occlusion of intact hydantoin rings cannot be estimated.

Table 4 reports the results of bacterial and fungal inhibition studies conducted with product E2P8. The 100-mg sample for each test contains 2.07×10^{-2} mmol (~730 μg) of active chlorine, which would be diluted to 0.73 ppm if it were homogeneously distributed without loss throughout the liter of bacterial suspension containing $>3.68 \times 10^{8}$ colony-forming units (CFU). Even at this challenge level, in all cases, direct plating of the challenge flask grew zero CFUs, and serial dilutions of the challenge flask yielded small, abnormal, “sickly looking” colonies.

Table 4. Attenuation of Viable Bacteria and a Fungus by Chlorinated E2P8 (BA-1 Boehmite Adduct) in Liquid Cultures According to M10.

E2P8	Total Colony-Forming Units (CFU)			
Organism	Chlorinated BA-1 Boehmite	Unchlorinated BA-1 Boehmite	Challenge/L	% Reduction
Staphylococcus aureus	2.92×10^7*	1.65×10^8	9.88×10^7	82.30
Klebsiella pneumoniae	7.50×10^7*	7.32×10^8	7.65×10^8	89.75
Aspergillus niger	3.10×10^7	3.83×10^7	2.87×10^7	19.06

[a] Adduct of BA-1 onto boehmite nanoparticles.
* Plating of the challenge flask grew no CFUs; colonies from the subsequent dilutions were abnormal and small.

One may conclude that preparation E2P8 of BA-1–boehmite adduct has bacteriostatic properties that persist in water and predict that, in sufficient quantities, BA-1–boehmite will exhibit potent biocidal properties. Reactivity of preparation E2P8 against three chemical agent surrogates is shown in Figure 19.

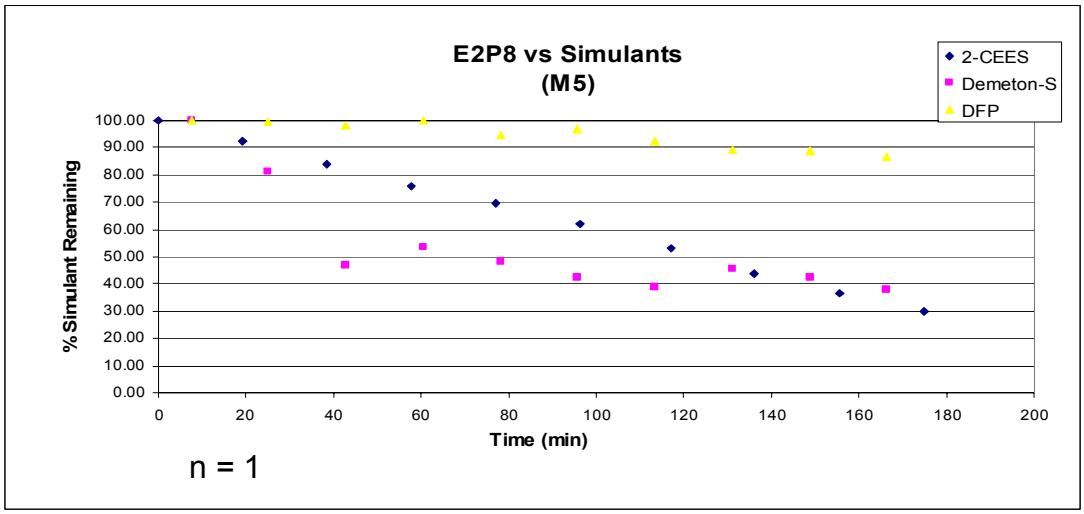

Figure 19. Removal from Solution of Surrogates for Mustard, VX and G-Agents by Heterogeneous-Phase Reaction with Chlorinated BA-1–Boehmite Adduct

Under M5 conditions, 100 mg samples of E2P8 reacted in three hours with 1.0 µL of the mustard agent surrogate 2-CEES and with 1.0 µL of VX agent surrogate demeton-S. These observations support the hypothesis proposed in the E1 discussion, that 5 ppt active chlorine delivered under M4 conditions from chloramine hydantoin modified polymers will be adequate to neutralize these two surrogates under M5 conditions. Verifying the predicted inactivity of the G-agent surrogate DFP under M5 conditions in effect added a control to the experiment.

E2.9 This experiment was designed to determine if microwave treatment could facilitate the attachment of the hydantoin siloxane to boehmite without catalysis. The solvent used was acetone, because it is nearly microwave transparent and has a low boiling point—an unreactive medium that will regulate the temperature of the reaction mixture by acting as a sink for

(evaporating to dissipate) the heat generated by the microwave-absorbing compounds in the reaction mixture, presumably the siloxane groups and the boehmite.[72-*b*]

This experiment was identical to the previous microwave-mediated experiments except that in E2.9 acetone was used as the solvent, and no catalyst was added. Product E2P9 took up 18.30 % more active chlorine than did product E2P2, again from 40% less BA-1, and possessed a C:N ratio, 3.65, closer to the ideal theoretical C:N ratio. The immediate hypothesis was proved—microwave radiation significantly facilitated the reaction in the absence of a chemical catalyst—but basic catalysis, as in E2.8, further improves the process.

E2.10 This experiment nominally scaled the E2.8 process up 50−fold, and moved it from the conventional microwave oven used, into a precision microwave reactor. However, the active chlorine content of product E2P10 increased more than 230% (by M4 titration), and the wt-% N from elemental analysis indicated that the quantity of BA-1 attached increased more than 220% compared to E2.8. The C:N ratio was similar to that of E2P6, perhaps showing that complete decomposition of the hydantoin ring to liberate the 3-silylpropylamine recovered some prominence in the microwave reactor. This dramatic, completely unexpected increase in hydantoin siloxane attachment and consequent increase in active chlorine was likely the result of a combination of scaling benefits and the use of a precision microwave

reactor, augmented by switching from glass to Teflon™ reaction vessels. Teflon™ is transparent to microwaves, while glass is not.

E2.11 The goal of this experiment was to attach the known biocide [3-(trimethoxysilyl)propyl]octadecyldimethylammonium chloride to AlO(OH) and test for biocidal efficacy. Once again, according to elemental analysis, the carbon and nitrogen elemental analyses indicate that more nitrogen is retained compared to carbon than predicted by the equivalent weight calculation reported in Table 3 for the quaternary ammonium salt siloxane E2P11. Considering the reaction conditions, this could be explained by a small percentage of the attached quaternary ammonium salts' undergoing Hoffman elimination of the octadecyl chain. The M10 data reported in Table 5 are inconclusive, presumably due to the extremely hydrophobic nature of E2P11.

Table 5. Activity of $C_{18}NMe_2(CH_2)_3Si$–Boehmite Adduct Against Two Bacteria and a Fungus.

E2P11	Total Colony-Forming Units (CFU)			
Organism	Treated	Untreated	Challenge/L	% Reduction
Staphylococcus aureus	1.33×10^8	3.68×10^8	3.68×10^8	63.86
Klebsiella pneumoniae	2.92×10^8	2.78×10^8	3.03×10^8	N/A
Aspergillus niger	4.13×10^7	4.27×10^7	3.77×10^7	3.28

III.3—Experiment 3 Discussion:

E3.0 This series of experiments addressed three goals: 1. to attach BA-1 to samples of the 50:50 cotton–nylon blend fabric used in the US military battle dress uniform (BDU), proposed to occur according to the scheme in Figure 20; 2. to evaluate the influence of varying reaction conditions on yield and quality of this product; and 3. to compare conventional heating methods to microwave-promoted addition.

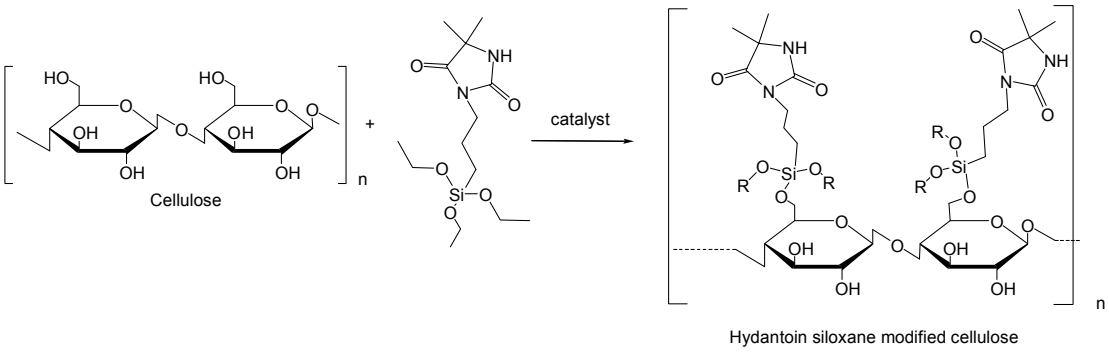

Figure 20. Reaction Scheme for Synthesis of BA-1—modified Cellulose

Table 6 displays the E3 series of experiments as a 4x5 array of four BA-1 dip treatments (neutral and acidic alcohol, neutral acetone and ethanolic hypochlorite) applied to 300-mg swatches of BDU fabric and heated according to five protocols (microwave irradiation for three one-minute intervals between dips, the same pattern repeated four times, microwave irradiation for two 3-minute intervals, no application of heating, and no heating, followed by an overnight bake at 75°C).

Table 6. Chlorine Uptake by BDU Fabric after Coupling with BA-1 under Various Reaction Conditions.

E3	Dip solution		μwave application sequence	FTIR/ ATR	mmol Cl^+/g	ppt Cl^+	wt % BA-1	% Cl^+ increase over heat treatment (M4)	% Error from M4 (+/-)
	Sol	Add	after dip		From M4 titration				
P1.1	E[a]		1,1,1 min		0.0276	0.96	0.54	10.86	4.83
P1.2	E	HCl	1,1,1		0.0390	1.37	0.76	7.82	3.02
P1.3	A[a]		1,1,1		0.0514	1.80	1.01	70.95	6.12
P1.4	E	OCl	1,1,1		0.0530	1.85	1.04	32.85	7.33
P2.1	E		(1,1,1)x4	+[c]	0.1217	4.26	2.39		2.78
P2.2	E	HCl	(1,1,1)x4	+	0.1051	3.68	2.06		2.00
P2.3	A		(1,1,1)x4	+	0.1414	4.95	2.77		1.93
P2.4	E	OCl	(1,1,1)x4	+	0.1310	4.59	2.57		4.55
P3.1	E		3,3		0.0331	1.16	0.66	32.95	8.40
P3.2	E	HCl	3,3		0.0367	1.29	0.72	1.53	11.18
P3.3	A		3,3		0.0432	1.51	0.85	43.88	3.96
P3.4	E	OCl	3,3		0.0495	1.73	0.97	24.06	7.87
P4.1	E		0,0,0		0.0000	0.00	0.00		--
P4.2	E	HCl	0,0,0		0.0005	0.02	0.01		37.99
P4.3	A		0,0,0		0.0000	0.00	0.00		--
P4.4	E	OCl	0,0,0		0.0019	0.07	0.04		62.18
P5.1	E		0,0,0/75C[b]		0.0249	0.87	0.49		10.42
P5.2	E	HCl	0,0,0/75C		0.0362	1.27	0.71		4.73
P5.3	A		0,0,0/75C		0.0300	1.06	0.59		5.94
P5.4	E	OCl	0,0,0/75C		0.0399	1.40	0.78		3.80

[a] Solvents: A—acetone. E—95% ethanol. [b] No microwave power applied, heated overnight at 75 °C. [c] Spectra were consistent with expected structure.

Comparing the M4 titration data among the sets of results reveals several trends:

1. E.4 shows that some form of energy absorption is necessary, and comparing E3.1.1 and .3 to E3.5.1 and .3 suggests that ethanol, for which tan δ = 0.941 indicating efficient absorption of microwave energy, acts largely by intercepting applied microwaves and raising the temperature (*T*) of the mixture—*i.e.*, dissipating much of the microwave power as heat—whereas acetone (tan δ = 0.054, almost transparent to microwave energy) allows direct excitation of the O–Si centers, driving the coupling reaction forward.

2. Comparing series E3.1.1 and .3 to E3.3.1 and .3 reinforces this interpretation, as the decrease in available chlorine on longer microwave exposure in acetone is consistent with microwave-induced degradation of the hydantoin ring upon prolonged exposure to microwaves, as proposed in the discussion of experiment series E2.

3. Comparing series E3.1 to E3.2 shows clearly that the degree of substitution (*ds*) of O-6 in BDU cellulose by BA-1 is relatively small after each treatment step. The large increase in chlorine uptake after four treatment cycles further suggest that *ds* at that stage remains significantly less than 1, and that additional cycles might lead to further useful increases in *ds* and Cl uptake.

4. Chlorine uptake across the acid-catalyzed series E3.*n*.3 is proportional to the amount of BA-1 applied but apparently independent of the mode of

application of energy. A similar trend is seen in the series to which hypochlorite was added, except that the higher values for 6-minute irradiation (E3P3.4) suggests that the reaction may be incomplete at the shorter irradiation and heating times.

III.4—Experiment 4 Discussion:

In this set of experiments, the results from E3 were used 1. to select and optimize a treatment process for attaching moieties such as BA-1, which are potentially active against chemical warfare agents, to 50:50 cotton–nylon BDU fabric and 2. to prepare and evaluate materials so produced for efficacy against chemical and biological warfare agent surrogates according to procedures M6 and M9. The M4 titration data presented in Table 7 show that all three E4 preparations containing BA-1 formed chloramines in quantities large enough to yield potent antimicrobial surfaces. Figure 21 demonstrates that BA-1-treated BDU fabrics yielded potent, broad-spectrum antimicrobials, except that the heat-treated product E4P1.3 was much less effective against spores. Products of both TTDD and of the C_{18} quaternary ammonium salt were ineffective against both spores and *S. aureus.*

Table 7. Chlorine Uptake by BDU Fabric Coupled with $R(CH_2)_3Si(OR')_3$ in Acetone Driven Either by Heat or by Microwave Irradiation.

E4	R =	Power	mmols Cl/g	ppt active Cl
P1.1	5,5-dimethyl-hydantoin-3-yl	Microwave	0.1649	5.77
P1.2		Microwave + np[b]	0.2109	7.38
P1.3		heat	0.1754	6.14
P3.1	2,4-dioxo-7,7,9,9-tetramethyl-1,3,8-diazaspirobicyclo[5,4]dec-3-yl[a]	Microwave	0.0106	0.37
P3.2		Microwave + np	0.0229	0.80
P3.3		heat	0.0089	0.31

[a] TTDD-3-yl [b] boehmite nanoparticles

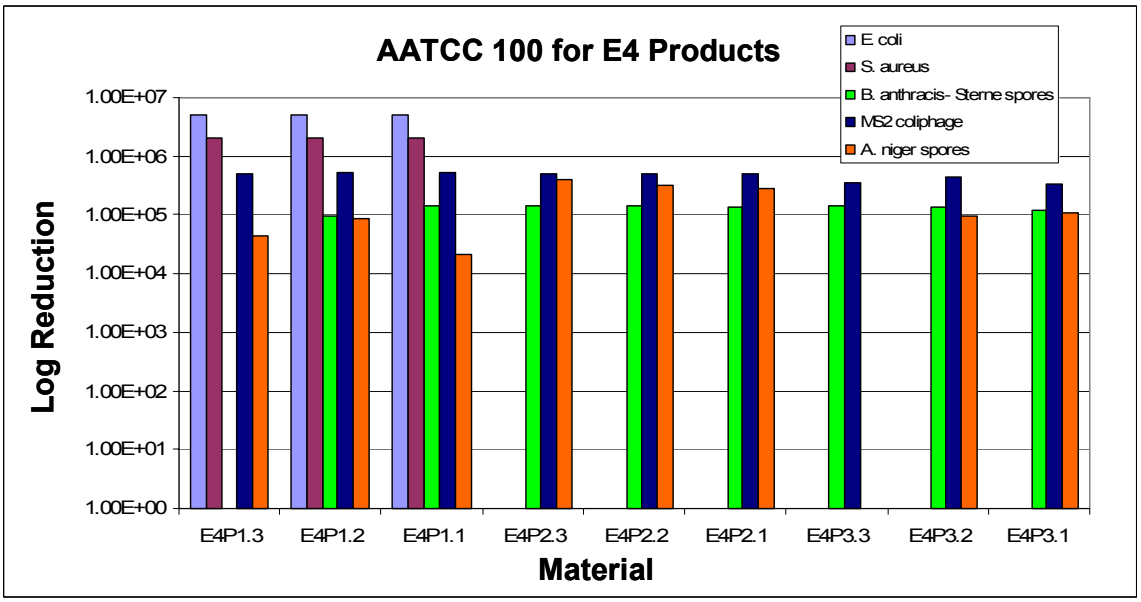

Figure 21. Antimicrobial Activity of BA-1, C18 Quaternary Ammonium and TTDD Derivatives of BDU Fabric by AATCC Method 100

The inability of the materials treated with QAC -1, $[C_{18}H_{37}(Me_2)N^{+}(CH_2)_3Si(OMe)_3]\,Cl^{-}$ (E4P2.1–E4P2.3), to kill *E. coli* is not surprising, since the biocidal action of this compound is dependent on membrane disruption.[18, 68, 69] Biocidal action via membrane disruption occurs when the hydrophobic tail of the alkylammonium salt (Figure 22) associates with the hydrophobic region of the cell membrane through Van der Waals interactions, while the positively charged alkylammonium

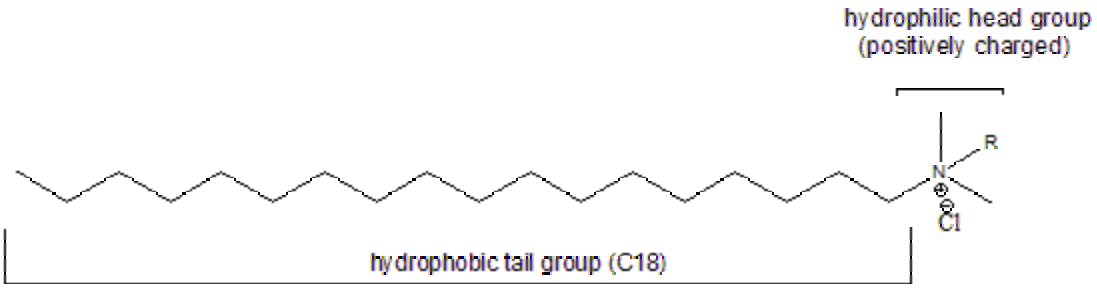

Figure 22. Structure of a Biocidal Quaternary Ammonium Salt

head group ion pairs with a hydrophilic, negatively charged head group of a bacterial membrane phospholipid, effectively changing the electronics of that region (Figure 23). While probably not significant as an isolated incidence, enough of these interactions destabilize/disrupt the phospholipid bilayer membrane and lyse the cell.

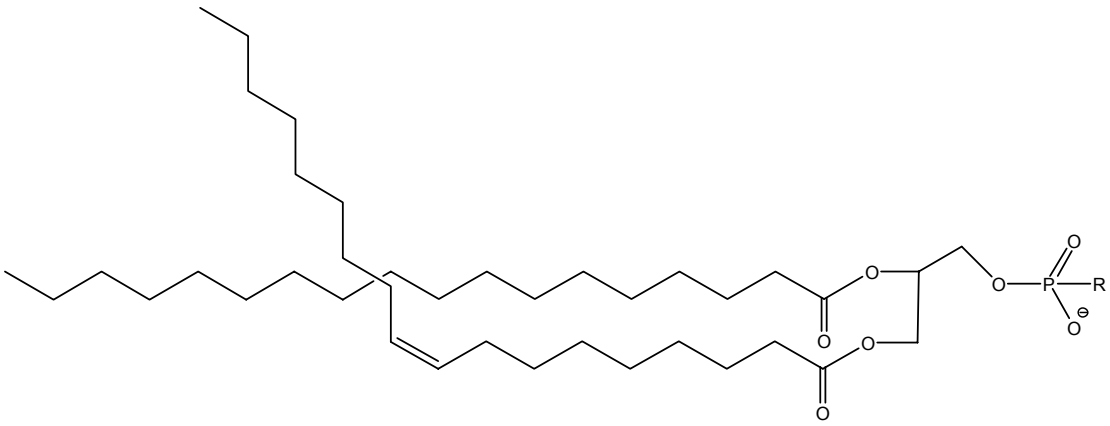

Figure 23. Structure of a Common Bacterial Membrane Phospholipid

Agents acting by these mechanisms have limited effect on Gram-negative organisms such as *E. coli*, because of the presence of a secondary outer membrane, that affords these organisms natural resistance to membrane-disrupting biocides. [70]

The inability of the materials treated with TTDD (E4P2.1–E4P2.3) to kill *S. aureus* could be attributed to their low chlorine content. One would expect materials treated with this compound to possess biocidal activity similar to E4P1.1–E4P1.3 since, TTDD and BA-1 have similar chemical functionality, and the materials treated with BA-1 demonstrated excellent biocidal properties against *S. aureus* (Figure 24).

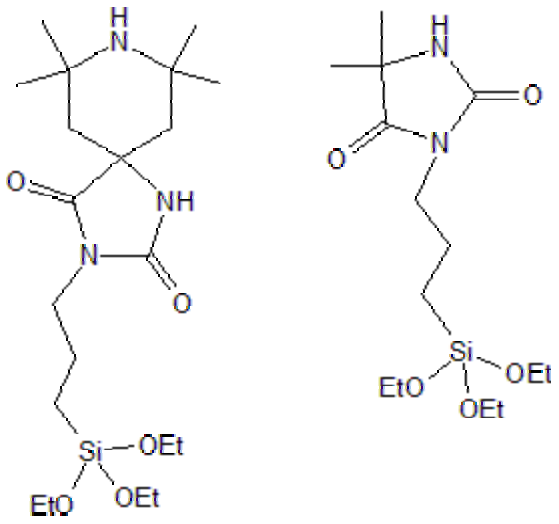

Figure 24. Structures of TTDD (left) and BA-1 (right)

This low chlorine loading of the material may also be the reason for the inability of E4P3.3 to kill *A. niger*.; however, enhanced efficacy caused by the microwave treatment can't be ruled out. In fact, the same phenomenon occurs in the E4P1 series materials. That E4P1.1 and P1.2 both demonstrated biocidal efficacy against spores of *B. anthracis* (Sterne strain), and E4P1.3 did not—even though E4P1.3 contained similar levels of active chlorine to P1.1 and P1.2—suggests that biocidal efficacy against *B. anthracis* spores derives from the microwave addition process. This

phenomenon is possibly caused by liberation of amines as suggested in discussion of E2 and E3, to induce conversion into vulnerable vegetative forms, or by a higher organization of the BA-1 on the materials treated with microwaves.

Reactivity to chemical agents in a relevant environment is desirable in any material used for chemical and biological warfare agent protection. The M5 test measures reactivity and degradation in solution, but this is rarely considered a valid test since it is well known that solution chemistry provides for ideal contact conditions between the substrate and the chemical agent surrogate. M6 is a vapor permeation test that is much more realistic than the M5 test (Figure 25).

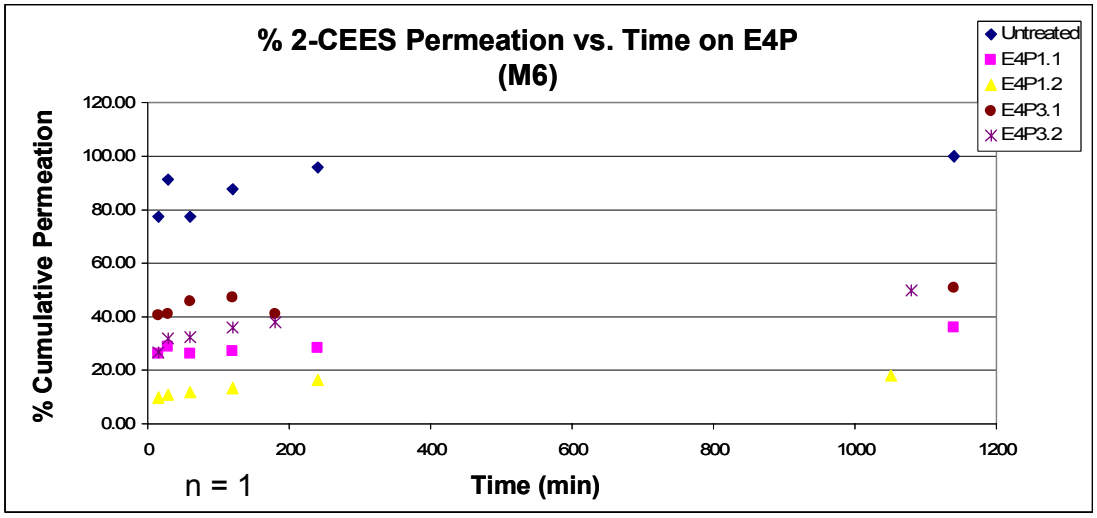

Figure 25. % 2-CEES Permeation vs. Time on E4P

The E4M5 data in Figure 25 show that all of the materials treated with chloramine-forming compounds demonstrated significant decreases in cumulative permeation of agent surrogate vapor compared to untreated

control fabrics. It is not surprising that the materials treated with nanoscale boehmite (P1.2 and P3.2) exhibited lower permeation than the equivalent materials without the boehmite (P1.1 and P3.1), since these materials possessed more active chlorine than their equivalent counterparts, and the boehmite possesses a high surface area that can slow permeation by acting as an adsorbent to the surrogate agent. GCMS data for the breakdown product are consistent for the sulfoxide analog of CEES. Natick Soldier Center verified that the breakdown products consist of ~94% CEES sulfoxide, ~3% CEES sulfone, and ~3% unidentified. That the primary product is the sulfoxide and not the sulfone is significant from a CWA protection aspect because HD sulfone is nearly as toxic as HD, while the HD sulfoxide is relatively nontoxic in comparison.[9, 10, 13] The M6 test was performed only with mustard agent surrogate because VX is non-volatile, and the E2M5 data revealed that the chloramine chemistry is inadequate for the destruction of diisopropyl fluorophosphonate (G-agent surrogate).

III.5—Experiment 5 Discussion:

To be of practical value, protection systems involving reactive chemistries must retain their reactivity during protracted storage or use in extreme environments. The E5 series of experiments was designed to establish a baseline of durability for the polymer-bound chloramines. Uneven coverage of boehmite across the fabric substrate is likely the cause of the significant variability in M4E5 data for boehmite-treated (E5P1.2 and E5P3.2) samples.

E5.1 Currently battlefield conditions are desert conditions. Desert temperatures commonly exceed 110 °F (43 °C) and can reach as high as 150 °F (66 °C) in cargo containers. Consequently, this experiment was designed to cover a range of temperatures up to 75 °C (167 °F). Figures 26–32 illustrate the rate of loss of chlorine equivalents from six boehmite–BA-1 adducts (prepared in experiment E2) during storage at room temperature, 50 °C and 75 °C, and recovery of activity after rechlorination.

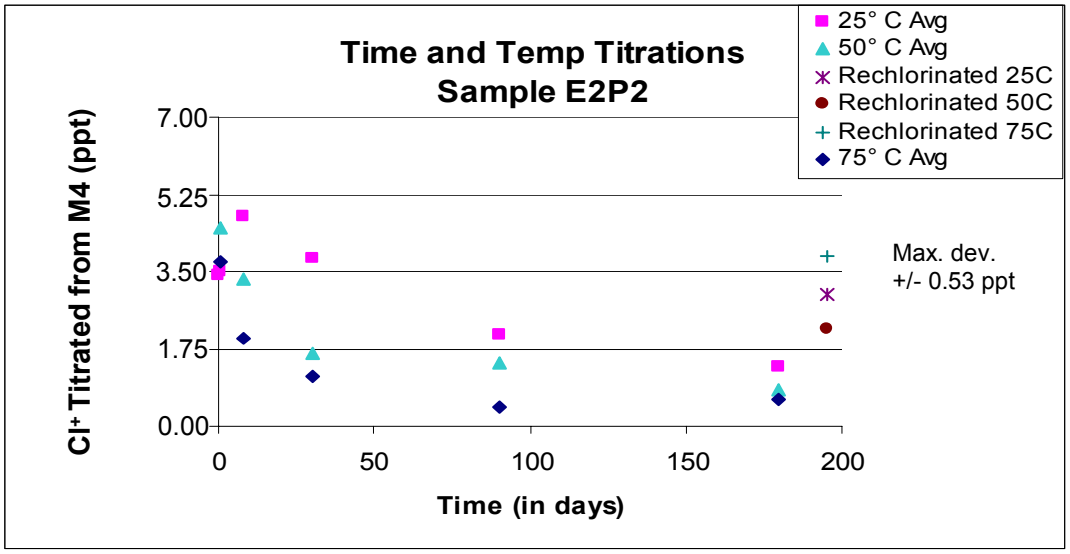

Figure 26. Loss of Chlorine from BA-1–Boehmite Nanoparticles E2P2 at Three Temperatures

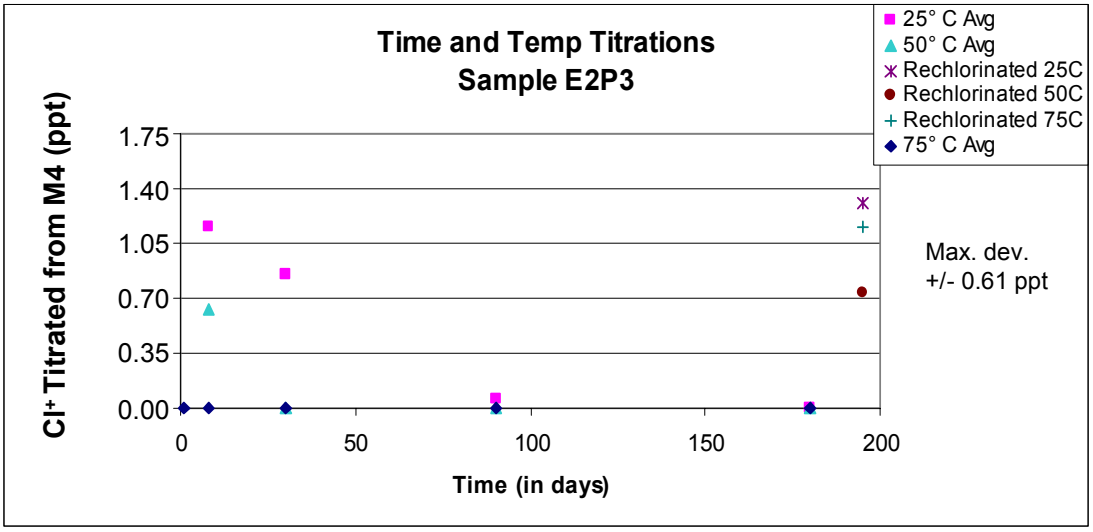

Figure 27. Loss of Chlorine from BA-1–Boehmite Nanoparticles E2P3 at Three Temperatures

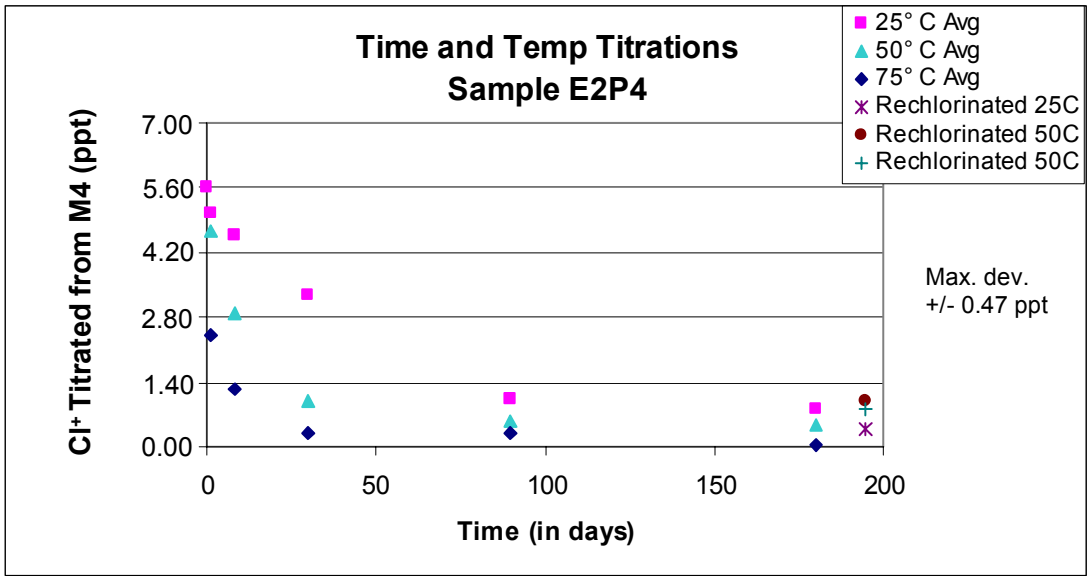

Figure 28. Loss of Chlorine from BA-1–Boehmite Nanoparticles E2P4 at Three Temperatures

The consistent observation in Figures 26–32 is that BA-1-modified boehmite gradually loses active chlorine over time at all three test temperatures, with rate of chlorine loss decreasing (from lower initial values) at higher temperature. This degradation is most likely caused by homolysis of the N–Cl by heat. This explanation is consistent the reactivity of other chloramides, such as N-chlorosuccinimide.[72] E2P2 and E2P6 demonstrated the highest temperature stability, retaining more than 0.5 ppt of active chlorine after 180 days at 75 °C. Additionally, upon rechlorination (procedure M1), E2P6 exhibited active chlorine values exceeding the time-zero active chlorine values. This indicates minimal degradation of the hydantoin ring, preserving higher availability of the chloramine-forming amide.

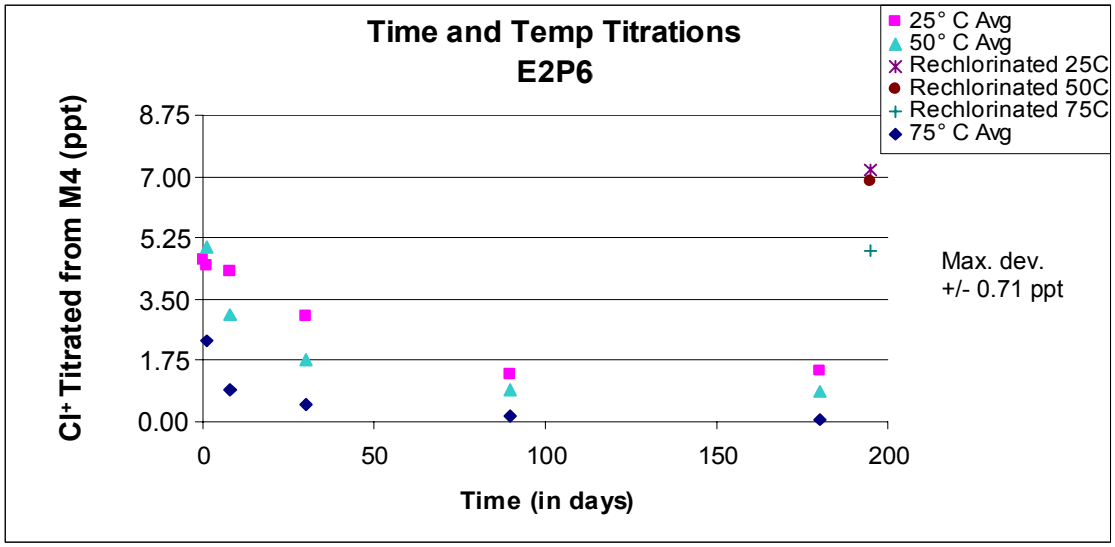

Figure 29. Loss of Chlorine from BA-1–Boehmite Nanoparticles E2P6 at Three Temperatures

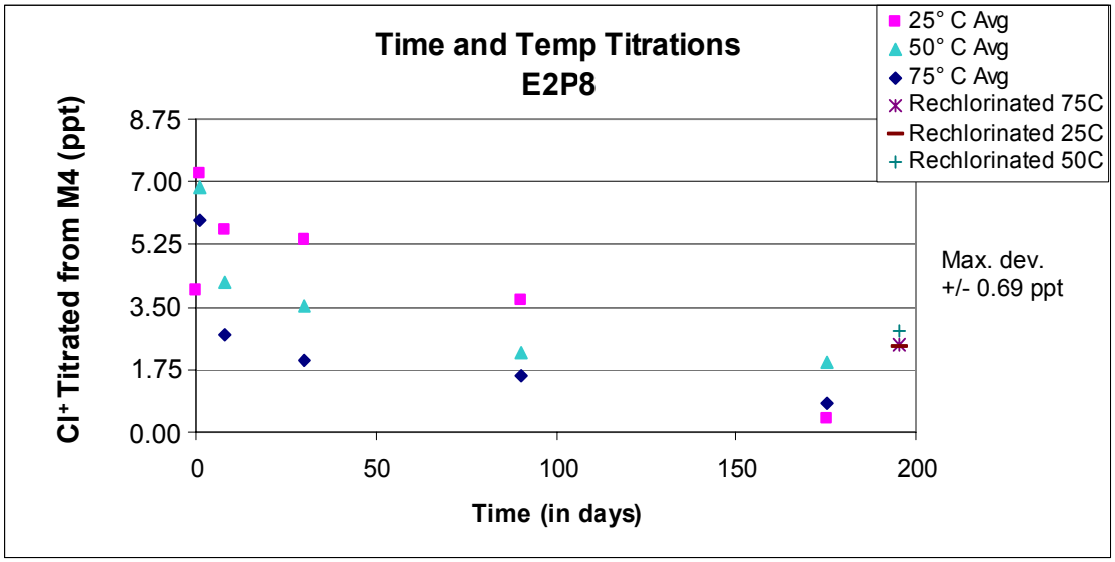

Figure 30. Loss of Chlorine from BA-1–Boehmite Nanoparticles E2P8 at Three Temperatures

Comparing to the E2 elemental analysis data in Table 2 to the corresponding data in Table 3 for E2P6 shows that 63% of the added hydantoin did not initially form the chloramine. Given that standards for storage stability typically specify a shelf life of 10 years or more, some form of matrix or supplemental stabilization will be needed if these adducts are to be used in practical protective equipment. The next three sets of experiments examine the adduct bound to swatches of BDU fabric.

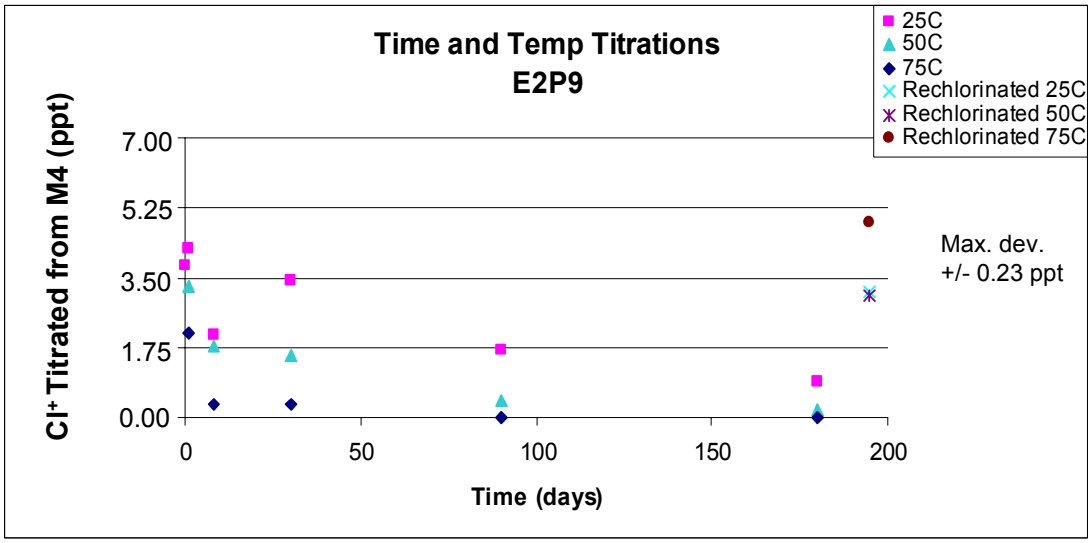

Figure 31. Loss of Chlorine from BA-1–Boehmite Nanoparticles E2P9 at Three Temperatures

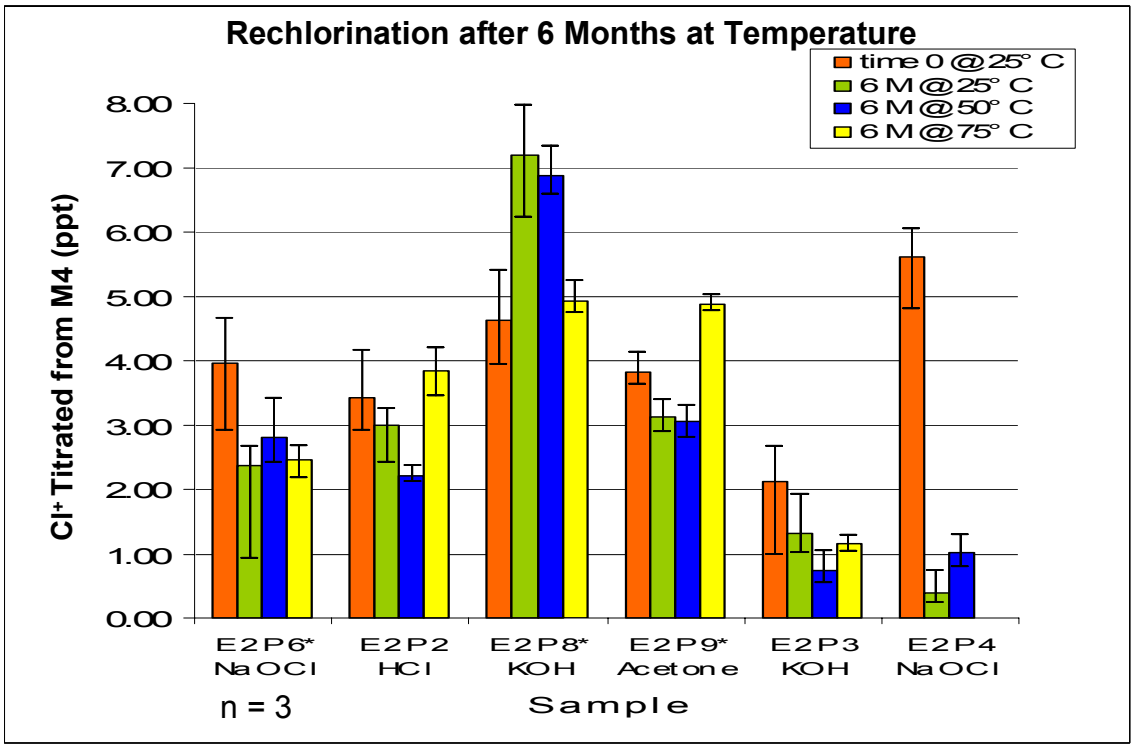

Figure 32. Recovery of Active Chlorine after Rechlorination of Heat-Inactivated BA-1–Boehmite Nanoparticles

E5.2–5.4 Current concept of operations requires that protective garments maintain their protection factor after one "cleaning." Although military protocol narrowly defines what constitutes "cleaning," this is often lost in translation in the field. Experiments E5.2–5.4 simulate conditions correlating to various "cleaning" methods.

E5.2 During a conventional wash cycle with detergent in chlorine-free water, BA-1-modified BDU fabrics E4P1.1, 2.1 and 3.1 retained 30~50% or greater active chlorine without the need for rechlorination (Figure 33). After two cycles in a conventional washing machine with detergent, followed by a rechlorination step, E4P1.1 recovered ~105%. E4P2.1 recovered ~50%, and

E4P3.1 recovered ~80% of the original active chlorine, as determined by M4 titration. The increased chlorine capacity of E4P1.1 is likely caused by a combination of the liberation of bound or occluded amide nitrogen and an increase in stability of the siloxane substrate graft compared to E4P2.1 and E4P3.1. The dramatic drop in active chlorine exhibited by E4P2.1 is likely caused by the "shedding" of unbonded BA-1-modified boehmite particles during the wash. Because the boehmite serves as a reservoir for the chloramide, a minimal loss of these particles will dramatically affect the active chlorine content of the treated materials.

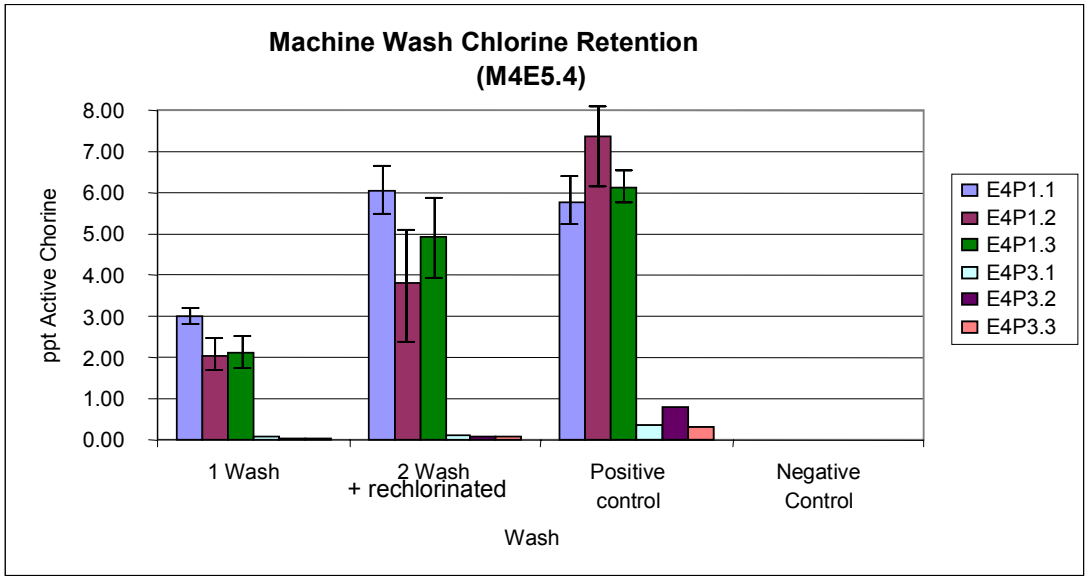

Figure 33. Retention of Chlorine by BA-1 and TTDD-Modified BDU Fabrics after Laundering

E5.3 Results from M5 titrations after prolonged boiling of the treated fabrics (Figure 34) demonstrated the moderate thermal instability of the bound chloramines in an aqueous environment: E4P1.1 retained ~60% (3.28 ppt),

E4P3.1 retained ~50% (0.33 ppt), E4P1.2 retained ~30% (2.02 ppt) and E4P3.2 retained ~30% (0.38 ppt) of their original active chlorine content after boiling for one hour. As in the preceding experiment, the dramatic loss of active chlorine within the boehmite-treated samples is attributed to shedding of unbound boehmite nanoparticles from the cloth during the experiment. This interpretation was supported by the recovery from the bottom of the boiling vessels from E4P1.2 and E4P3.2 of white powdery residues that yielded a positive M4 test for active chlorine. E5.3 was designed to include a rechlorination step followed by an M4 test of the fabric swatches, but the materials were lost during preparations for a mandatory hurricane evacuation.

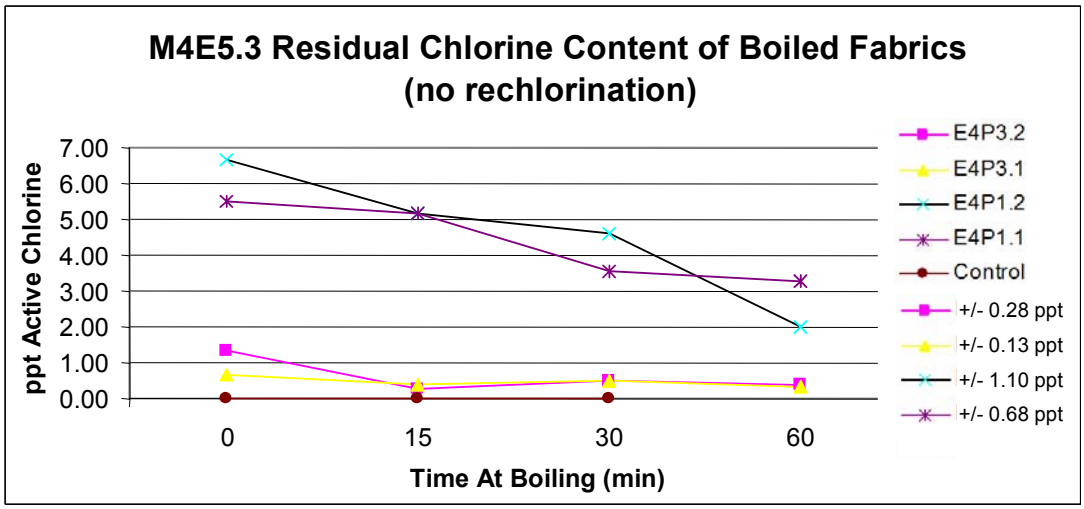

Figure 34. Loss of Chlorine from BA-1 and TTDD-Modified BDU Fabrics after Boiling Chlorinated Samples in Water

E5.4 examined the stability of the fabric-bound chloramines to steam. Neither of the materials treated with BA-1 (E4P1.1 and E4P1.2) exhibited residual chlorine after autoclaving, but the materials treated with TTDD (E4P3.1 and

E4P3.2) retained a measurable amount of active chlorine, ~14% (0.09 ppt) and ~18% (0.24 ppt), respectively (Figure 35). All four samples recovered significant activity upon rechlorination: E4P1.1 ~65% (3.70 ppt), E4P3.1 ~85% (0.54 ppt), E4P1.2 ~80% (5.24 ppt) and E4P3.2 ~90% (1.18 ppt) of their respective original active chlorine content, showing that the hydantoin rings were intact. The persistent activity of E4P3.1 and E4P3.2 is likely a result of chlorination of N-8 in the six-membered ring. Steric and inductive effects of the four methyl groups make this chloramine much more stable than the hydantoin ring chloramide.

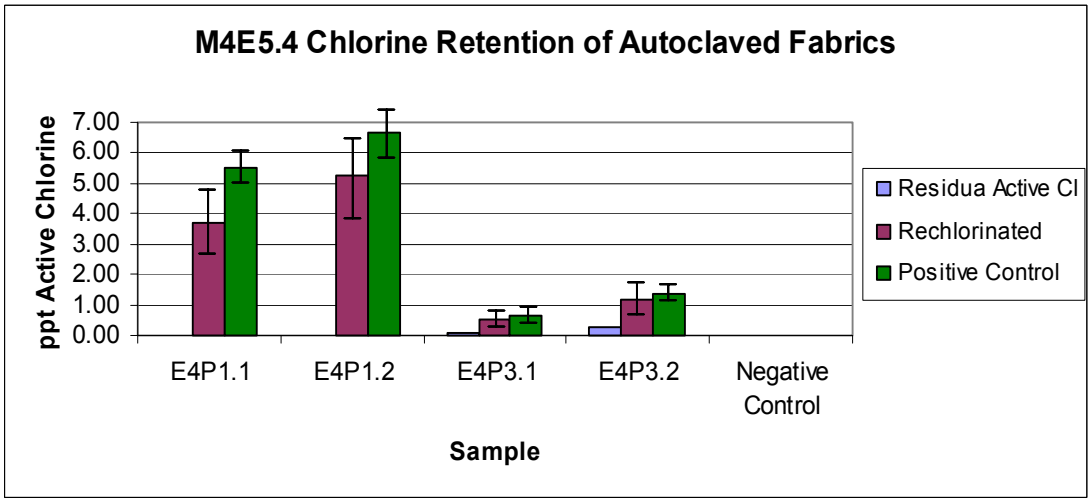

Figure 35. Loss of Chlorine from BA-1- and TTDD-Modified BDU Fabrics after Autoclaving Chlorinated Samples

The materials treated with boehmite exhibited a higher chlorine content compared to the treated materials without boehmite across all facets of E5.4. This suggests that, under E5.4 conditions, the boehmite is either acting as a reservoir for or stabilizing the active chlorine, and indicates that the boehmite-

bound chloramines exhibit greater stability than similar chloramines bound directly to the fabrics. These findings support the hypothesis presented in discussion of E2, that attachment to boehmite stabilizes the bound chloramines from heat and moisture degradation.

E5.5–5.6 Desert conditions are intensely sunny conditions. Sun damage is common in polymeric systems, causing fading and chain shortening of polymers.[71] Additionally, it is known that, in aqueous solution, chloramines degrade rapidly in sunlight.[72] These experiments were designed to provide a baseline of stability for chloramine-treated materials exposed to sunlight and weathering.

E5.5 Sunlight falling within the UV range of the electromagnetic spectrum contains the highest-energy photons that reach the earth's surface. This experiment measured UV-A degradation of treated materials under controlled laboratory conditions prior to an actual weathering test (Figure 36). After irradiation under a UV lamp for 24 hours, E4P1.1 retained ~20% (1.01 ppt), E4P3.1 none, E4P1.2 ~30% (0.99 ppt) and E4P3.2 ~20% (0.72 ppt) of their original active chlorine content. The modest increase in stability of each boehmite-bound chloramine is consistent with, but not conclusive evidence for, the hypothesis in E2 that the boehmite will stabilize and/or shield the bound chloramines from UV degradation.

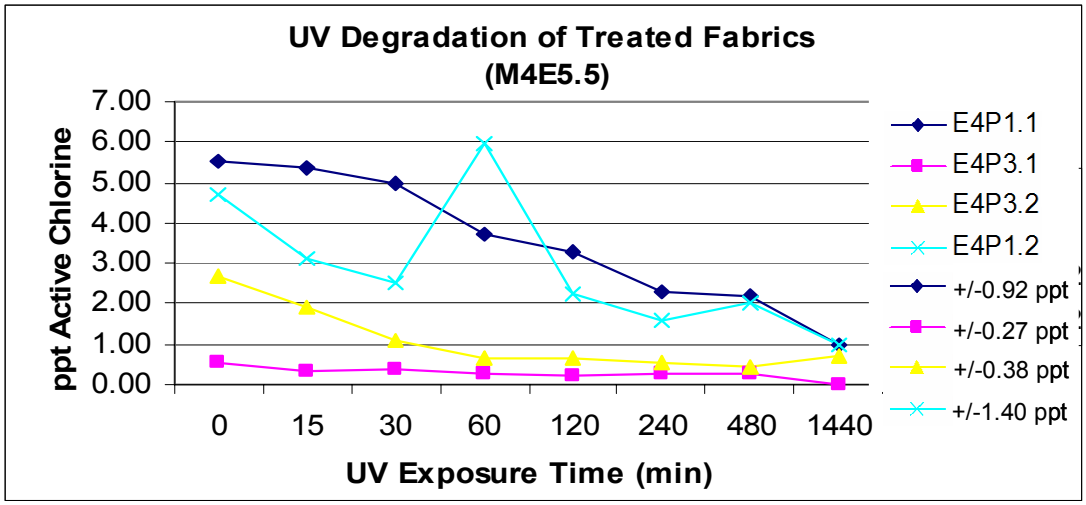

Figure 36. Loss of Chlorine from Chlorinated BA-1 and TTDD-Modified BDU Fabrics after Exposure to UV Radiation.

E5.6 Laboratory environmental conditions do not adequately represent the dynamic natural environment, which includes temperature, wind, rain, humidity, and sunlight exposure as variables. This experiment was designed to provide a weathering durability baseline for the treated materials. None of the materials in Figure 37 retained any active chlorine after 30 days of continuous exposure to the elements in the Florida summertime. E4P1.3 consistently exhibited higher active chlorine contents than any of the test samples through day 14.

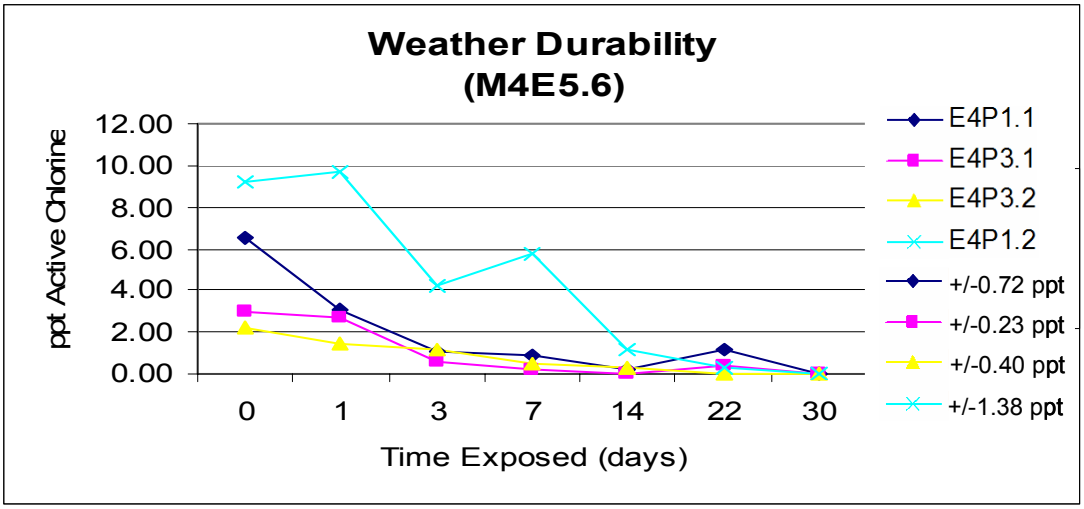

Figure 37. Loss of Chlorine from Chlorinated BA-1- and TTDD-Modified BDU Fabrics Exposed Outdoors.

All of the exposed samples took up a significant amount of active chlorine upon rechlorination according to procedure M1: E4P1.1 recovered ~65% (4.17 ppt), E4P1.2 ~30% (2.72 ppt), E4P3.1 ~75% (2.29) and E4P3.2 recovered ~65% (1.42 ppt) of the original active chlorine, as determined by M4 (Figure 38). The observation of significant rechlorination excludes decomposition of the hydantoin ring caused by UV-induced homolysis of the N–Cl bond as the principal mechanism of chlorine loss. The lower recovery of the boehmite-bound BA-1 adduct E4P1.2 may be caused in part by loss of unbound particles, and the TTDD derivatives started with lower initial activities, so it is possible that some of the "recovery" of the E4P3 fabrics involved exposing shrouded binding sites. However, one is left to conclude from this experiment that TTDD is at least as stable as BA-1 under the conditions of weathering experienced, and that boehmite did not measurably

stabilize either of the chloramines against degradation by the combination of UV, heat, and moisture experienced.

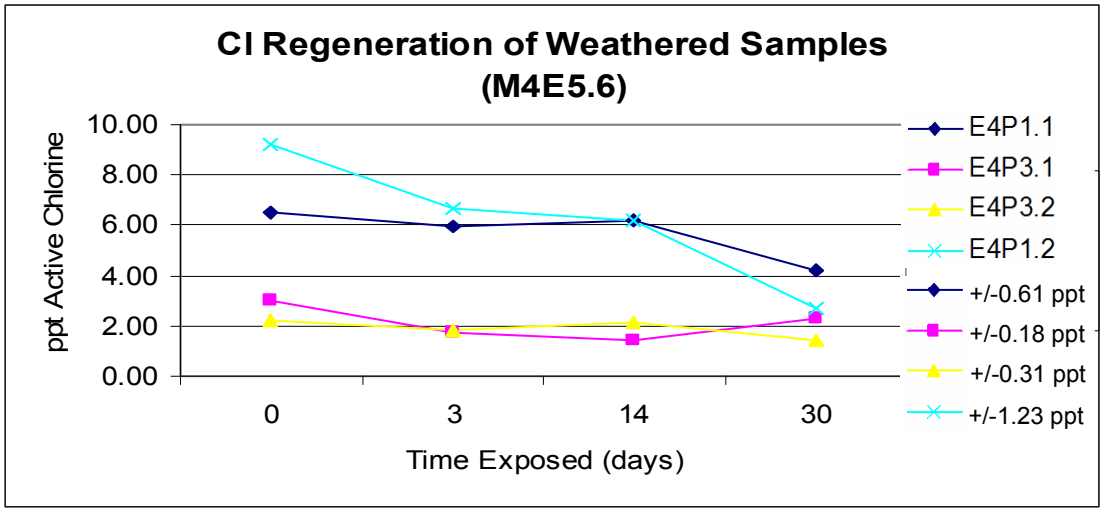

Figure 38. Uptake of Active Chlorine by BA-1 and TTDD-Modified BDU Fabrics after Weathering Outdoors

III.6—Experiment 6 Discussion:

The novelty and efficiency of the microwave-assisted siloxane grafting procedure spurred curiosity about the extent of its utility for other siloxanes and substrates. E6 explores the generality of this method with various substrates and siloxanes. Because boehmite is a Lewis acid, mechanism of reaction in this series of reactions is predicted to be nucleophilic attack of an oxygen atom (on silicon) at the aluminum atom, with subsequent release of the corresponding hydroxide, water, or alcohol.[63-a]

E6.1 This experiment examined the microwave-promoted reactivity of boehmite with a series of siloxanes and silanols, listed in Table 8. That the elemental analyses of all 11 examples (Table 9) revealed wt-% C significantly larger than untreated boehmite demonstrated that microwave-assisted addition of organosiloxanes to boehmite is not restricted to the organosiloxanes previously studied in this work.

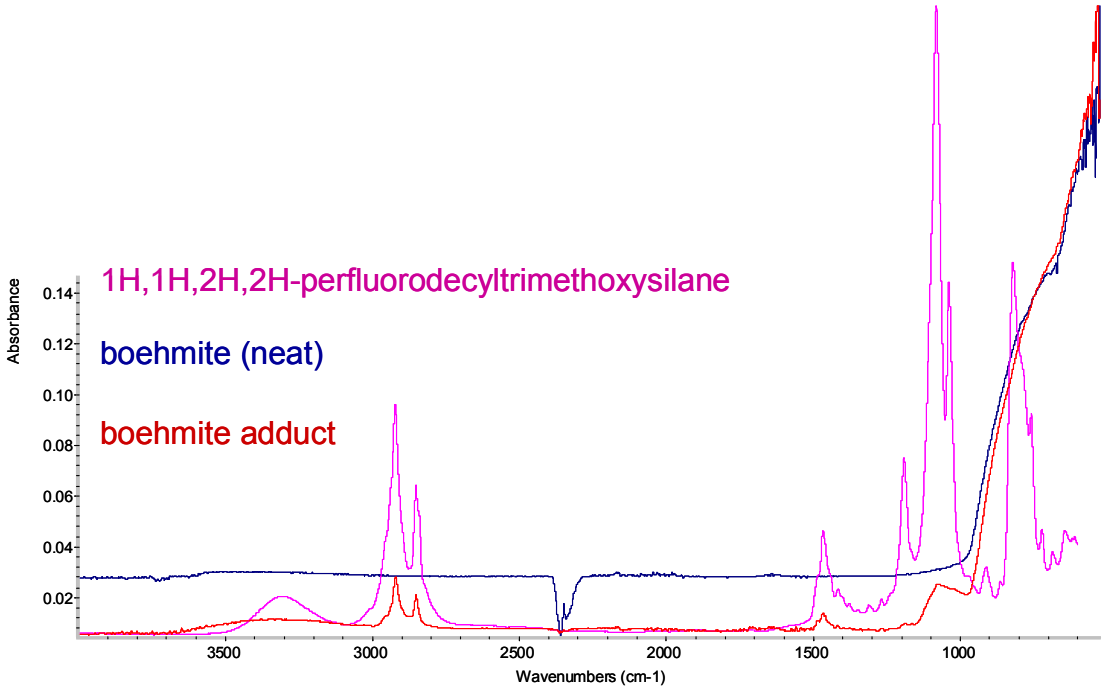

Figure 39. Example of a Typical Positive FTIR/ATR Result on Boehmite

Table 8. Elemental Analyses for Products of the Microwave-Promoted Reaction between Boehmite Nanoparticles and 11 Different Siloxanes or Silanols.

E6P	Siloxane	% C (EA)	% N (EA)	FTIR/ ATR	SD-C (EA) +/-	SD-N (EA) +/-
1.1	Octadecyltrimethoxysilane	1.985%	0.000%	+	0.004	
1.2	Methoxydimethyloctylsilane	1.268%	0.000%	+	0.007	
1.3	Triisopropylsilanol	1.988%	0.000%	+	0.004	
1.4	potassium trimethylsilanolate	0.680%	0.000%	-	0.008	
1.5	(3-chloropropyl)triethoxysilane	0.469%	0.000%	+	0.004	
1.6	(3-chloropropyl)dimethoxymethylsilane	0.570%	0.000%	+	0.010	
1.7	3-aminopropyltriethoxysilane	0.556%	1.827%	+/-	0.009	0.210
1.8	*N*-[3-trimethoxysilyl)propyl]-ethylenediamine	0.723%	1.175%	+/-	0.010	0.172
1.9	3-(trimethoxysilyl)propyl methacrylate	1.109%	0.000%	+	0.004	
1.10	3-glycidoxypropyltrimethoxysilane	1.059%	0.000%	+	0.010	
1.11	1H,1H,2H,2H-perfluorodecyltrimethoxysilane	N/A	N/A	+	N/A	N/A
	Negative Control (washed boehmite)	0.120%	0.082%	-	0.013	0.102

Table 9. Calculated Weight Addition of –Si-R from Carbon and Nitrogen Elemental Analysis.Assuming 3-Point Attachment (Figure 16).

E6P	Theor C (g)	Theor N (g)	Actual C (g)	Actual N (g)	C mol (xE-04) from Elemental Analysis	N mol (xE-03) from Elemental Analysis	Wt-%C from Elemental Analysis	Wt-%N from Elemental Analysis
1.1	0.2942	0.0000	0.0201	0.0000	0.930		2.593	
1.2	0.1454	0.0000	0.0128	0.0000	1.067		1.820	
1.3	0.1177	0.0000	0.0201	0.0000	1.859		2.897	
1.4	0.0665	0.0000	0.0068	0.0000	1.893		1.381	
1.5	0.0815	0.0000	0.0049	0.0000	1.328		1.390	
1.6	0.0740	0.0000	0.0058	0.0000	1.215		1.462	
1.7	0.0928	0.0361	0.0057	0.0185	1.591	1.323	1.356	11.27
1.8	0.1087	0.0507	0.0072	0.0118	1.205	0.420	1.559	5.43
1.9	0.1404	0.0000	0.0123	0.0000	1.463		2.057	
1.10	0.1369	0.0000	0.0108	0.0000	1.500		2.126	

Product E6P1.1 demonstrates the microwave addition of octadecyltrimethoxysilane, a hydrocarbon siloxane, to boehmite. Preparation of E6P1.1, 1.2, 1.5, and 1.6 demonstrated that microwave addition is also effective for siloxanes containing one, two, or three silyl ether functional groups, and that the chemistry works on methyl and ethyl silyl ethers. The molar equivalent yield from addition of (3-chloropropyl)triethoxysilane was 10% higher than for (3-chloropropyl)dimethoxymethylsilane. This difference was most likely caused by the presence of the third silyl ether group. Formation of products E6P1.3 and E6P1.4 demonstrated the ability of this microwave addition chemistry using silanols and silanolates. The addition of 3-(trimethoxysilyl)propyl methacrylate and 3-glycidoxypropylltrimethoxysilane without apparent interference from or change in functionality of the reactive

methacrylate or epoxide groups, as determined by FTIR diamond ATR, illustrates the precise selectivity of the chemistry.

In contrast, the corresponding products from addition of organosiloxanes containing amine groups yielded unexpeted FTIR diamond ATR spectra and elemental analysis C:N ratios that were much too low (~0.12 vs. ~2.6 predicted for E6P1.7 and ~0.36 vs ~1.9 predicted for E6P1.8) to be consistent with simple siloxane addition to an alumina particle. A competing process of nucleophilic attack of the amine nitrogen at an aluminum or silicon atom to form an aluminum or silicon nitride followed by hydrolytic cleavage of the propylsiloxane portion of the amine would yield ratios of negligible carbon and ~0.47 nitrogen, respectively, in much closer agreement with observed values. This route could also be invoked as contributing to the elevated wt-% N values observed for several of the E2 products.

E6.2 The complement to the preceding set of experiments, this set of tests qualitatively examined the products of microwave-promoted attachment of BA-1 to a wide array of diverse substrates, applying the M3 color assay after chlorination. The results, catalogued in Table 10, suggest that the microwave-assisted addition of BA-1 is a highly versatile method for attachment of siloxanes to polymeric substrates. A loose correlation can be discerned between hydroxyl content and M3 color intensity, which corresponds to active chlorine content. That hydroxyl-terminated hydroentangled nylon produces a positive M3 response, whereas nylon

hosiery, which contains no hydroxyl functional groups, did not produce a positive M3 response. This observation demonstrates a requirement for the availability of hydroxyl groups in the substrate.

Table 10. Qualitative Measurements of Active Chlorine Uptake by Polymeric Substrates after Microwave Promoted Attachment of BA-1 and Chlorination According to M1.

E6P	Substrate	M3 Color (no indicator)	M3 Color (indicator)
2.1	activated aluminum oxide (neutral *p*H)	lt yellow	dark blue
2.2	silica gel	lt yellow	dark blue
2.3	borosilicate glass beads	yellow	black
2.4	titanium dioxide	dk yellow	black
2.5	$Mg_3SiO_{10}(OH)_2$ (talc)	lt yellow	dark blue
2.6	$CaAl_2O_{10}(OH)_2$ (montmorillonite)	dk brown	black
2.7	$Al_2 Si_2O_5(OH)_4$ (kaolinite)	dk brown	black
2.8	$(Mg_2,Fe_2^{++},Al_4)_3Si_4O_{10}(OH)_2 \cdot 4(H_2O)$, (vermiculite)	dk brown	black
2.9	$(Na_{16})(Al_{16}Si_{24}O_{80}) \bullet 16H_2O$ (zeolite)	dk brown	black
2.10	cotton fabric 100%	dk brown	black
2.11	raw wool	lit yellow	dark blue
2.12	cured cowhide leather	dk brown	dark blue
2.13	nylon hosiery	none	none
2.14	hydroentangled hydroxyl-terminated nylon	dk yellow	black

III.7—Experiment 7 Discussion:

This series of experiments was designed to prepare small siloxane–substrate model compounds using the microwave-mediated coupling. Because of the novel nature of the siloxane and silanol chemistry developed in this study, it was necessary to prepare and characterize one or more model examples of the chemistry that can then represent a broad category of compounds for which this chemistry can be applied. All work up to this point was performed on polymer matrices. Unfortunately, the size and available variability in cross-linking within these polymeric systems makes it impracticable to try to obtain a pure compound that can be accurately and reproducibly synthesized, and thus also impossible for the chemical structure to be discerned with any degree of confidence. Consequently, this task was undertaken to identify compounds that would undergo representative reactions and still provide consistently pure, isolable products for analysis. This task proved much more difficult than originally anticipated.

E7.1–E7.2 Since the reaction of BA-1 with cellulose occurs fastest at the O-6 position of cellulose (the only primary alcohol within the polymer), methyl α-D-glucopyranoside, a monomeric, hydrolytically stable compound comparable to one repeating unit of cellulose (Figure 40) was chosen as a first attempt at model compound synthesis (Figure 41). Glucose could not be used because it is a hemiacetal, so the anomeric OH is labile and pyranose–furanose ring isomerization occurs readily in solution.

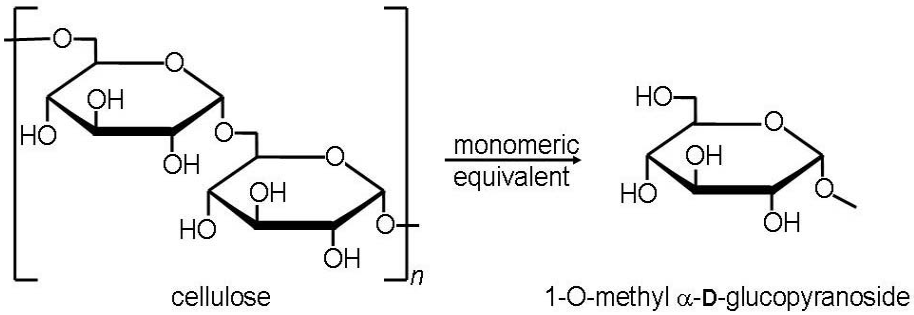

Figure 40. Structures of Cellulose and α-Methyl Glucoside

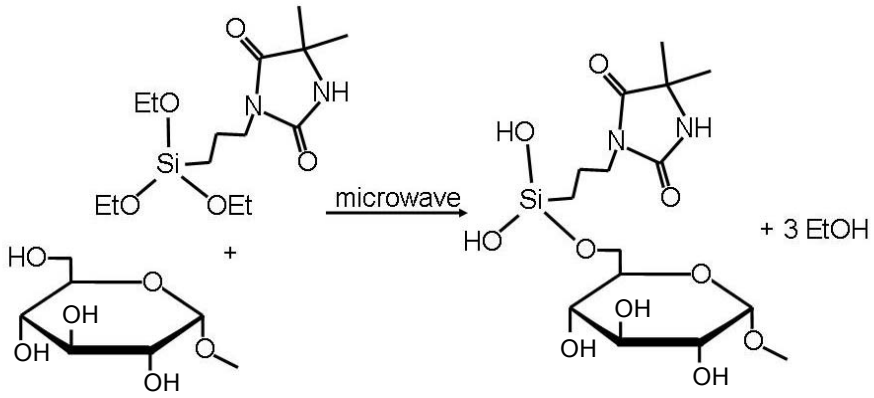

Figure 41. Proposed Reaction Scheme between
BA-1 and α-Methyl Glucoside

Unfortunately, based on the physical characteristics of the products—broad melting range, the glass-like texture, and the insolubility in organic solvents, it was apparent that uncontrolled cross-linking resulted in random polymerization (Figure 42).

While theoretically this cross-linking should be controllable by stoichiometry, solvent dilution, and the rate at which BA-1 is added to the reaction mixture, in practice every attempt led to the cross-linked product. When chlorinated

according to M1, resultant polymers were able to oxidize iodide from KI to elemental iodine, signifying that the amines were still intact and able to form the chloramine derivative. Additionally, two strong peaks at approximately 1750 cm^{-1} were detected in the FTIR spectra of the samples, representing the two amide carbonyls from the bound hydantoin and further supporting the conclusion that the hydantoin ring was still intact.

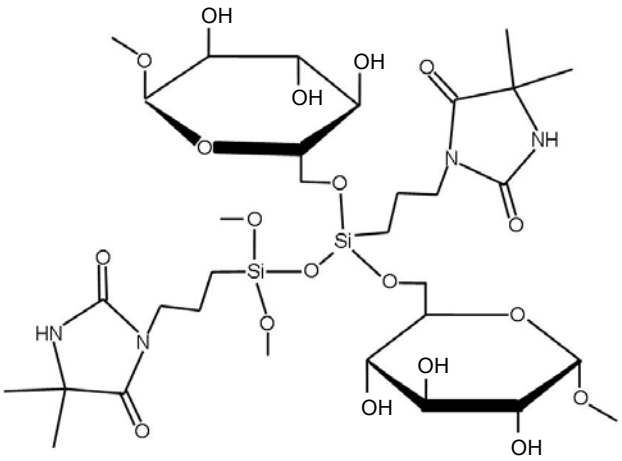

Figure 42. Example of Uncontrolled Cross-linking between BA-1 and α-Methyl Glucoside

E7.3 It is known that siloxane reagents are prone to polymerizing upon exposure to moisture. At this point the monomeric purity of the BA-1 was questioned. To alleviate concerns, the equivalent reaction was performed with a fresh bottle of 3-aminopropyltriethoxysilane (>99.0 %) resulting, once again, in a glass-like polymer with similar physical characterstics. The FTIR spectroscopic data indicated the presence of a primary amine, signifying that

the amine functionality did not significantly participate in the polymeric cross-linking.

E7.4 – E7.11 To achieve a relatively pure and low-molecular-weight compound to analyze, it was necessary to inhibit cross-linking and to maintain quality control with regard to the purity of the siloxanes. Consequently, commercially available 3-aminopropyltriethoxysilane (>99.0 %; APS) was used as a suitable siloxane to ensure quality control. Glycerol and ethylene glycol were identified as reactants that could result in bonding to all three of the silyl ether oxygens in the siloxanes. In addition to possessing primary and secondary hydroxyl groups that are relatively similar to the hydroxyl groups found in cellulose, the second and third intramolecular siloxane couplings with glycerol would form a spirosilicate containing two interconnected, five-membered rings. The expectation was that because the coupling to either of these two compounds would result in an intramolecular ring closure reaction and the formation of two kinetically favored five-membered rings, this reaction should occur much faster than competing intermolecular reactions (Figure 43).

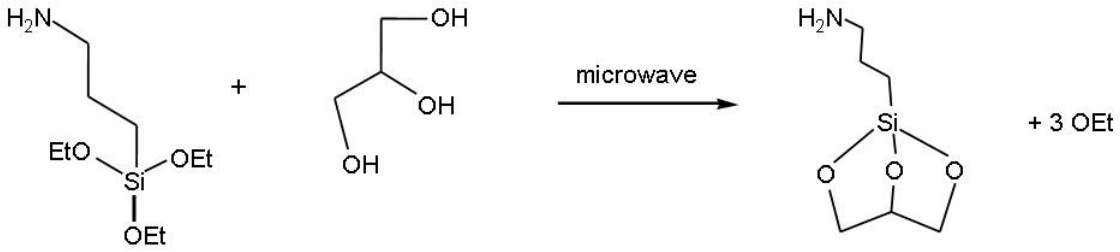

Figure 43. Proposed Reaction Scheme between Glycerol and Aminopropyltriethoxysilane

In the case of ethylene glycol, using a 1.5:1.0 molar ratio of ethylene glycol to siloxane, the formation of a silicate dimer (Figure 44) was expected.

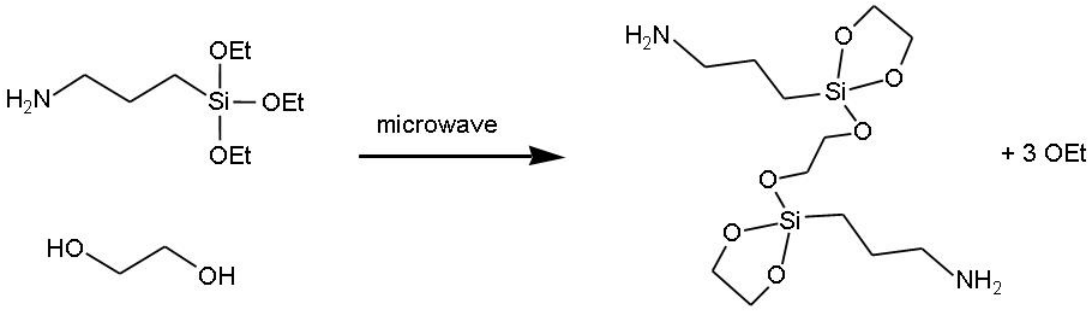

Figure 44. Proposed Reaction Scheme between Ethylene Glycol and Aminopropyltriethoxysilane

Neither of these reaction attempts resulted in products whose structures could be analytically confirmed. However, it is significant to note that the crystalline products observed transiently in experiments involving ethylene glycol are atypical of the equivalent base-catalyzed reaction using conventional heating, which yields a viscous polymeric liquid.[18, 60-62] Unfortunately, upon exposure to air these crystals and crystalline solids liquefied into viscous oils. The ^{1}H NMR of these products yield spectra

consistent with a polymer—broad, undifferentiated signals, particularly at the key protons bonded to the crosslinking agents. Consequently, the narrow signal near δ 3.4, corresponding to the two geminal protons that would have definitively identified the structure as the ethylene glycol spirosilicate, was not apparent. Products from the acid-catalyzed, base- catalyzed, hypochlorite-catalyzed, and neat microwave-promoted reactions involving ethylene glycol and glycerol yielded FTIR diamond ATR spectra within each respective reaction series that were nearly indistinguishable from one another. This signifies that the microwave chemistry proceeds in the absence of chemical catalysts, and proceeds independent of pH conditions. The FTIR spectroscopic data from all of the products involving APS indicated the presence of a primary amine, signifying that the amine functionality did not significantly participate in the polymeric cross-linking.

E7.12–E7.14 Several attempts to synthesize caged siloxane compounds using a triol, such as glycerol, have been reported in the literature, but none were successful when coupling was attempted through tetrahedral geometry. Bond angle strain induced from the vacant 3*d* orbital inhibits the formation of caged siloxanes with tetrahedral geometries.[73] However, hypervalent compounds with pentacoordinate and hexacoordinate caged siloxane compounds are well known.[18, 40-43, 50, 52, 53, 60-62, 74-78]

E7.12–E7.13 According to precedents for the preparation of crystalline bis(catechol)silane derivative, APS was combined with two equivalents of catechol, quickly forming solid product E7P12, respectively, which was characterized by ^{1}H nmr spectroscopy (Figure 45).[44, 53]

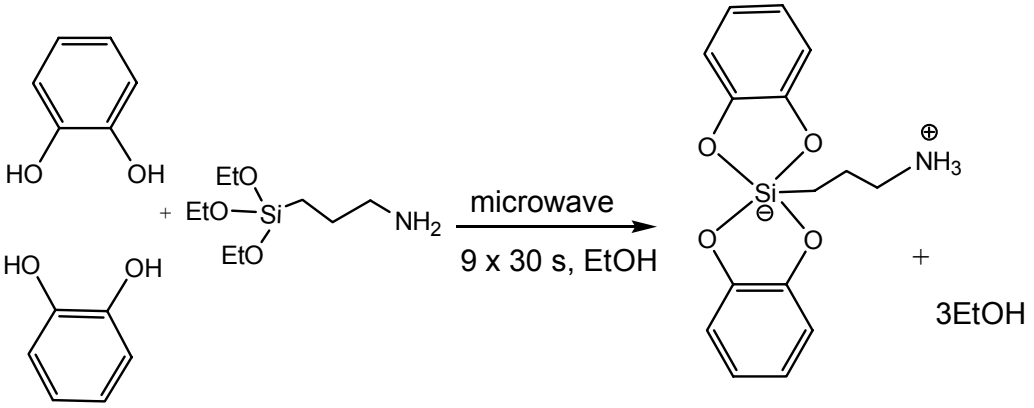

bis(1,2-phenylenedioxy)-(3-aminopropyl)silane

Figure 45. Reaction for the Synthesis of E7P12

E7.14 Again according to a precedent— for a reported triethanolamine–siloxane adduct—APS and triethanolamine were combined and reacted in a few minutes in the microwave to form a solid that was characterized as E7P14 by nmr spectroscopy and mass spectrometry.[53, 74-76] After recrystallization, a single-crystal X-ray diffraction determination yielded the structure in Figure 46, in which the extended conformation of the sidechain shows that cyclization by coordination of the $–NH_2$ group from the aminopropyltriethoxysilane with Si does not occur in the solid phase, and that the short Si–N distance, 2.176 Å, corresponding to the N in the triethanolamine, clearly indicates a bonding relationship.[75, 79]

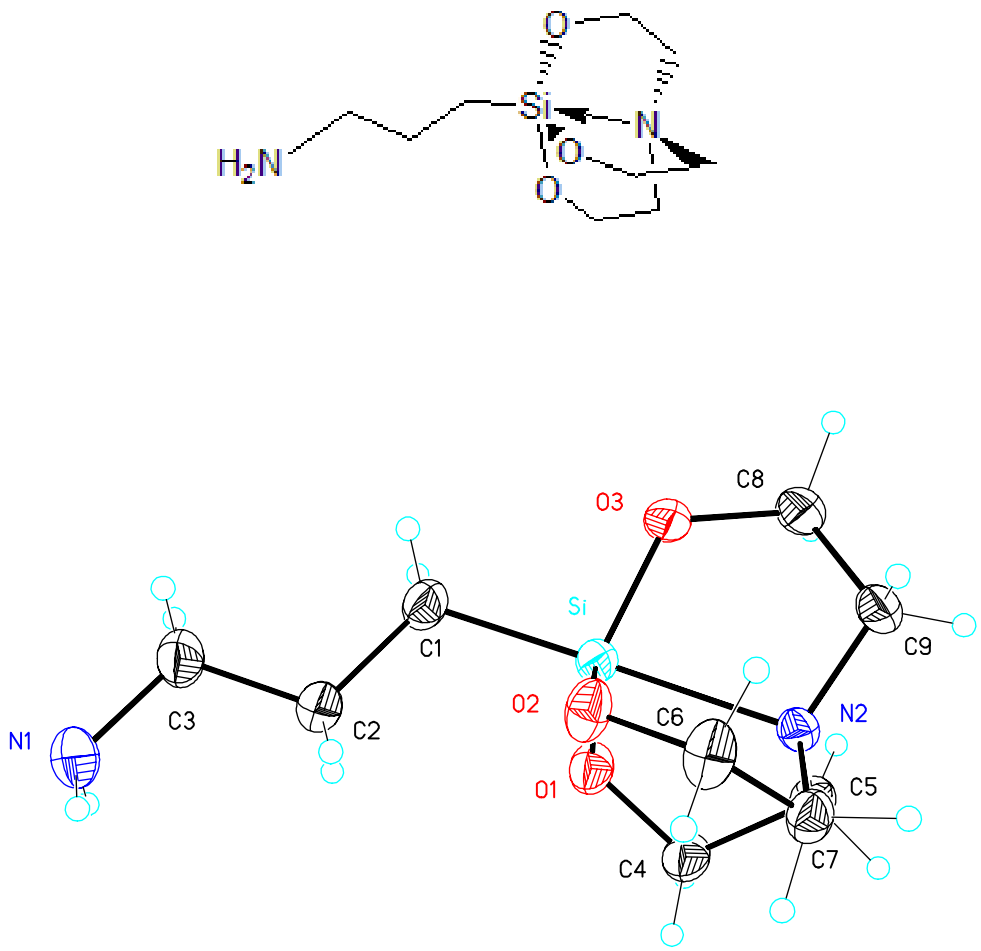

3-(2,8,9-trioxa-5-aza-1-sila-bicyclo[3.3.3]undecan-1-yl)propan-1-amine
$C_9H_{20}N_2O_3Si$
Exact Mass: 232.1243
Mol. Wt.: 232.3522
m/e: 232.1243 (100.0%), 233.1277 (9.7%), 233.1239 (5.1%), 234.1212 (3.3%)
C, 46.52; H, 8.68; N, 12.06; O, 20.66; Si, 12.09

Figure 46. X-Ray Crystallographic Structure of E7P14

Table 11. Bond lengths [Å] and angles [°] about the silicon in E7P14 from X-Ray Crystallography Data.

Atoms comprising the bond angle	Bond angle around Si in degrees (+/-)	Si-X Ligand	Bond Length in Å (+/-)
O3-Si-O2	117.17(8)	Si-O3	1.670(1)
O3-Si-O1	118.75(8)	Si-O2	1.673(1)
O2-Si-O1	119.53(8)	Si-O1	1.677(1)
O3-Si-C1	97.53(8)	Si-C1	1.878(2)
O2-Si-C1	96.47(8)	Si-N2	2.176(2)
O1-Si-C1	97.38(9)		
O3-Si-N2	83.27(7)		
O2-Si-N2	82.82(6)		
O1-Si-N2	82.55(6)		
C1-Si-N2	179.11(8)		

Table 12. Average bond lengths [Å] and angles [°] for the ring system in E7P14.

Atoms comprising the bond angle	Bond angle around Si in degrees (+/-)	Si-X Ligand	Bond Length in Å (+/-)
Si-O-C	122.6(1)	Si-O	1.673(2)
O-C-C	108.8(2)	O-C	1.423(2)
C-C-N	106.0(2)	C-C	1.522(3)
C-N-Si	105.1(1)	C-N	1.472(2)
N-Si-O	82.88(7)		
O-Si-O	118.48(8)		
C-N-C	113.5(2)		

The bond lengths and bond angles in E7P14 are consistent with historical reference.[52] The Si ← N interaction in silatranes presents an atypical bond in many respects, and the extraordinary chemical properties of silatranes have been attributed to the unusual electronic structure imposed by the polycyclic ring system. In the solid-state, the length of the Si ← N bond varies from 1.97 to 2.24 Å and is strongly influenced by the nature of the

trans-substituent.[76] This bond-length has been calculated to increase in the gas phase, typically by 0.28 Å relative to solid-state determinations.[50] This bonding-interaction is shorter than the sum of the van der Waals radii (~3.5 Å) but longer than those found for Si – N bonding interactions in typical tetravalent Si systems (~1.7 Å).[52] The increase in ligand bond lenths reflects the increased Lewis acidity of the hypervalent system. Consequently, the ligands of the hypervalent species possess greater electron density is compared to their tetracoordinate counterparts. [75-78]

Table 13. E7P14 Bond Lengths and Angles Compared to Other Cited Silatrane Work.

X =	Si-N length in Å	Si-O Ave.	Reference
H	2.15		Greenberg, A.; Wu, G. Struct. Chem. 1990, I , 79-85.
OEt	2.11		Iwamiya, J. H.; Maciel, G. E. J. Am. Chem. SOC. 1993,115,6835-6842.
SCN	2.01		Narula, S. P.; Shankar, R.; Kumar, M.; Chadha, R. K.; Janaik, C. Inorg. Chem. 1997, 36, 1268-1273.
Cl	2.02		Voronkov, M. G.; Baryshok, V. P.; Petukhov, L. P.; Rahklin, R. G.; Pestunovich, V. A. J. Organomet. Chem. 1988, 358, 39-55.
F	2.04		Voronkov, M. G.; Baryshok, V. P.; Petukhov, L. P.; Rahklin, R. G.; Pestunovich, V. A. J. Organomet. Chem. 1988, 358, 39-55.
Me	2.18	1.68	Matters, R.; Fenske, D.; Tebbe, K. F. Chem. Ber. 1972, 105, 2089.
$CH_2CH_2CH_2NH_2$	2.176	1.673	this work

An early hypothesis during this program of study had attributed the increased biocidal efficacy in BA-1–boehmite powders E4P1.1 and E4P1.2 (compared to the heat-prepared equivalent product) to a polarization of the lone pair electrons from an amide carbonyl to form a weak coordinate covalent interaction with the silicon and ultimately rearranging to form a bicyclo[7.5] zwitterion (Figure 47). Seven-membered-ring closure is not

usually entropically favored, but the rigid arrangement of four of the seven atoms and the inclusion of the Si atom were considered possible mitigating factors. However, the absence of evidence for formation of the more-favored five-membered ring by E7P14 does not support the existence of the proposed zwitterions (Figure 48).

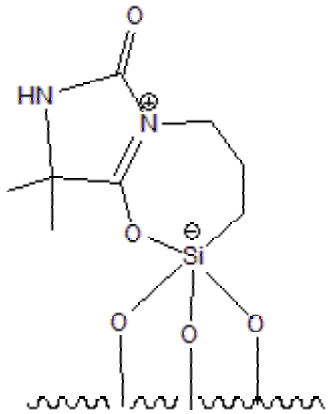

Figure 47. Initially Proposed Structure from the Reaction Between BA-1 and Boehmite

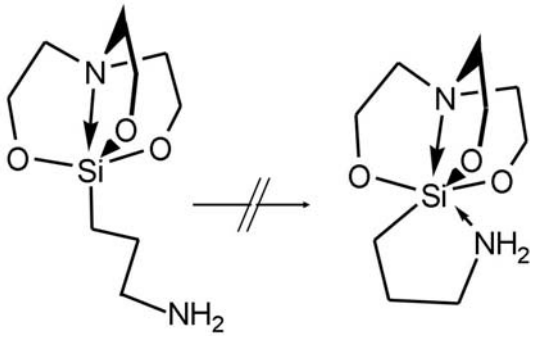

Figure 48. Model Compound Empirical Evidence does not Support the Formation of the Aforementioned Zwitterion (Figure 47)

The products from experiments E7.12–E7.14 illustrate the microwave-promoted synthesis of hypercoordinate silicon compounds in >90% yield with reaction times of <5 minutes, a >35% improvement to yield over the equivalent classical preparation of the compound by C. L. Frye, which represents a considerable improvement over these classical conditions. [42] Thus, this result begs the question as to whether or not the chemistry can be advantageously applied to the synthesis of other hypervalent compounds, and raises a question as to the mechanism of action responsible for this dramatic increase. Unfortunately, the considerable academic debate over the presence, or lack thereof, of nonthermal effects underscores the relative infancy of microwave promoted synthetic chemistry in comparison to its conventional counterpart.[32-38, 80] The ethanol solvent condition, coupled with the highly polar nature of all of the reactants, under which this set of reactions was carried out, necessitates a degree of dielectric heating. While recognized as important in microwave promoted chemistry, it is as yet unclear what roll the solvation complex plays within these reactions.[38] Additionally, it is well known that solid substrates are locked into a rigid lattice, and cannot contribute to orientational polarization, but, can lower the potential energy required for a reaction, by interacting with neighbors within the lattice.[38] These are important issues to consider within this set of reactions because, while it is not clear when crystal nucleation occurs during each of these reactions, once it does, the conditions within the reaction, and the mechanisms that drive the reaction may change considerably.

Finally, the reaction products in E7P12-14 satisfy the requirement for model compounds showing the C–O–Si linkages proposed throughout this dissertation as products from the microwave-assisted addition of siloxanes to alcohols.

III.8 Comparison of Thermal and Microwave-Induced Siloxane Reactions

A holistic review of the data from experiments E2–E7 reveals consistent empirical evidence that the microwave siloxane chemistry can produce products discretely different from the heat-treated analogs:

- In E2 the microwave chemistry demonstrated that addition of BA-1 could be achieved independent of acid or base catalysis; that the heat treated analog products yielded higher C:N ratios; and that, according to the elemental analysis data, the *ds* of BA-1 onto the boehmite was consistently higher than the heat treated analog—yet the % of chloramine-forming functionality from M4 data compared to *ds* of BA-1 from elemental analysis data of the same was consistently lower than for the heat-treated analog.

- In E3 BDU fabrics treated with BA-1 in the presence of microwaves consistently yielded higher active chlorine than their heat-treated analogs.

- In E4 BDU fabric treated with BA-1 in the presence of microwaves demonstrated inactivation of *Bacillus* spores, whereas the heat-treated analog containing similar amounts of active chlorine did not; a similar result is present for TTDD-treated BDU materials and *Aspergillus*.

- E5 materials treated using microwaves displayed different characteristic UV, heat, and moisture stabilities compared to heat-treated analogs.

- In E6 an epoxide functionality was attached using microwaves without opening the epoxide to a diol, as would be expected if an analogous heat treatment were employed.[72]

- In E7 neat reactions of appropriate siloxanes and alcohols produced higher yields of hypervalent product compared to conventional reactions of this type.

IV. CONCLUSIONS

The E1 set of experiments verified that the known broad-spectrum antimicrobial properties of 1-chloro-5,5-dimethylhydantoin are preserved in polymeric derivatives of BA-1. They also demonstrated the promising ability of these chloramines to oxidize reduced sulfur compounds to the corresponding S→O products. The examples selected for study suggest that this property may be of value in neutralizing the chemical agent HD, but its utility against VX is uncertain.

Attachment of BA-1 to the ceramic nanoparticle boehmite comprised a step forward in antimicrobial science and technology, enabling the use of sol–gel methods to prepare a wide spectrum of composite antimicrobial materials, the scope of which was shown in experiment sets E5 and E6 to be expansive. The extensive exploration of reaction conditions in experiment E2 established practical reaction conditions to accomplish addition of BA-1 and other siloxanes to boehmite in high yield and with preservation of most of the hydantoin functionality. Similar optimization of the coupling of other siloxanes to –OH or the –O– of –OR groups in other polymeric substrates will be straightforward and is left to succeeding generations to accomplish.

The principal contribution from this program of study derived from recognition of the highly beneficial influence of applying sufficient quantities of microwave energy to Si–O bonds in siloxane reagents upon siloxane-coupling reactions performed in nonabsorbing media. Systematic development of this observation produced a practical, general route for synthesis of composite polymers with reactive functionality. Among the latter, the BA-1-treated Battle Dress Uniform (BDU) fabric prepared in experiment E4 is of immediate interest as a possible material for use in daily-wear garments providing a moderate measure of protection from chemical and biological warfare agents.

A basic contribution to understanding the alumina–siloxane chemistry came from the quest for, and eventual preparation of, characterizable small molecules as products. The failure of α-methyl glucoside to produce a monomeric product suggested that it would be prudent to target a cyclic product, and the subsequent failures with glycerol and ethylene glycol, ideal simple substrates for forming three Si–O bonds to an Si center, triggered a detailed search for examples of cyclic siloxanes, whence precedents were found that suggested successful routes to three crystalline solids, all containing a hypervalent Si center—of which one, after patient recrystallization, yielded a single crystal of sufficient quality for a definitive structure determination by X-ray crystallography.

The simplest substructure consistent with the sol–gel chemistry performed and with the structures of the solid products prepared is the

tricyclic configuration illustrated below, which is structurally similar to the hydrocarbon adamantane. Although evidence herein is far from conclusive for this structure, it is consistent with all of the information at hand and it (R = 5,5-dimethylhydantoin-3-yl) is therefore proposed to describe the BA-1–boehmite adduct. It is left to subsequent investigators to confirm or revise this assignment.

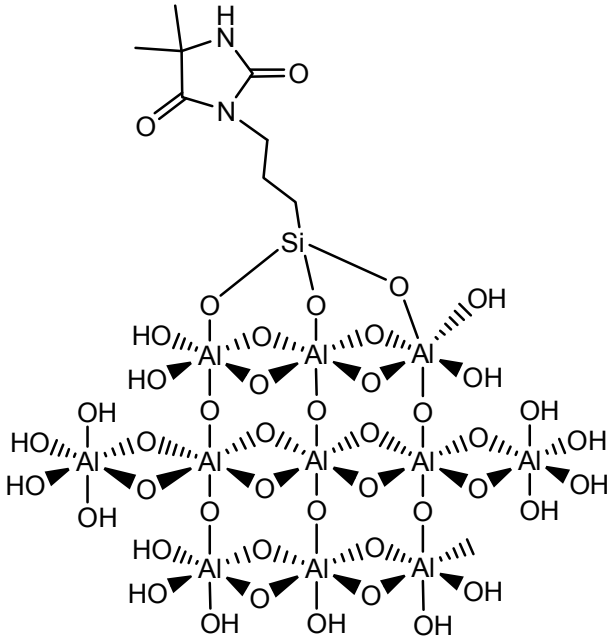

Figure 49. Proposed Structure of BA-1 Modified Boehmite

V. RECOMMENDATIONS FOR FUTURE WORK

A rich array of opportunities exists to expand on this work, particularly in expanding our understanding of the differences between microwave irradiation and conventional heating. It is speculated that the application of microwaves facilitates polarization of the d-orbital of silicon, and that this polarization is, at least in part, responsible for the dramatic increases in the degree of substitution, particularly in the case of the formation of hypervalent silicon species. A thorough investigation using *ab initio* molecular modeling would confirm this assumption, as well as providing a better understanding of the effects of microwaves on the molecular orbitals of various siloxanes. Ideally, empirical experiments would be designed to test the results of the model as a second step. The logical next step entails building a semi-empirical model and expanding the model to include solvent and substrate effects, which should include as a parameter microwave absorbency of the solvents and substrates. Once such a model can predict the results reported in this work, it will both provide a deeper understanding of the questions that have arisen from it and it will spawn additional topics for laboratory investigation.

REFERENCES

1. Cornwell, J., *Hitler's Scientists: Science, War, and the Devil's Pact*. 2003: Penguin Group.
2. Cordesman, A.H., *Asymmetric and Terrorist Attacks with Chemical Weapons*, in *Defending America*. 2001, Center for Strategic and International Studies.
3. Panel, A., *National Strategy: Assessment of Domestic Response Capabilities for Terrorism Involving Weapons of Mass Destruction*, in *Report to the President and Congress*. 2004. p. 1-191.
4. Day, S.E., *DS2: Development, Improvements, and Replacements*. D.T.I. Center, Editor. 1996, Defense Technical Information Center. p. 7-35.
5. Donahue, K.L., *Chemical and Biological Barrier Materials for Collective Protection Shelters*. 2003, Soldier and Biological Chemical Command: Natick, MA. p. 1-10.
6. *Final FY 2004 GPRA Annual Performance Plan*, U.S.D.o.H.a.H. Services, Editor. 2003, Center for Disease Control.
7. *Joint Service Functional Concept of Operations*, D.o. Defense, Editor. 2004, Joint Requirements & Inetegration Office. p. 1-22.
8. Coleman, D.R.; Thomas, T.R., *Application of Reactive Mircrocapsules for Deactivation of Toxic Agents*. D.T.I. Center, Editor. 1983, Defense Technical Information Center. p. 10-52.
9. Yang, Y.-C.; Baker, J.A.; Ward, R.J., *Decontamination of Chemical Warfare Agents.* Chemistry Reviews, 1992. 92: p. 1729-1743.
10. Yang, Y.-C.; Wagner, G.W., *Rapid Nucleophilic/Oxidative Decontamination of Chemical Warfare Agents*. Ind. Eng. Chem. Res. 2002. **41**(8): 1925-1928.
11. Karwacki, C.; Peterson, G.; Maxwell, A., *Filtration Technology*, in *Chemical & Biological Individual Protection Conference*. 2006, Edgewood Chemical & Biological Center: Charleston, South Carolina.
12. Rivin, D.; Kendrick, C. E., *Adsorption Properties of Vapor-protective Fabrics Containing Activated Carbon.* Carbon. 1997. **35**(9): p. 1295-1305.
13. Yang, Y.-C., *Chemical Reactions for Neutralising Chemical Warfare Agents.* Chemistry & Industry, 1995: p. 334-337.
14. http://www.bio.psu.edu/People/Faculty/Whittam/apdbase/. *Minimal Infective Doses for Airborne Viruses of Pathogenic Concern*. 2003.
15. Services, U.I.H. (2003) *Filtering Facepiece Respirators*.

16. Fisk, W.J.; Faulkner, D.; Palonen, J.; Seppanen, O., *Performance and costs of particle air filtration technologies.* Indoor Air, 2002: p. 223-234.
17. Eknoian, M.W., *Novel Biocidal Polymers*, in *Chemistry*. 1998, Auburn University: Auburn, Ph.D. [Organic Chemistry] dissertation.
18. Sauvet, G.; Dupond, S.; Kazmierski, K.; Chojnowski, J., *Biocidal Polymers Active By Contact. V. Synthesis of Polysiloxanes with Biocidal Activity.* Journal of Applied Polymer Science, 2000. **75**(8): p. 1005-1012.
19. Sun, G.; Chen, T.J.; Worley, S.D., *A Novel Biocidal Styrenetriazinedione Polymer.* Polymer, 1996. **37**(16): p. 3753-6.
20. Sun, G.; Xiangjing, X., *Innovative Durable and Regenerable Antimicrobial Finishing of Textile Materials*. in *American Association of Textile Chemists and Colorists 1999 Annual Conference and Exhibition*. 1999. Charlotte, NC.
21. Sun, G.; Xu, X., *Durable and Regenerable Antibacterial Finishing of Fabrics: Fabric Properties.* Textile Chemist and Colorist, 1990. **31**(1): p. 21-24.
22. Sun, G.; Xu, X., *Durable and Regenerable Antibacterial Finishing of Fabrics: Chemical Structures.* Textile Chemist and Colorist, 1999. **31**(5): p. 31-35.
23. Worley, S.D.; Chen, Y.; Wang, J-W; Cho, R.U.; Broughton, R.M.; Kim, J.; Wei, C-I; Williams, J.F.; Chen, J.; Li, Y., *Novel N-Halamine Siloxane Monomers and Polymers for Preparing Biocidal Coatings*. in *Hygienic Coatings & Surfaces*. 2004. Orlando FL.
24. Worley, S.D.; Kim, J.; Wei, C.I.; Williams, J.F.; Owens, J.R.; Wander, J.D.; Bargmeyer, A.M.; Shirtliff, M.E., *A Novel N-halamine Monomer for Preparing Biocidal Polyurethane Coatings.* Surface Coatings International Part B: Coatings Transactions, 2003. **86**(4): p. 273-77.
25. Worley, S.D.; Williams, J.F., *CRC Critical Reviews in Environmental Control.* 1988. **18**(2): p. 133.
26. Yanagisawa, Y.; Akiyama, M.; Okawara, J., *Synthesis and Reactions of Functional Polymers Containing N-halosuccinimide Structure.* Chemical Abstracts, 1969. 72: p. 1399-1402.
27. Overberger, C.G.; Vorchheiver, N., *Imidazole-Containing Polymers. Synthesis and Polymerization of the Monomer 4(5)-Vinylimidazole.* Journal of American Chemical Society, 1963. 85: p. 951-955.
28. Ko, L.L.; Shibamoto, T.; Sun, G., *A Novel Detoxifying Pesticide Protective Clothing for Agricultural Workers.* Textile Chemist and Colorist & American Dyestuff Reporter, 2000. **32**(2): p. 34-38.
28-*a*. Sun, Y.; Sun, G., *Durable and Regenerable antimicrobial textile materials prepaared by a continuous grafting process.* Journal of Applied Polymer Science, 2002. **84**(8): p. 1592-1599.

29. Liang, J.; Owens, J.R.; Worley, S.D., *Biocidal hydantoinylsiloxane polymers. IV. N--halamine siloxane-functionalized silica gel.* Journal of Applied Polymer Science, 2006. **101**(5): p. 3448-3454.
30. Kappe, O.C., *Controlled Microwave Heating in Modern Organic Synthesis.* Angewandte Chemie, 2004. 43: p. 6250-6284.
31. Yu, X.; Huang, X., *Microwave-Assisted Tandem Nucleophilic Substitution-Wittig Reaction of α-Hypervalent Iodine Functionalized Phosphonium Ylide* Synthetic Letters, 2002: p. 1895-1897.
32. Binner, J.G.P.; Hassine, N.A.; Cross, T.E. *The Possible Role of the Pre-exponetial Factor in Explaining the Increased Reaction Rates Observed During the Microwave Synthesis of Titanium Carbide.* Journal of Material Science, 1995. 30(5389-5393).
33. Haz, A.; Diaz-Ortiz A.; Andres, M., *Microwaves in Organic Synthesis. Thermal and Non-thermal Microwave Effects.* Chemical Society Reviews, 2005. 34: p. 164-178.
34. Jacob, J.; Chia, L.H.L.; Boey, F.Y.C., *Thermal and non-thermal Interaction of Microwave Radiation with Materials* Journal of Material Science, 2004. **30**(21): p. 5321-5327.
35. Kuhnert, N., *Microwave-Assisted Reactions in Organic Synthesis - Are There Any Nonthermal Microwave Effects?* Angewandte Chemie International Edition, 2002. **41**(11): p. 1863-1866.
36. Stuerga, D.A.C.; Gaillard, P., *Microwave Athermal Effects in Chemistry: A Myth's Autopsy.* Journal of Microwave Power and Electromagnetic Energy, 1996. **31**(2): p. 87-100.
37. Wroe, R.; Rowley, A.T., *Evidence for a non-thermal Microwave Effect in the Sintering of Partially Stabilized Zirconia.* Journal of Material Science, 1996. 31: p. 2019-2026.
38. Loupy, A., *Microwaves in Organic Synthesis*. 2nd ed. 2003: Wiley.
39. Musher, J.I., *The Chemistry of Hypervalent Molecules.* Agnew. Chem. Int'l. Ed., 1968. 8: p. 54-68.
40. Frye, C.L., *Quaternary Phosphonium Silicon Complexes*. 1970, Dow Corning Corporation: United States.
41. Frye, C.L., *Pentacoordinate Silicon Derivatives. IV. Alkylammonium Siliconate Salts Derived from Aliphatic 1,2-Diols.* Journal of the American Chemical Society, 1970. **92**(5): p. 1205-10.
42. Frye, C.L.; Vincent, G.A.; Finzel, W.A., *Pentacoordinate Silicon Compounds. V. Novel Silatrane Chemistry.* Journal of the American Chemical Society, 1971. **93**(25): p. 6805-11.
43. Laine, R.M.; Blohowiak, K.Y.; Treadwell, D.R.; Mueller, B.L.; Hoppe, M.L.; Jouppi, S.; Kansal, P.; Chew, K.W.; Scotto, C.L.S.; Babonneau, F.; Kampf, J., *Synthesis of Pentacoordinate Silicon Complexes from SiO_2.* Nature, 1991. 353: p. 642-6.
44. Lee, C.L.; Johannson, O.K., *Polymerization of Hexamethylcyclotrisiloxane With A Biscatecholsiliconate. I. Nature of Polymerization.* Journal of Polymer Science, 1975. **14**(3): p. 729-742.

45. Ratner, M.A.; Satner, J.R., *Some Symmetry Considerations Concerning the Role of Atomic d Orbitals in Chemical Bonds: Discussion and Some Calculational Examples.* Journal of American Chemical Society, 1977. 99: p. 3954-3960.
46. Sun, X., *Pentacoordinated AB5-Type Main Group Molecules Favorably Adopt sp^2 Hybridization in the Central Atom: Bonding Without d-Orbital Participation.* Chem Educator, 2002. 7: p. 11.
47. Sun, X., *Three-Center, Four Electron Bond in Hexacoordinated AB6-Type Main Group Molecules: An Alternative Model of Bonding Without d-Orbital Participation in the Central Atom.* Chem Educator, 2002. 7: p. 261.
48. Michels, H.H.; Montgomery, J.A. Jr., *Chemical Bond in Phosphoranes: Comparative ab initio Study of Difluorophosphorane Phosphorane* Journal of Physical Chemistry, 1990. **93**(3): p. 1805.
49. Kar, T.; Sanchez-Marcos, E.S., *Three-Center Four Electron Bonds and Their Indexes.* Chemical Physics Letters, 1992. 192: p. 14-20.
50. Hajdasz, D.J.; Ho, Y.; Squires, R.R., *Gas-Phase Chemistry of Pentacoordinate Silicon Hydride Ions.* Journal of American Chemical Society, 1990. 116: p. 10751-10760.
51. Cahill, P.A.; Dykstra, C.E.; Martin, J.C., *The Structure and Stability of the 10-F-2 Trifluoride Ion, a Compound of a Hypervalent First Row Element.* Journal of American Chemical Society, 1985. 107: p. 6359-6362.
52. Boer, F.P.; Flynn, J.J.; Turley, J.W., *Structural Studies of Pentacoordinate Silicon.* Journal of the American Chemical Society, 1968. **90**(25): p. 6973-77.
53. Chuit, C., *Reactivity of Penta and Hexacoordinate Silicon Compounds and Their Role as Reaction Intermediates.* Chemical Reviews, 1993. **93**(4): p. 1368-1448.
54. *Water Chlorine (Residual) No. 1*, E.P. A., 1969, Analytical Reference Service.
55. *Antibacterial Activity Assessment of Textile Materials: Parallel Streak Method*, in *Test Method 147*. 1998: AATCC.
56. *Standard Test for Determining the Activity of Incorporated Antimicrobial Agent(s) in Polymeric or Hydrophobic Materials*, in *ASTM Method E2180-1*. 2002, ASTM.
57. *Antibacterial Finishes on Textile Materials: Assessment of*, in *Test Method 100*. 1999, AATCC.
58. *E2149-01 Standard Test Method for Determining the Antimicrobial Activity of Immobilized Antimicrobial Agents Under Dynamic Contact Conditions*. 2004, ASTM. p. 1-4.
59. Chung, J.S.; Kim, D.J.; Ahn, W.S.; Ko, J.H.; Cheong, W.J., *Synthesis, Characterization, and Applications of Organic-Inorganic Hybrid Mesoporous Silica.* Korean Journal of Chemical Engineering, 2003. **21**(1): p. 132-139.

60. Jitchum, V.; Chivin, S.; Wongkasemjit, S.; Ishida, H., *Synthesis of Spirosilicates Directly from Silica and Ethylene Glycol/Ethylene Glycol Derivatives.* Tetrahedron, 2001. 53: p. 3997-4003.
61. Blohowiak, K.Y.; Robinson, T.R.; Hoppe, M.L., *Synthesis of Penta-alkoxy and Penta-aryloxy Silicates Sirectly from SiO_2*, in *Inorganic and Organometallic Polymers with Special Properties*. 1992, Khuwgr Academic Publishers. p. 99-111.
62. Shea, K.J.; Loy, D.A., *A Mechanistic Investigation of Gelation. The Sol--Gel Polymerization of Precursors to Bridged Polysilsesquioxanes.* Accounts of Chemical Research, 2001. **34**(9): p. 707-716.
63. Klabunde, K.J., *Nanoscale Materials in Chemistry*. 2004: Wiley.
63-*a*. Wright, J.; Sommerdijk, N., Sol-Gel Materials: *Chemistry and Applications*. 2001: Taylor and Francis Books Ltd.
63-*b* Padmaja, P.; Warrier, K.; Padmanabhan, M.; Wunderlich, W.; Berry, F.; Mortimer, M.; Creamer, N., *Structural Aspects and Porosity Features of Nano-size High Surface Area Alumina–silica Mixed Oxide Catalyst Generated Through Hybrid Sol–gel Route.* Mat. Chem. Phys., 2006. 95: 56-61.
63-*c* Szabo, I.; Blickle, T.; Ujhidy, A.; Jelinko, R., *Kinetics of Aluminum Oxide Chlorination.* Ind. Eng. Chem. Res., 1991, 30: p. 298-303.
64. Bandgar, B.P.; Kasture, S.P., *Chemoselective Protection of Hydroxyl Groups and Deprotection of Silyl Ethers.* Chemical Monthly, 2001. 132: p. 1101-1104.
65. Hajipour, A.R.; Mallakpour, S.E.; Mohammadpoor-Baltork, I.; Khoee, S., *An Efficient Method for Selective Deprotection of Trimethylsilyl Ethers, Tetrahydropyranyl Ethers, Ethylene Acetals, and Ketals Under Microwave Irradiation.* Synthetic Communications, 2002. **32**(4): p. 611-20.
66. Heravi, M.M.; Oskooie, H.A.; Yazdanpanah, S.; Mojtahedi, M., *Oxidative Deprotection of Trimethylsilyl Ethers Using Bismuth Nitrate Supported Onto Montmorillonite k-10 Under Microwave Irradiation in Solventless System.* Journal of Chemical Research, 2004. 2(February): p. 129-130.
67. Mojtahedi, M.M.; Saidi, M.R.; Heravi, M.M.; Bolourtchian, M., *Microwave Assisted Deprotection of Trimethylsilyl Ethers Under Solvent-free Conditions Catalyzed by Clay of a Palladium Complex.* Chemical Monthly, 1999. 130: p. 1175-1178.
68. Augusta, S.; Gruber, H.F.; Streichsbier, F., *Synthesis and antibacterial activity of immobilized quaternary ammonium salts.* Journal of Applied Polymer Science, 1994. **53**(9): p. 1149-1163.
69. Jiang, S.; Wang, L.; Yu, H.; Chen, Y.; Shi, Q., *Study on antibacterial behavior of insoluble quaternary ammonium.* Journal of Applied Polymer Science, 2006. **99**(5): p. 2389-2394.
70. Atlas, R.M., *Basic and Practical Microbiology*. 1986, Macmillan.

71. Hamid, H.S.; Hamidi, A., *Handbook of Polymer Degradation*. 2nd Ed., K.F.I.o.P.a. Minerals. 2000, Dhahran, Saudi Arabia: Marcel Dekkar.
72. Smith, M.B.; March, J., *Reactions, Mechanisms, and Structure*. 5th ed. March's Advanced Organic Chemistry. 2001: Wiley.
72-*a* Clark, T. *Fabrication of SiC - AIN alloys*, 1986, patent, #4687.
72-*b* Bram, G.; Loupe, A.; Majdoub, M., *Alkylation of Potassium Acetate in "Dry Media" Thermal Activation in Commercial Microwave Ovens.* Tetrahedron, 1990. **46**(15): p. 5167-76.
73. Bedard, T.C.; Corey, J.Y., *Conversion of Hydrosilanes To Alkoxysilanes Catalyzed By Titanocene Dichloride-butyllithium.* Journal of Organometallic Chemistry, 1992. **428**(3): p. 315-333.
74. Carre, F.; Cerveau, G.; Chuit, C.; Corriu, R.J.P.; Nayyar, N.K.; Reye, C., *Hexacoordination at Silicon. The Case of Silatranes.* Organometallics, 1990. **9**(7): p. 1989.
75. Cerveau, C.; Chuit, C.; Corriu, R.J.P.; Nayyar, N.K.; Reye, C., *Pentacoordinate Silicon Compounds. Reactions of Silatranes with Nucleophiles.* Journal of Organometallic Chemistry, 1990. **389**(2): p. 159-168.
76. Corriu, R.J.P., *Hypervalent Species of Silicon: Structure And Reactivity.* J. of Organometallic Chem., 1990. 400: p. 81-106.
77. Dobado, J.A.; Martinez-Garcia, H.; Molina, J.M.; Sundberg, M.R., *Chemical Bonding In Hypervalent Molecules Revised: Application of the Atoms In Molecules Theory To Y_3 and Y_3XZ (Y= H or CH_3 X=N, P, or As; Z=O or S) Compounds.* J. Amer. Chem. Soc., 1998. 120: p. 8461-8471.
78. Holmes, R.R.; Deiters, J.A., *Enhanced Reactivity of Pentacoordinated Silicon Species. An ab Initio Approach.* Journal of American Chemical Society, 1990. 112: p. 7197-7202.
79. Corriu, R.J.P.; Mix, A.; Flanneau, G.F., *Intramolecular Nitrogen Ligand Stabilization of Phenyl-imidazolidine Derived Silicon Species.* Journal of Organometallic Chemistry, 1998. **570**(2): p. 183-193.
80. Raner, K.; Strauss, C.; Vyskoc, F.; Mokbel, L., *A Comparison of Reaction Kinetics Observed under Microwave Irradiation and Conventional Heating.* J. Org. Chem., 1993. 58: 950-3.